The Hemispherical Asymmetry of the Residual Polar Caps on Mars

Contract No. NASW-4444

Semi-Annual Progress Report

Submitted Apr. 1, 1991

by Bernhard Lee Lindner

TECHNICAL REPORT STANDARD TITLE PAGE

1. Report No.	2. Government Accession No.	3. Recipient's Catalog No.

4. Title and Subtitle	5. Report Date
The Hemispherical Asymmetry of the Residual Polar Caps on Mars	March 1, 1991
	6. Performing Organization Code
7. Author(s)	8. Performing Organization Report No.
Bernhard Lee Lindner	
9. Performing Organization Name and Address Atmospheric and Environmental Research, Inc. 840 Memorial Drive Cambridge, MA 02139-3794	10. Work Unit No.
	11. Contract or Grant No. NASW-4444
	13. Type of Report and Period Covered Semi-Annual Progress Report 9/1/89 - 3/1/91
12. Sponsoring Agency Name and Address NASA Headquarters Headquarters Contract Division Washington, DC 20546	14. Sponsoring Agency Code EL
15. Supplementary Notes	

16. Abstract A model of the polar caps of Mars has been created which allows for light penetration into the cap, allows ice albedo to vary with age, latitude, hemisphere, dust content and solar zenith angle, includes the radiative effects of clouds and dust, allows for diurnal variability, and includes heat transport as represented by a thermal wind. The model reproduces polar cap regression data very well, including the survival of CO_2 frost at the south pole and not the north pole, and reproduces the general trend in the Viking Lander pressure data, although further improvement is needed. Papers were presented at six conferences and in the Journal of Geophysical Research, and have been submitted to Icarus. The research plan for the next reporting period involves further publishing and presenting of our results.

17. Key Words (Selected by Author(s))	18. Distribution Statement
planets, Mars, polar cap	

19. Security Classif. (of this report)	20. Security Classif. (of this page)	21. No. of Pages	22. Price*
Unclassified	Unclassified	79	

*For sale by the Clearinghouse for Federal Scientific and Technical Information, Springfield, Virginia 22151.

Table of Contents

I. Abstract for the project

Computer simulation of the condensation and sublimation of CO_2 frost in the martian polar caps has been fairly successful in reproducing the annual cycle in atmospheric pressure observed by the Viking Landers. However, these studies have not been able to uniquely explain why CO_2 frost survives southern summer. We propose to study several mechanisms which might explain this phenomenon: an improved treatment of cloud and atmospheric-dust effects; the decrease in the importance of heat conduction due to existing CO_2 ice; an improved treatment of sublimation microphysics; the variance in ice albedo with solar zenith angle, ice age, and dust/ice ratio; the bidirectional reflectance of ice; snowfall accumulation in addition to surface frost formation; insulating residues on the ice; wind shifting of ice and brightening of ice under exposure to sunlight. To perform this study, we will integrate two existing models of the martian polar caps and combine them with an accurate model of martian atmospheric radiation and parameterizations of the processes described above. The model will be used to identify combinations of parameters which will allow a reproduction of seasonal observations of atmospheric pressure and the latitudinal and seasonal extent of the polar cap, and the hemispherical asymmetry in the residual polar caps. A better understanding of the martian polar caps will have direct implications for our understanding of the climate and atmospheric dynamics of Mars and the Earth, as well as provide insight for the observations planned for the Mars Observer mission.

II. Summary of Research to date

II.1. Jakosky Model Acquired

The Principal Investigator, Dr. Lindner, flew to Colorado in September 1989 to meet with the Co-Investigator, Dr. Jakosky. The polar cap model of Dr. Jakosky was obtained. Dr. Lindner became familiar with the code in discussions with Dr. Jakosky, and through exercising the model on Dr. Jakosky's computer system. Dr. Lindner and Dr. Jakosky also held in-depth discussions of the overall approach to be taken on the project to meet the objectives.

II.2. Lindner and Jakosky Models Integrated

The Jakosky model was loaded onto the AER computer system and combined with the Lindner model, as discussed in the proposal. The hybrid model was debugged of errors.

II.3. Comparison to Kieffer's surface model

Kieffer (1990) described a model which is similar to ours, which he used for ice metamorphism studies. I set up the code to use the same inputs as Kieffer did in his Figure 3, and plotted the results on the same figure (deleting all but the case I compared to). The agreement is good, as can be seen in Figure 1. Since I don't know exactly what all of his input parameters were (such as emissivity, seasonal ice albedo, etc.), I consider the agreement a validation of our code. The only different behavior is why his figure doesn't show a seasonal temperature "pulse" which makes it's way down in depth (i.e.

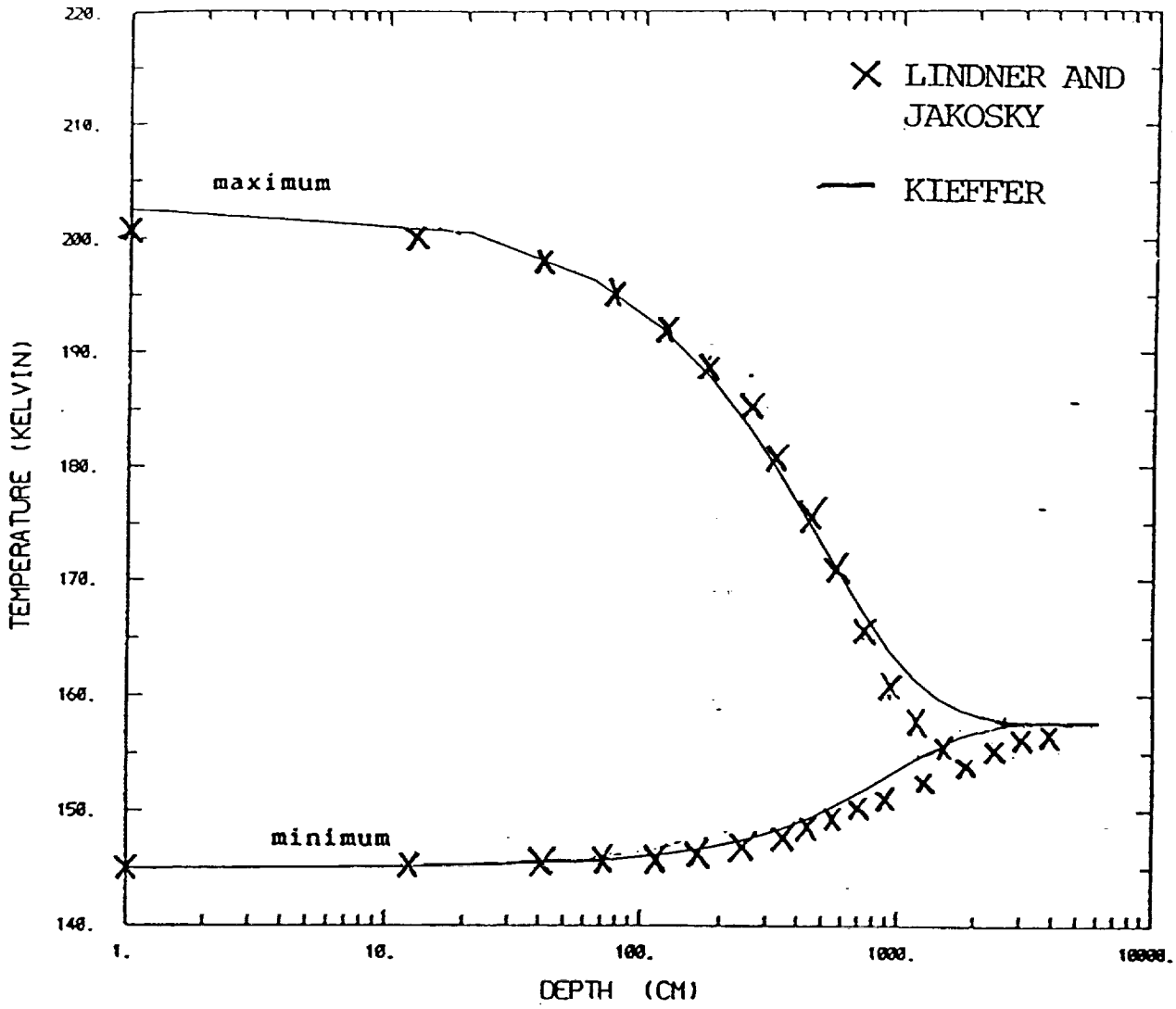

Fig. 1. Temperatures within the north polar ice cap (shown are the annual minimum and maximum). Lindner and Jakosky values are for the current study (L_s = 260 and 280 degrees), and Kieffer values are taken from Kieffer (1990). The albedo of the residual ice is 0.41, and the thermal inertia is 0.04 cal cm-2 sec-0.5 K-1. Surface values are shown as 1 cm depth.

when the surface is at a maximum, the temperature at 10 m should be at a relative minimum, as our results show). Perhaps Kieffer is showing the maximum temperature for all year at each depth, rather than a snapshot in time when the surface reaches a maximum (as I've plotted).

II.4. Ice Microphysics Parameterization

Section 2.3 of the proposal discussed the inclusion of improved ice microphysics in the model. Discussions were held with Dr. Gary Clow as to the nature of his ice microphysics models and the results he has obtained recently. In the proposal, we mentioned that the depth to which radiation penetrates into the cap has never been included in polar cap sublimation models, although it could be important. We have done calculations that show that this is not important for thick CO_2 ice, or thin CO_2 ice overlying a dust surface. For the thick ice case, the integral of sublimation is independent of where it occurs within the ice. The distribution of absorption within the polar cap is important for studies of the internal physics of the cap, but not for overall sublimation rate. For the thin CO_2 ice over dust case, the surface thermally reradiates the absorbed solar radiation primarily back to the polar cap where most is reabsorbed. The top few grains of dirt absorb the incoming solar radiation which penetrates the polar cap, and it is much easier for these top few grains to conduct or radiate heat back to the overlying polar cap than deep into the surface.

A thin CO_2 ice polar cap overlying a residual water ice deposit is different. Solar radiation which passes through the CO_2 ice cap may penetrate quite deeply into the H_2O ice. This will effect CO_2 ice lifetimes over the residual polar cap, but won't affect overall polar-cap recession or the annual variation in surface pressure, both of which current models reproduce. I incorporated this effect in the model by apportioning the absorbed solar flux between the sublimation of the ice, and the heating of the subsurface. Clow (1987) has already calculated the absorption of solar flux as a function of depth in CO2 ice on Mars, and I have reproduced a figure from his paper in Figure 2, which we used in the model. Based on Clow's figure, I obtained a % of solar flux absorption as a function of depth for 41 depth steps. The code already calculates the thickness of CO_2 ice, and I use this depth with Clow's work to determine how much sunlight penetrates the seasonal ice. This fraction that penetrates the seasonal ice is further apportioned between the individual subsurface layers, again using Clow's figure.

Both Kieffer (1990) and Moore (1988) have deduced that ice grain radii in the residual cap are over 100 μm and that dust concentrations are less than 1/1000, so any one of Clow's profiles could be legitimate. I've tried them all, and found the largest deviation was for clean, fine ice. This is understandable, since solar radiation penetrates the deepest in clean, fine ice. In our work, we have assumed that the seasonal ice was fine, and the residual ice was coarse.

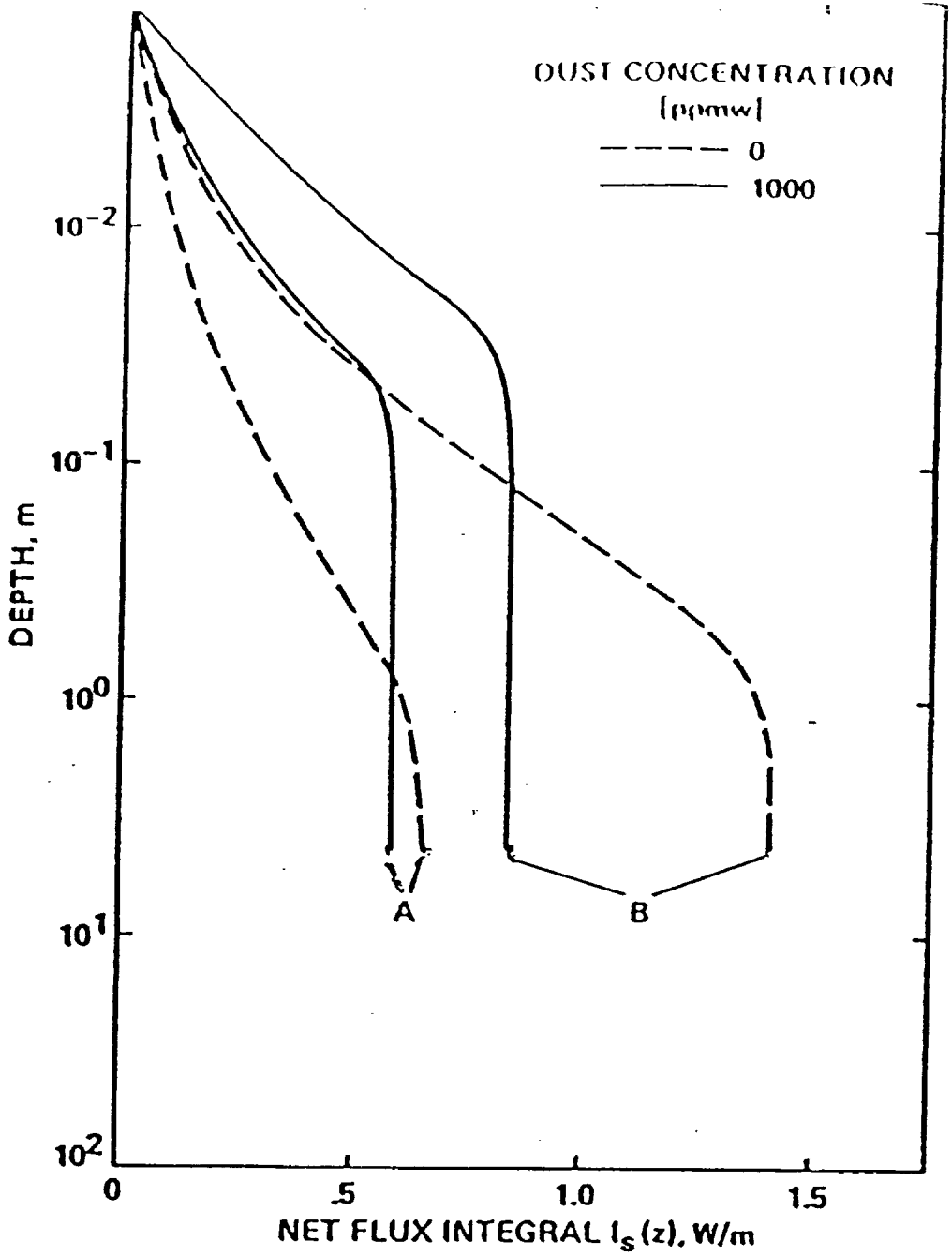

FIG. 2. The integral of net shortwave flux with respect to depth for clean and dusty snow, using the mean-annual incident solar flux at latitude −38°. Mean-annual temperature profiles in snow are proportional to the flux integral $I_s(z)$, which is generally greater for coarse-grained than for fine-grained snows. Curves (A) correspond to a snow with ice grain radii of 50 μm and bulk density 50 kg m^{-3} while curves (B) are for a snow with 1000-μm ice grains and a density of 400 kg m^{-3}. [from Clow (1987)]

I have plotted in Figure 3 the difference in the depth profile of temperature between the code with no penetration of light and the modified code using penetration appropriate for clean ice for L_S = 260° (just before the last of the seasonal ice sublimes). The radiation which penetrates the cap heats the subsurface by up to 3°K. Most of the radiation gets absorbed near the surface, but that easily conducts away to the surface. The greatest heating occurs at 1 m depth. The scale on the right side of the figure is for the "difference" curve. The surface temperature is plotted as 1 cm depth on this plot.

Figure 4 shows the profiles for L_S=280°, when the maximum surface temperature occurs, as well as the maximum deviation at depth between the codes (9K). The surface is actually a couple of degrees cooler for the penetrating radiation case, as we expected. Again, the maximum subsurface heating occurs at 1 m depth.

Figure 5 shows how the surface temperature varies with L_S for both codes. Surface temperatures are cooler from L_S = 270° to L_S = 310° for the penetration code, since solar radiation is absorbed at depth, and must conduct to the surface. From L_S = 310° to 360°, the surface is actually warmer than for the original code, due to the increased conduction by the warmer subsurface.

Figure 6 shows depth profiles of temperature for every 10 sols through the year for clean ice penetration, and Figure 7 shows the same for the no-penetration code. Again, the heating of the subsurface can be seen for summer (just before the

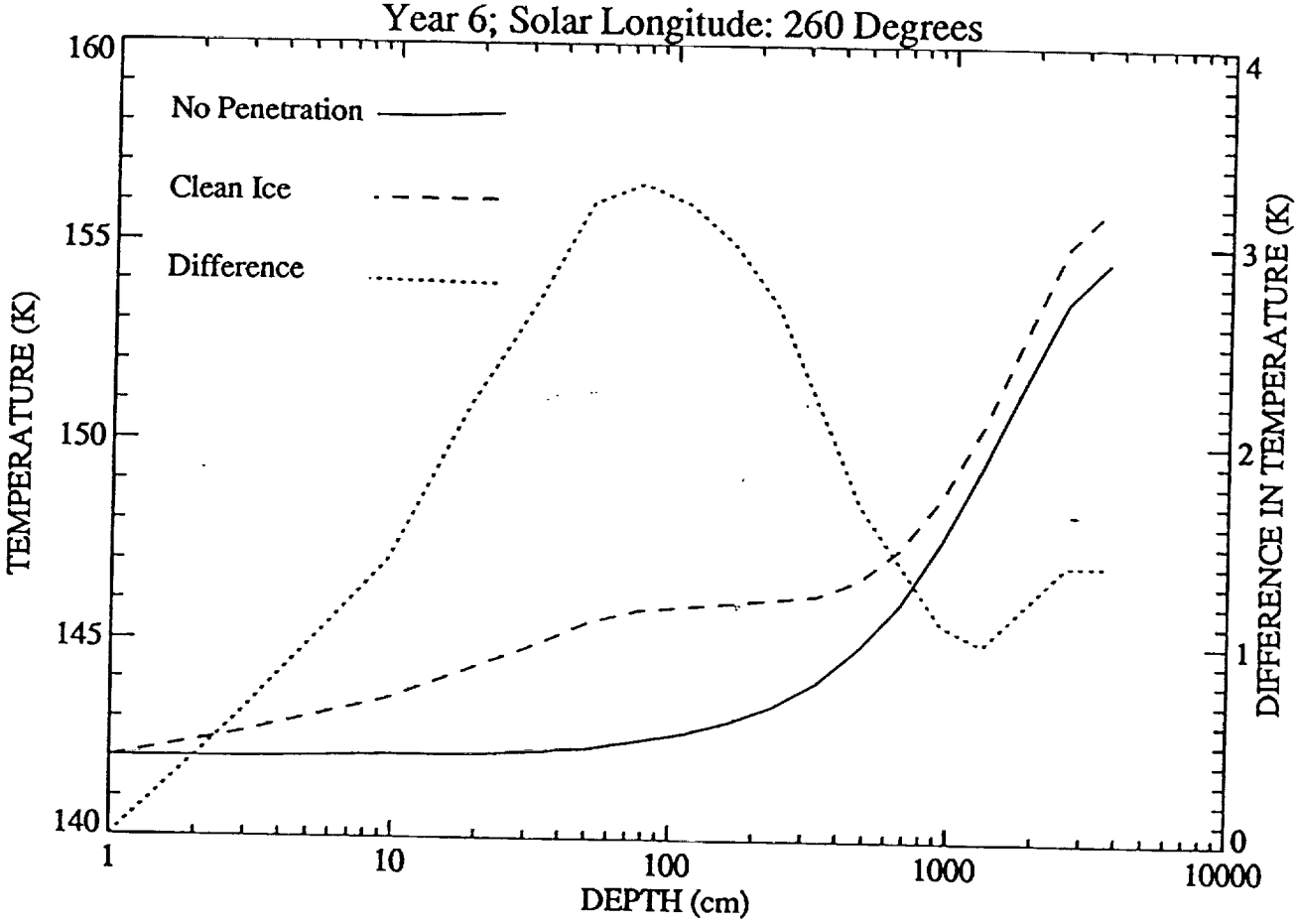

Fig. 3. Temperature versus depth in the south polar cap for L_s of 260 degrees simulated including the effect of light penetration for "clean" ice, and simulated without penetration. The difference between with and without is also plotted, using the scale on the right side. Surface values are shown at 1 cm depth.

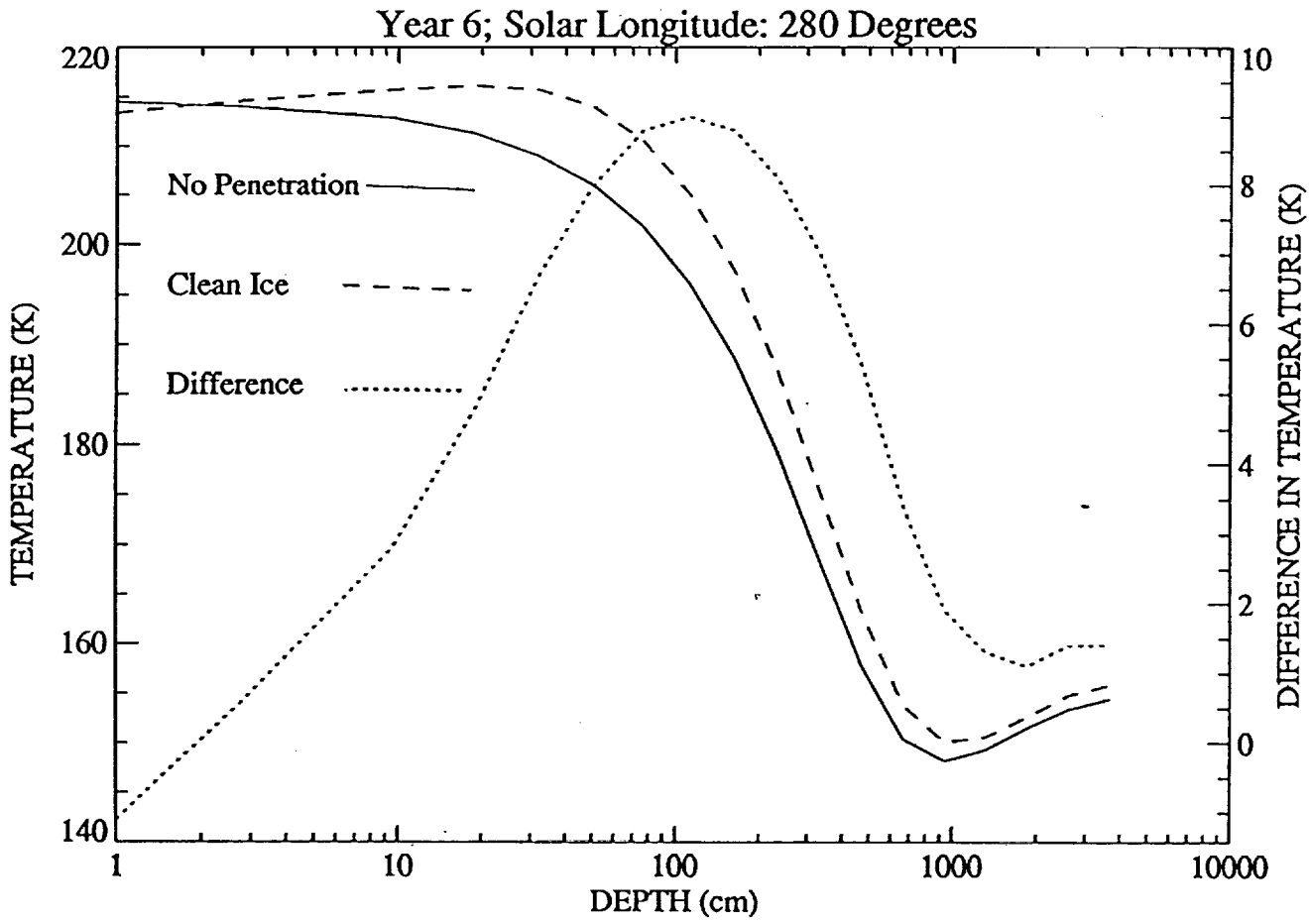

Fig. 4. Temperature versus depth in the south polar cap for L_s of 280 degrees simulated including the effect of light penetration for "clean" ice, and simulated without penetration. The difference between with and without is also plotted, using the scale on the right side. Surface values are shown at 1 cm depth.

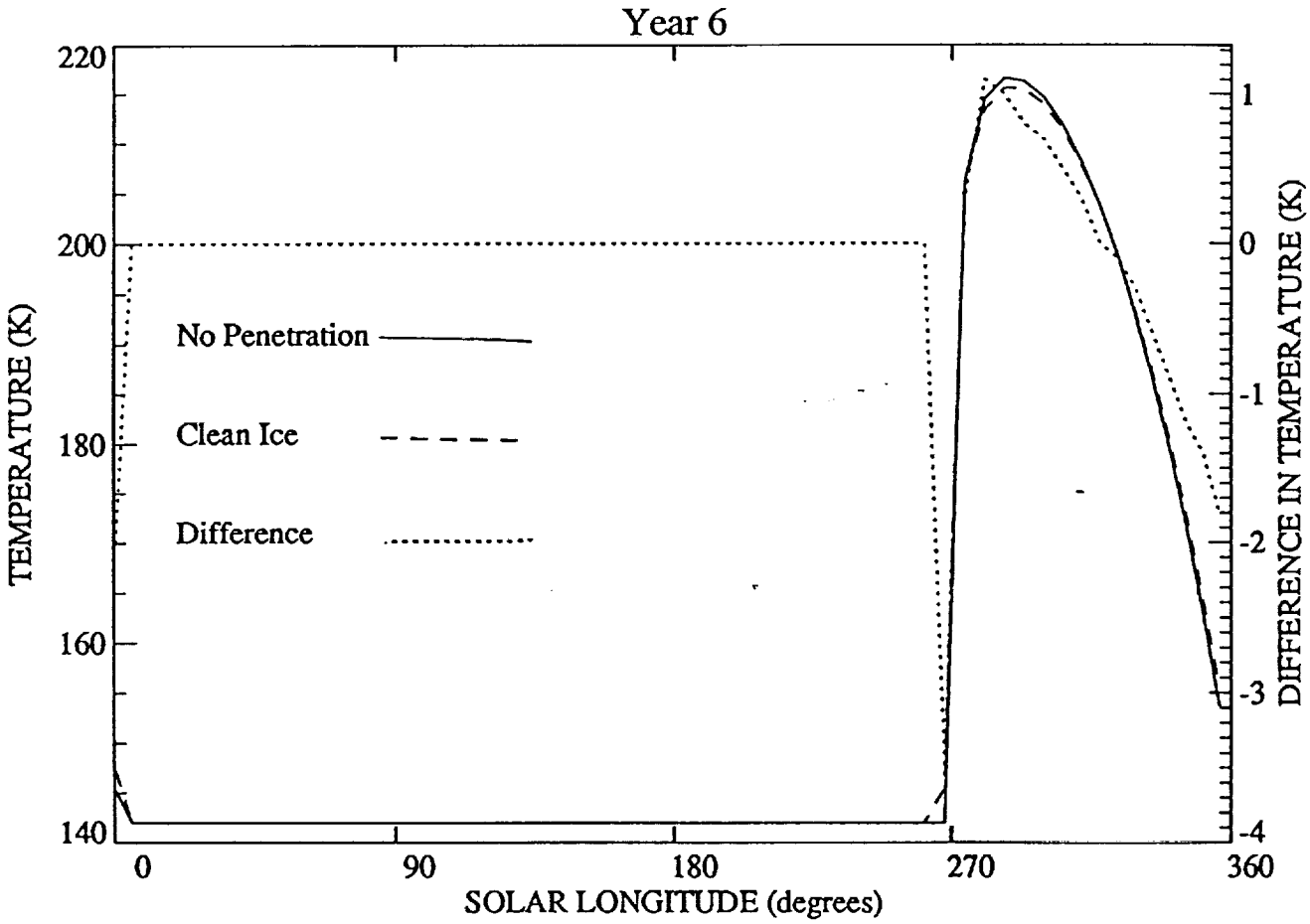

Fig. 5. Surface temperature of the south pole versus Solar Longitude simulated including the effect of light penetration for "clean" ice, and simulated without penetration. The difference between with and without is also plotted, using the scale on the right side.

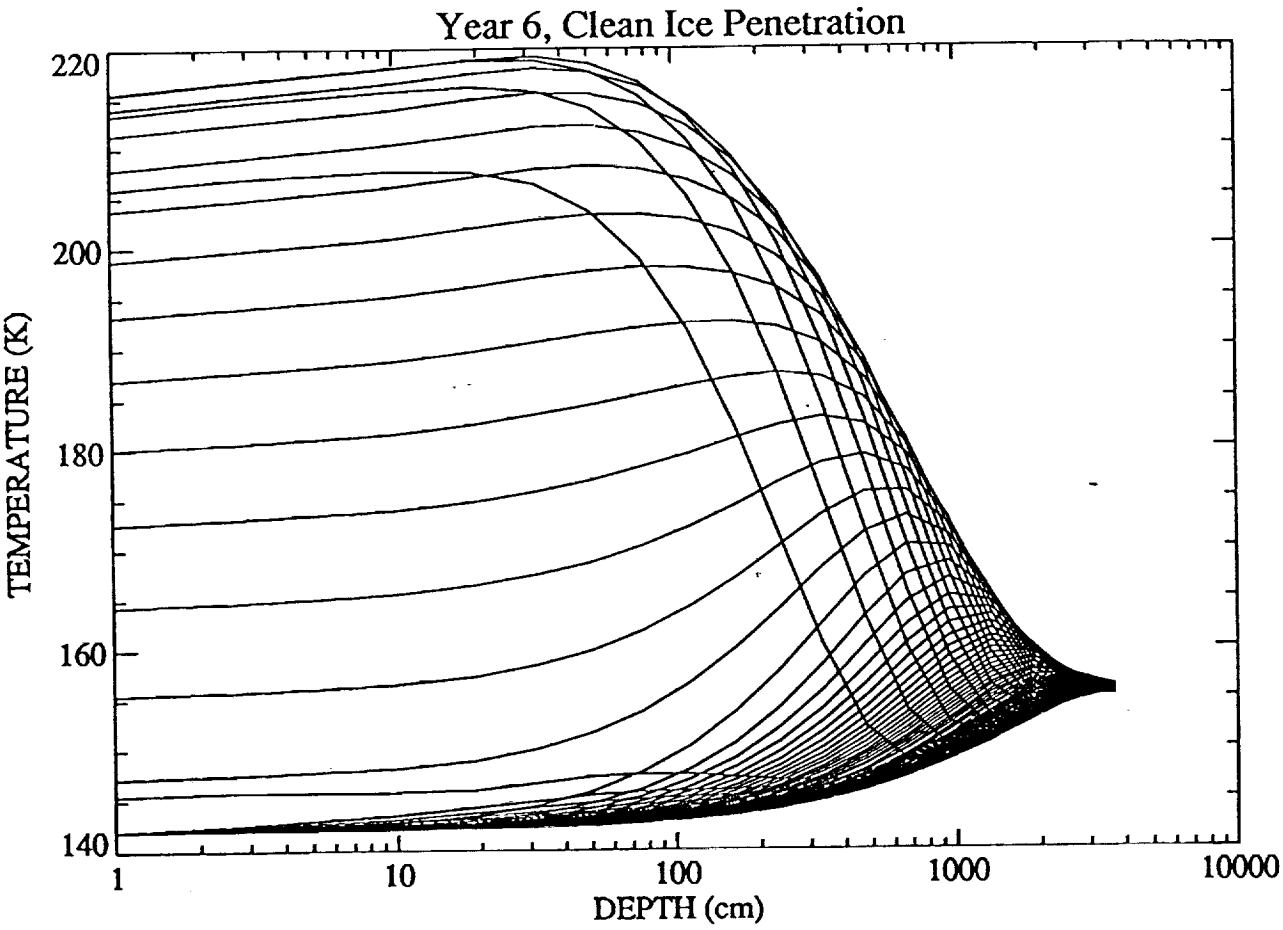

Fig. 6. Temperature versus depth in the south polar cap for every 10 sols through one year simulated including the effect of light penetration for "clean" ice. Surface values are shown at 1 cm depth.

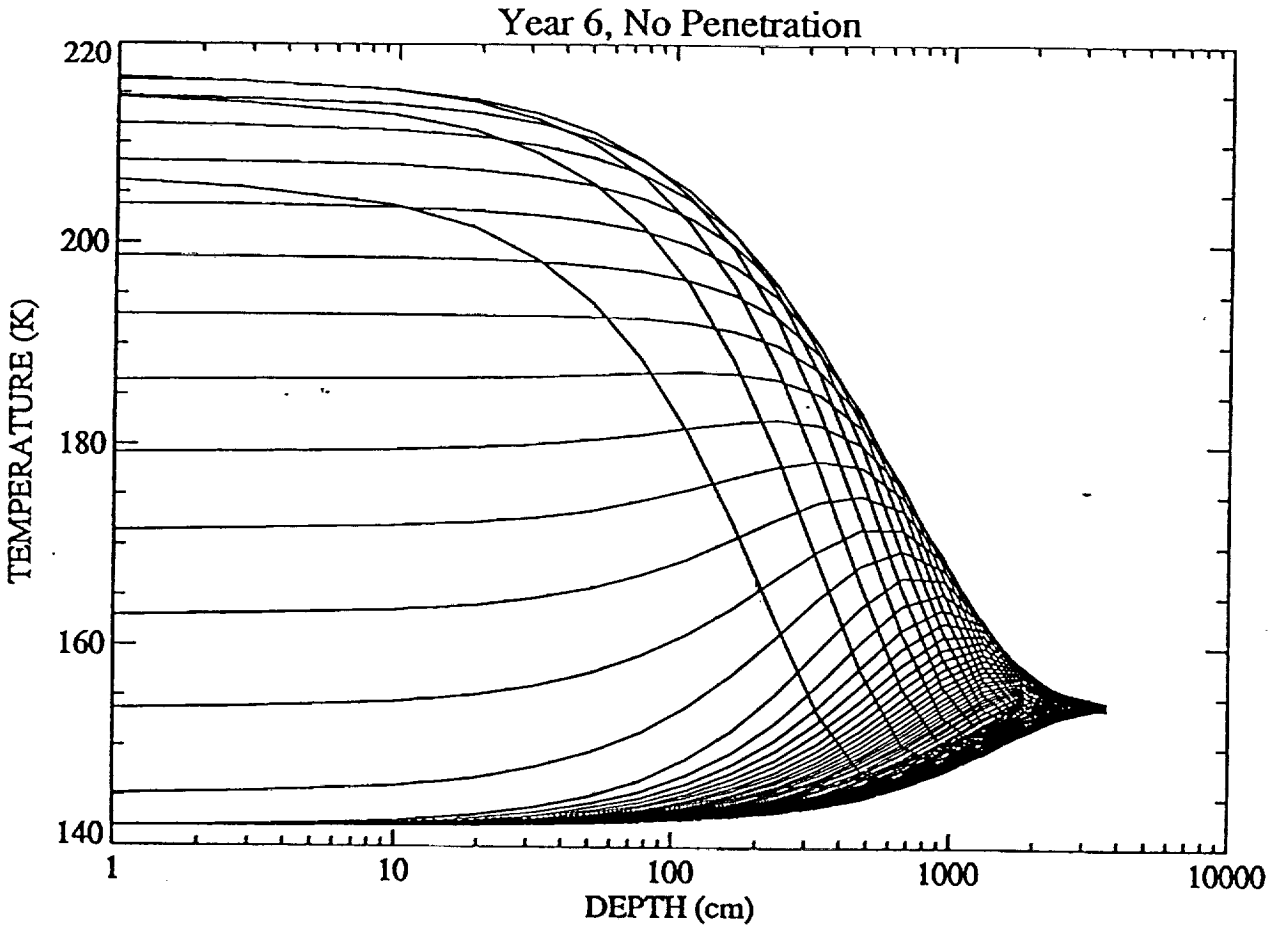

Fig. 7. Temperature versus depth in the south polar cap for every 10 sols through one year simulated without the effect of light penetration. Surface values are shown at 1 cm depth.

surface ice sublimes away) and in the warm subsurface at the maximum temperatures. We also see that very little annual variation in temperature occurs at 4 m depth.

Figures 8 and 9 show the annual variation in temperature, with each curve representing a different depth (at z=0, 2.8, 9.5, 19.0, 32.2, 50.6, 76.5, 112.7, 163.4, 234.4, 333.7, 472.8, 667.5, 940.1, 1321.8, 1856.2, 2604.2, and 3651.5 cm). The deepest depths show the least variation (almost a straight line at 36 m. The ice-covered heating of the subsurface can be seen between L_S = 180° and 270°.

Figure 10 shows the effect of light penetration on surface frost between the two models in the first year of iteration (starting from the same initial conditions of an isothermal surface of 154K, and no frost). Since the sun doesn't shine from L_S=0° to 180°, no difference is seen then. As the cap thins in the spring, the effect of sunlight penetrating the cap becomes more important (as expected from Clow's figure). Thus the ice in the model which includes penetration lasts longer in Year 1.

Figure 11 shows the same for Year 6, by which time the models have converged. Now the model which includes penetration has less ice all year. This is because the subsurface heats up more in the summer due to light penetration, and this heat decreases the amount of condensing frost in the fall and winter, resulting in an increasing difference between the models from L_S=0 to 180°. After L_S=180°, this difference decreases because of light penetration as we saw for Year 1, but not enough to

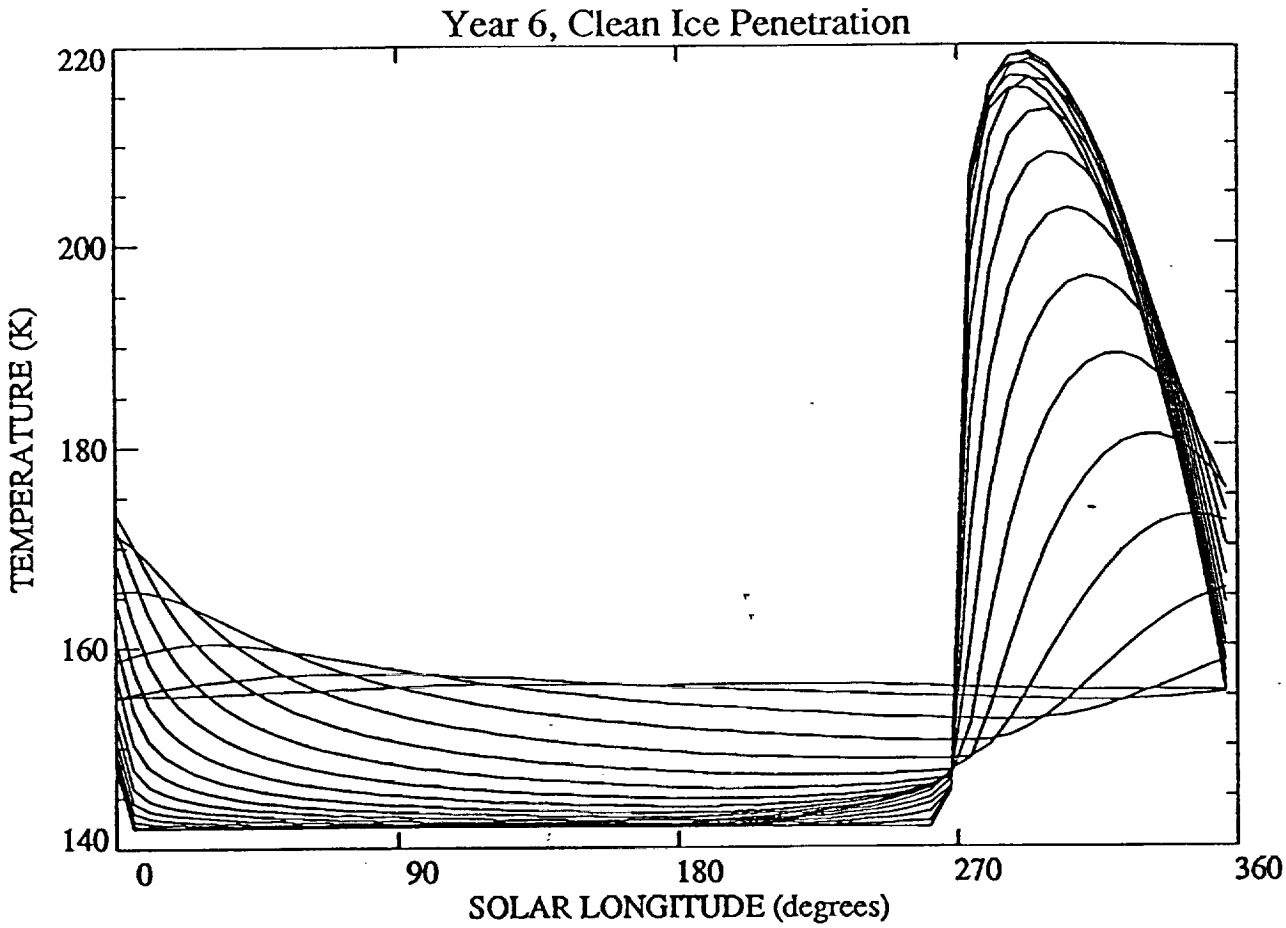

Fig. 8. Surface temperature of the south pole versus Solar Longitude, simulated including the effect of light penetration for "clean" ice. Each curve represents another layer in the model, ranging from the surface to 3.5m depth.

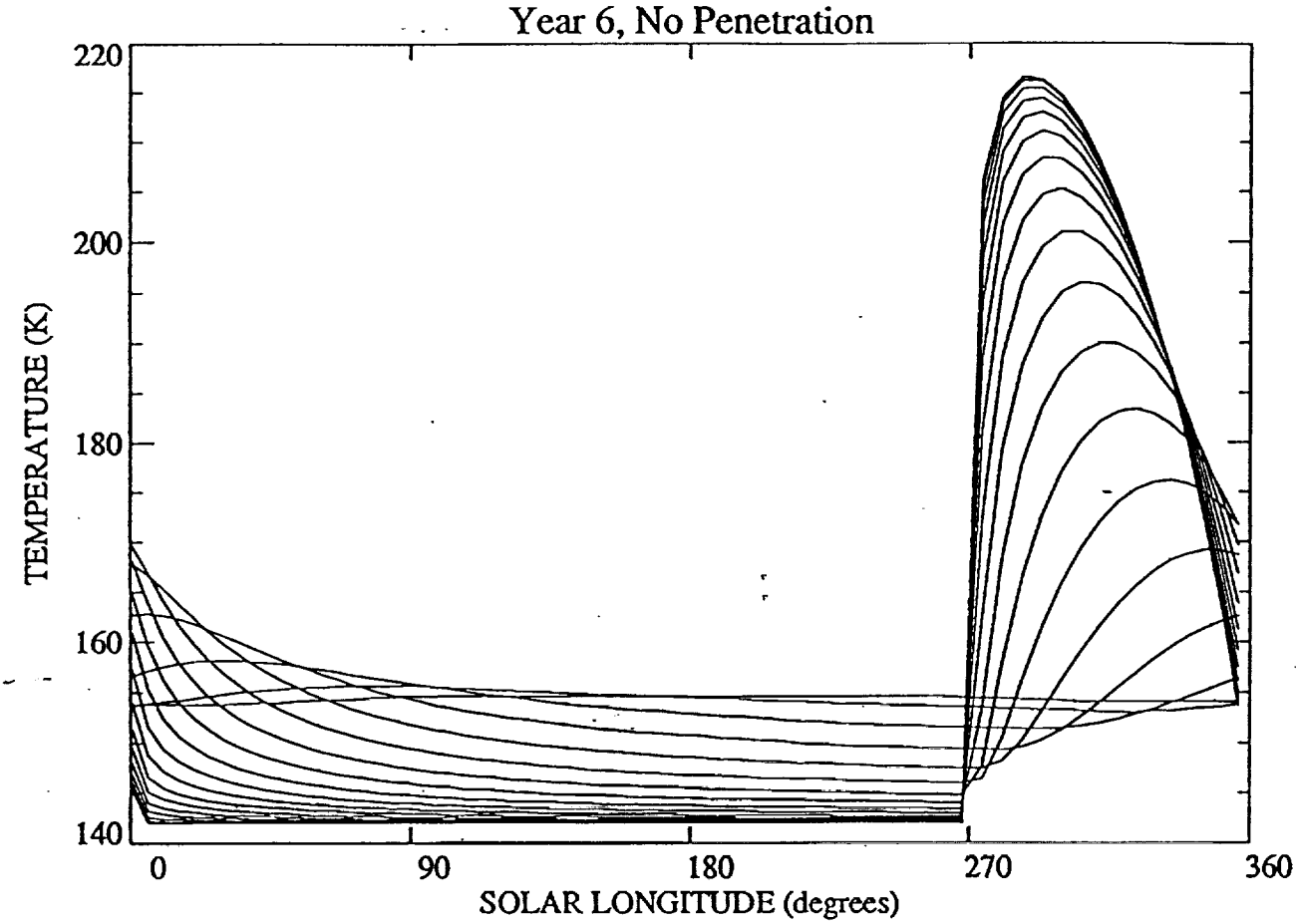

Fig. 9. Surface temperature of the south pole versus Solar Longitude, simulated without the effect of light penetration for "clean" ice. Each curve represents another layer in the model, ranging from the surface to 3.5m depth.

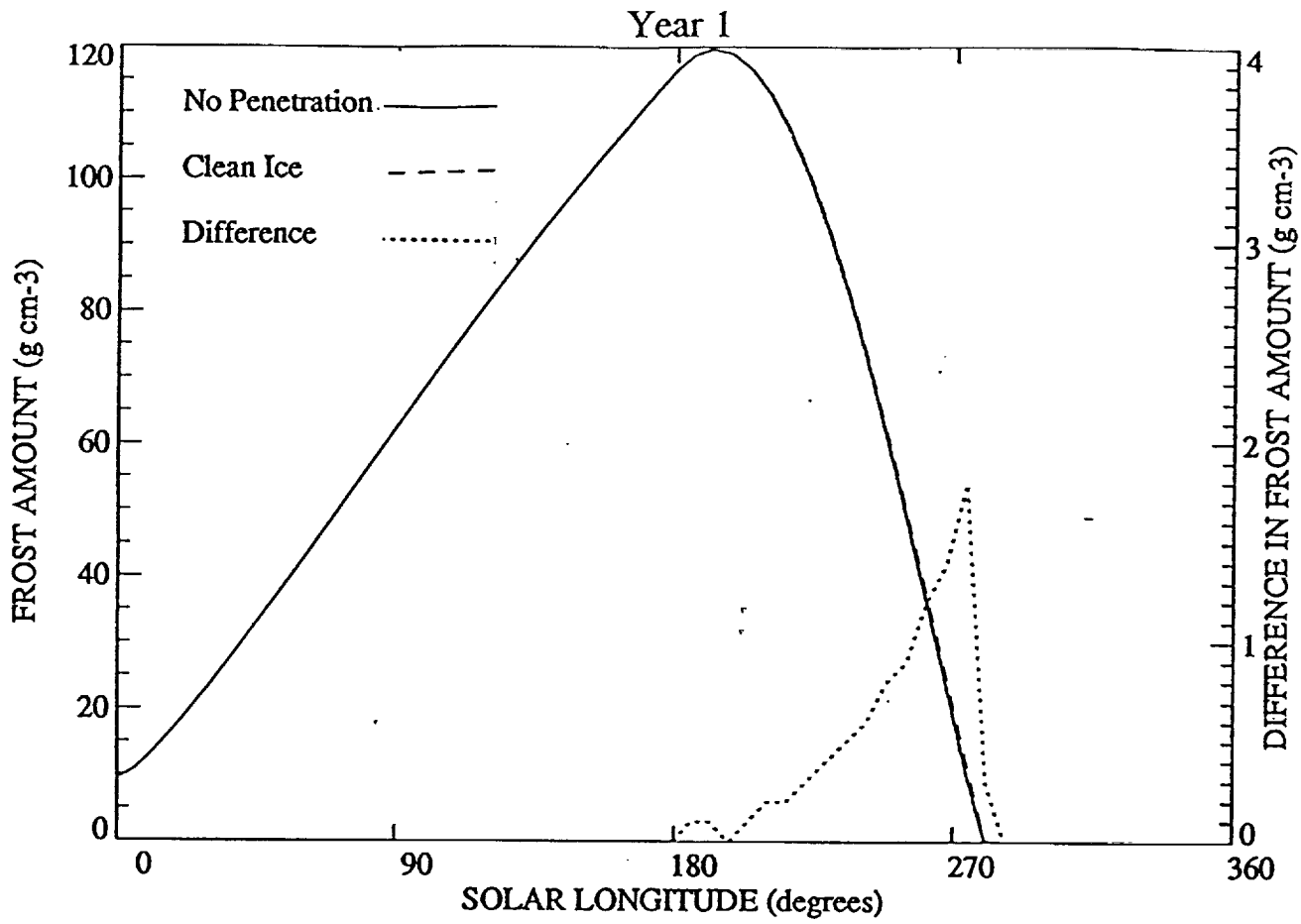

Fig. 10. Frost amount at the south pole versus solar longitude, simulated including the effect of light penetration for "clean" ice, and simulated without penetration. The difference between with and without is also plotted, using the scale on the right side. Results are for the first year of model iteration, starting from an isothermal 154K surface and 10g cm-3 of frost.

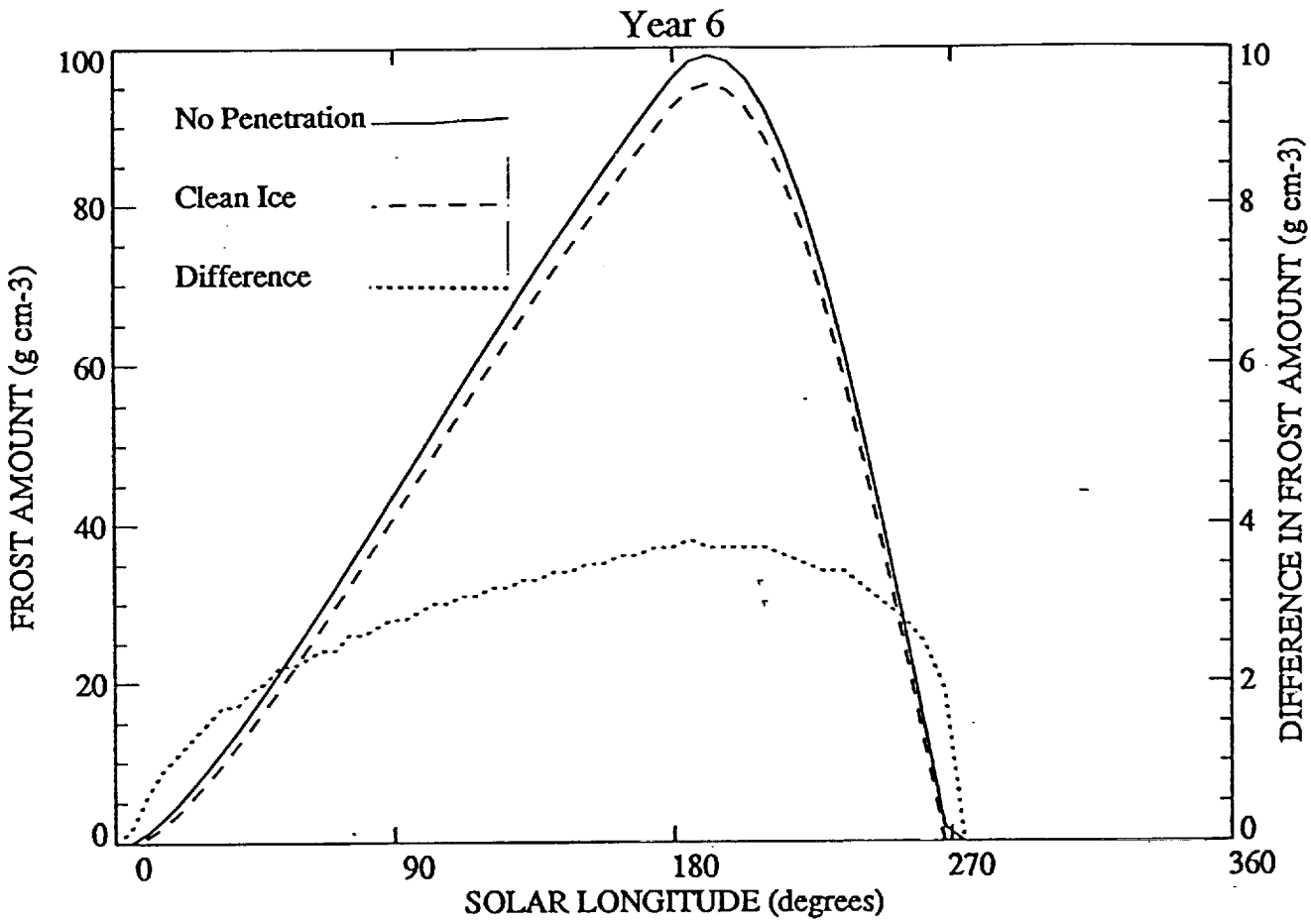

Fig. 11. Frost amount at the south pole versus solar longitude, simulated including the effect of light penetration for "clean" ice, and simulated without penetration. The difference between with and without is also plotted, using the scale on the right side. Results are for the sixth year of model iteration.

compensate completely, and the ice sublimes away earlier for the model which includes penetration.

Figures 12 and 13 show the depth profiles of temperature for the dirty ice case versus the no-penetration model. The differences in temperature exhibit the same behavior as with clean ice, but of a much lower magnitude (as we expected). Figure 14 shows surface temperature as a function of L_S for dirty ice and the original code, again exhibiting the same behavior as for clean ice, but with a smaller magnitude. Figure 15 shows the effect of light penetration on the frost budget for dirty ice, again showing the same behavior as for clean ice, but with a smaller magnitude.

I have checked to make sure that these deviations in temperature are not caused by the modifications to the code. To check that these changes weren't altering the code in its original form, I ran one case where all solar radiation is absorbed in the top mm of ice, rather than distributed over the top meter or so. This case gave the same results as Jakosky's original code, and Kieffer's model.

Obviously, the code had to be run with very thin layers at the surface (a 5 cm surface layer thickness for this case). Thicker layering caused an error, which was determined by comparing to the original Jakosky code. Even a 26 cm top layer caused a 3 sol increase in the number of ice-free days, and a 100 cm top layer caused a 15 sol error. This is obvious, since the layering needs to be on the same scale as the penetration depth.

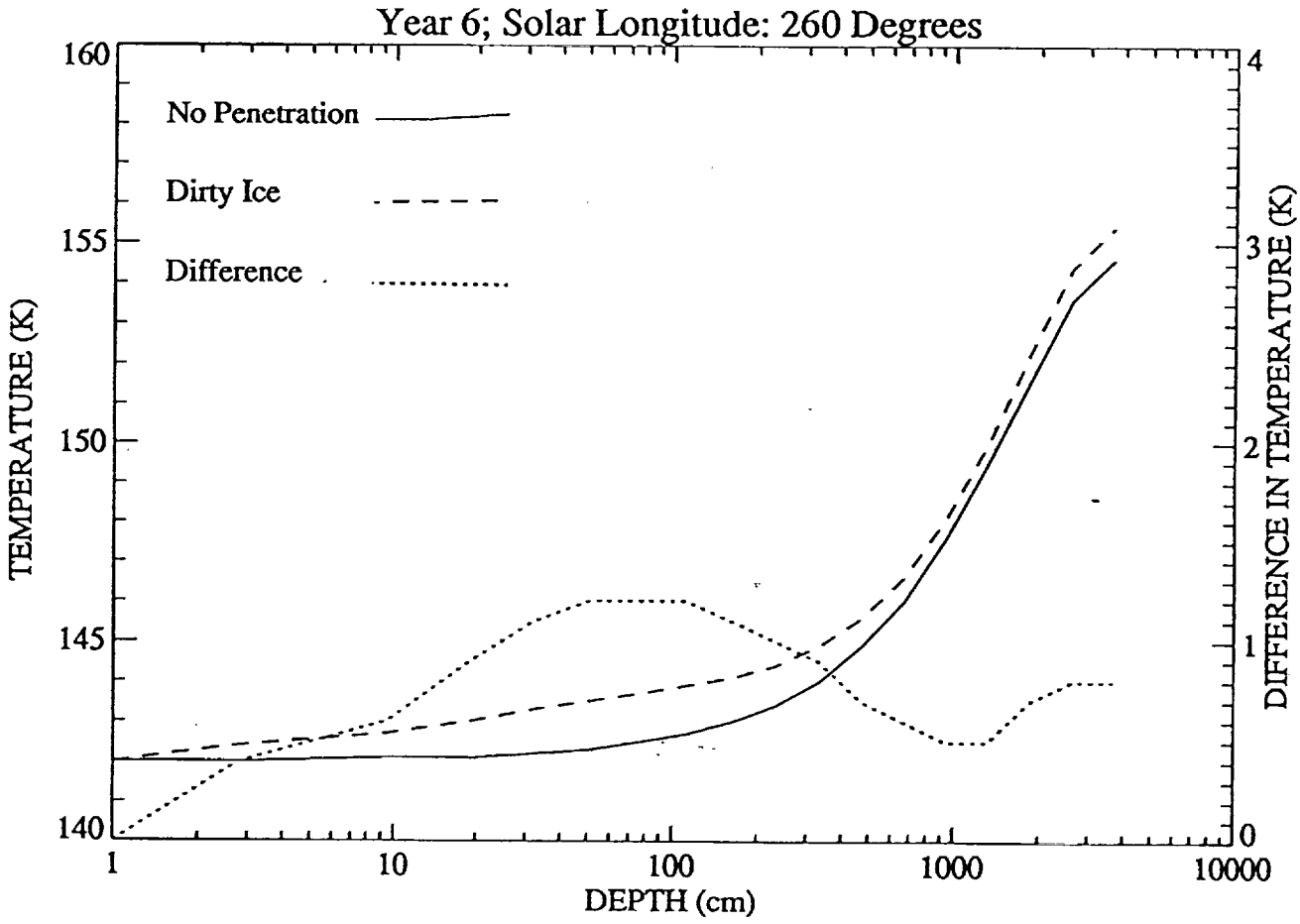

Fig. 12. Temperature versus depth in the south polar cap for L_s of 260 degrees simulated including the effect of light penetration, and simulated without the effect, for "dirty" ice. The difference between with and without is also plotted, using the scale on the right side. Surface values are shown at 1 cm depth.

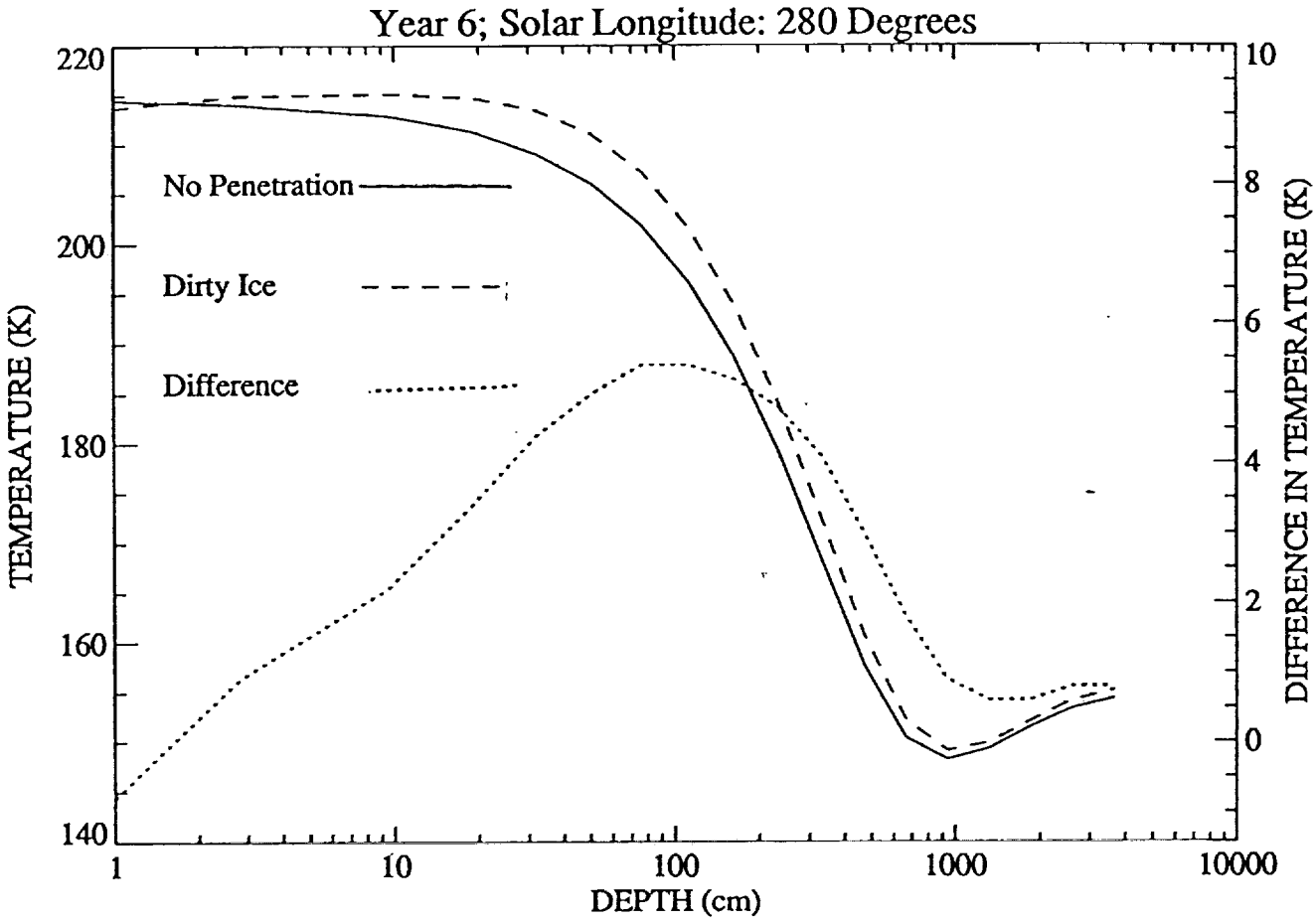

Fig. 13. Temperature versus depth in the south polar cap for L_s of 280 degrees simulated including the effect of light penetration for "dirty" ice, and simulated without penetration. The difference between with and without is also plotted, using the scale on the right side. Surface values are shown at 1 cm depth.

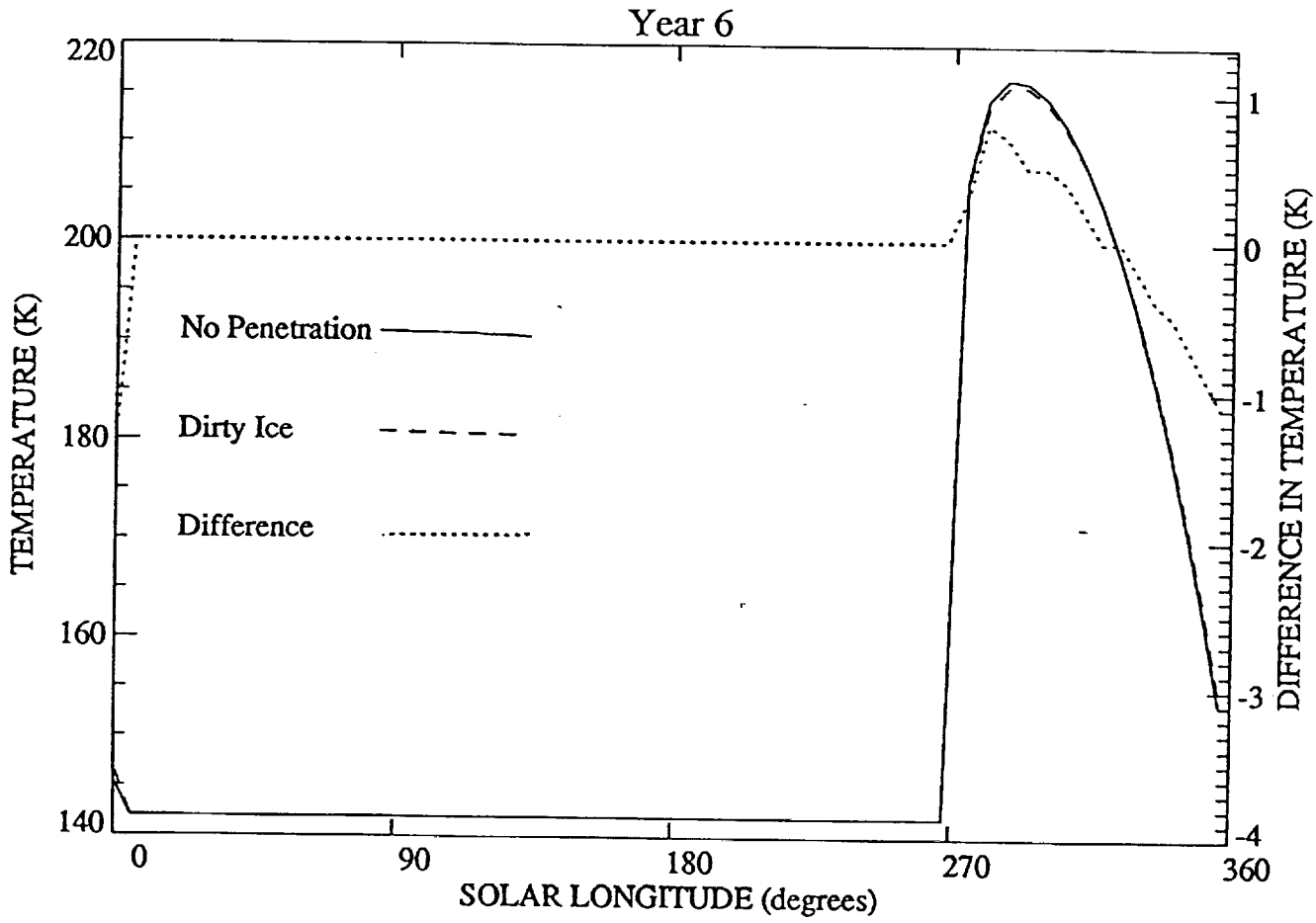

Fig. 14. Surface temperature of the south pole versus solar longitude, simulated including the effect of light penetration for "dirty" ice, and simulated without penetration. The difference between with and without is also plotted, using the scale on the right side.

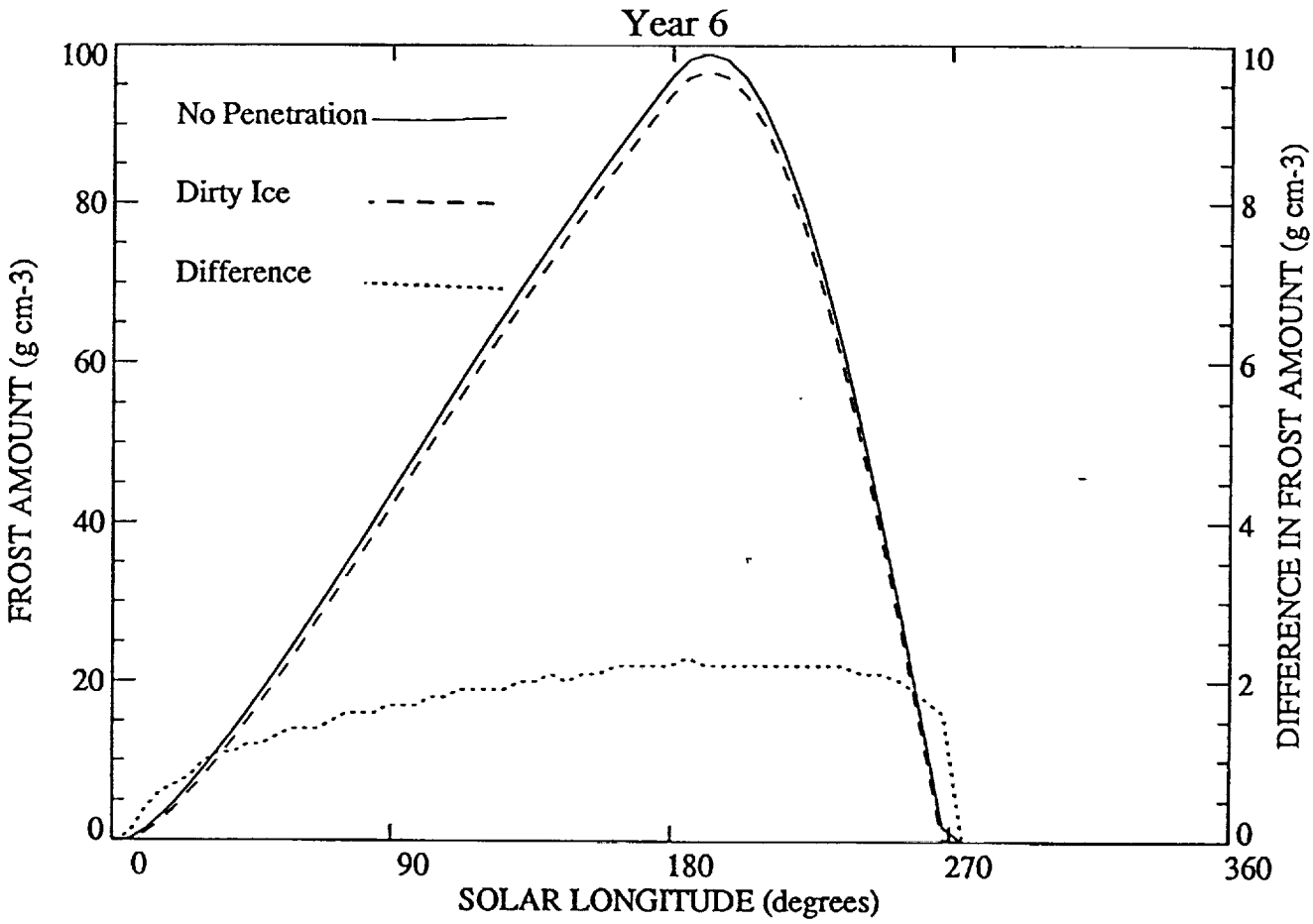

Fig. 15. Frost amount at the south pole versus solar longitude, simulated including the effect of light penetration for "dirty" ice, and simulated without the effect. The difference between with and without is also plotted, using the scale on the right side. Results are for the sixth year of model iteration.

The results do depend on the input parameters (albedo of ice, inertia, albedo of surface, emissivity, etc.). For example, a low thermal inertia (0.01) yields a much hotter subsurface and dramatic reduction in ice-covered sols due to light penetration. Also, the albedo needed to keep ice year-round is ~0.04 higher for frost emissivity of 0.95 versus 1.0 (obviously, since a reduction in emissivity reduces amount of heat lost, and a higher albedo reduces the absorbed solar radiation to maintain balance). The results do not depend strongly on which hemisphere is studied. However, the results do depend on the type of ice (coarse/fine and clean/dirty). A dirty, coarse ice has much less light penetration than a clean, fine ice. But all cases result in fairly small changes, and can be neglected given the uncertainties in other parameters.

I did run one case with soil as the underlying surface. As we had stated earlier, there is no difference between the no-penetration code and a code which allows light to penetrate the seasonal cap and get absorbed in the top mm of soil. Almost all the penetrating radiation returns to sublime the seasonal ice from this depth.

However, this does imply that the seasonal CO_2 frost sublimes away more quickly over the residual cap in the spring than over the neighboring soil, and condenses more slowly over the residual cap in the fall than over the surrounding soil. This might tend to move the residual cap around a bit on a climatic timescale, but would probably be a small effect.

II.5. Solar zenith angle dependence of albedo.

The albedo of ice depends on solar zenith angle (SZA). This SZA dependence has been theoretically predicted for CO_2 frost on Mars by Warren et al. (1990). I assumed that the co-albedo (1-albedo) varied with the SZA dependence given by Warren, no matter what the albedo was. This will give reasonable albedos when near the 0.7 base albedo used in Warren's calculations, but is speculative for albedos far from this value. Fortunately, the values considered here are very close to this value.

As mentioned by Warren et al. (1990), his calculations are for a flat surface. Because of surface roughness on a natural snow surface, the effective zenith angle is usually much less, and rarely over 80° (Warren et al., 1990). I have simply adjusted the SZA to be 10° less than given by orbital mechanics as a simple approximation for surface roughness.

I find that the influence of the sun on ice stability is significantly reduced in spring and fall, when SZA's are large. This significantly lowers the albedo required to maintain ice on the south pole year-round, by about 5%.

II.6. All parameterizations considered together, with the best fit to the data.

The results discussed up to now dealt strictly with ice at 90°N and 90°S latitude. The problem with polar cap models to date has been that they cannot maintain CO_2 ice on the south pole without also maintaining it on the north pole, unless a

hemispherical asymmetry in ice albedo is assumed. Having noted that the effects of clouds and dust can correct this problem (Lindner, 1990), and having seen that the SZA effect on albedo can allow for reasonable albedos to accomplish this, I set out to run the model at all latitudes and seasons to see if the observed data on polar cap regression and atmospheric pressure could be reproduced.

The Lindner (1985) polar cap model was modified to allow for light penetration into the cap, to allow ice albedo to vary with age, latitude, hemisphere, dust content and solar zenith angle, to include the radiative effects of clouds and dust, to allow for diurnal variability, and to include heat transport as represented by a thermal wind, as discussed in the proposal. Ice albedo was chosen to have either the albedo for old ice or new ice, depending upon whether frost was condensing or subliming, with a gradual transition from the albedo of new ice to that of old ice over a period of 10 days. The albedo of old ice was usually assumed to be less than that of new ice, although several cases of brightening of ice with age of the type postulated by Paige (1985) were investigated. Ice albedo also was allowed to vary linearly with distance from the edge of the polar cap, being up to 10% higher if the edge of the polar cap were 50° in latitude away. The transport of dust into the winter polar region is ineffective and there are no sources of dust when the soil is ice-covered. Changes in albedo due to dust content within the ice and hemispherical asymmetries in albedo were allowed to vary at random to obtain the best fit to the data.

The radiative effects of clouds and background dust (i.e. other than during dust storms) as computed by Lindner (1990) were incorporated. The cloud opacity was assumed to be hemispherically asymmetrical, with an opacity of 0.5 in the north and 0.2 in the south, and to vary linearly with the annual cycle in atmospheric surface pressure observed by the Viking Lander. Clouds were assumed to exist only where CO_2 frost existed. The annual cycle in background dust opacity was taken from Pollack et al. (1977). Dust opacity was assumed to vary linearly with distance from the edge of the polar cap, so that it was only half that at the equator if the edge of the polar cap was 50° in latitude away. Both background dust and cloud opacity were also assumed to vary linearly with the changes in airmass due to changes in elevation. The radiative effects of CO_2 vapor were also included (NIR absorption of solar radiation and emission of IR radiation). The scientific basis for all of these approximations were discussed in Lindner (1990) and in the proposal to this contract and will not be repeated here.

Heat transport was simply incorporated by the use of the thermal wind approximation. Future versions of this model will use a full GCM calculation. The thermal wind is based on the temperature difference across the edge of the polar cap, and various efficiencies for heat transport were chosen for model comparisons.

The model was also run with time steps of 1/50 of a day, small enough to account for diurnal variations in solar zenith angle, surface temperature, and frost condensation/sublima-

tion. The model was run for every 2° in latitude to account for latitudinal variation in model parameters. An albedo of 0.45, a thermal inertia of 0.03 cal cm^{-2} $s^{-1/2}$ K^{-1} and a surface density of 0.93 g cm^{-3} were chosen for the residual polar caps (Kieffer, 1990; Jakosky and Haberle, 1990), while values for bare soil of 0.25 for albedo, 0.006 cal cm^{-2} $s^{-1/2}$ K^{-1} for thermal inertia, and 1.5 g cm^{-3} for surface density were chosen for other latitudes. Frost temperature was allowed to vary with atmospheric pressure.

I ran hundreds of combinations and permutations of model parameters. Rather than present hundreds of graphs, charts, etc., allow me to summarize the results and show the best fit to the data. The penetration of light into the polar cap was not deemed to be important, as discussed in section II.4. The division of albedo between old and new ice was also not very important. The fits to the data were not markedly different whether old ice was chosen to be higher or lower than new ice. The dependence of ice albedo on SZA and the radiative effects of clouds and background dust were only important right at the pole itself, and not for the overall polar cap regression or atmospheric pressure, as postulated by Lindner (1990). The radiative effects of global dust storms were not investigated, and could be important. Running the model including diurnal variability versus in a diurnally-averaged mode also made little difference to the fit to the data. The inclusion of heat transport was significant, and therefore warrants the inclusion of more accurate GCM simulations.

Figures 16 through 19 show the regression of the polar caps as predicted by the model versus observations. Agreement is good, particularly in the northern hemisphere. An exact comparision is difficult, considering that the edge of the polar cap is usually patchy and ill-defined, in large part due to terrain. Further, observations of the polar cap are conducted during the daylight. Near the cap edge, ice frequently forms at night and sublimes away completely during the day. Thus, the edge of the polar cap is also diurnally-variable.

Figures 20 and 21 show the comparison of the atmospheric pressure predicted by the model for the elevations of the Viking Landers to the actual observations. The agreement is good, although the annual cycle in pressure predicted by the model is slightly out of phase with the data. This is a problem noted with all runs of the model, no matter what sets of input parameters were used. The model is still ignoring or poorly treating some process which forms ice sooner in the fall, and sublimes it away more quickly in the spring. Some suggestions for what these may be are presented in the section on plans for future work.

Figures 22 and 23 show model predictions for the amount of frost at particular latitudes throughout the year. These values can be converted to a depth of frost by using a density of 0.93 g cm^{-3}. Frost forms as equatorward as 50°S and 54°N latitude with typical maximum depths of a meter. Note that frost forms later and sublimes earlier at lower latitudes. Note also that once ice begins to sublime, it does so rapidly.

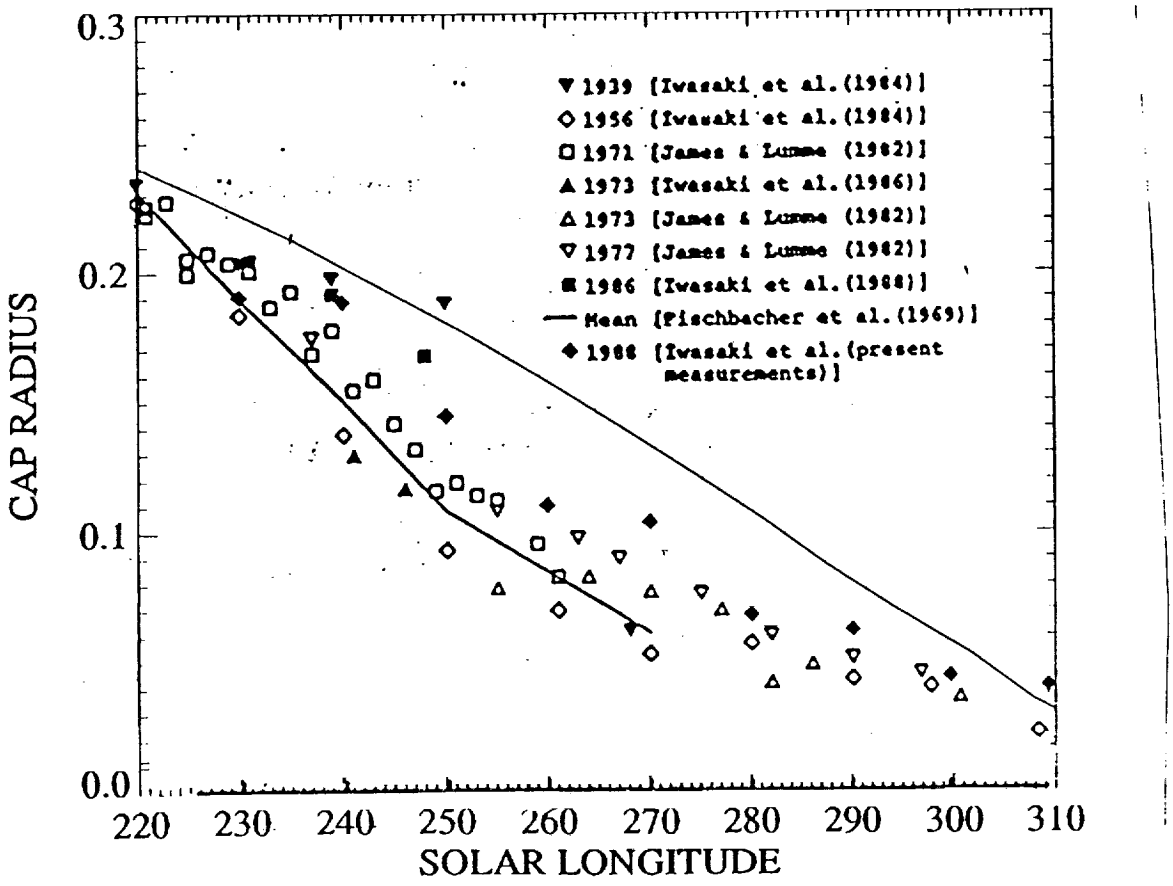

Fig. 16. The regression of the south polar cap, as observed for various years (taken from Iwasaki et al., 1990) and as simulated by our model (thin line), as a function of the aerocentric longitude of the sun (L_s). The cap radius is that whcih would be measured on a polar stereographic projection of the south polar region; the units of the radius are fractions of the planetary radius of Mars.

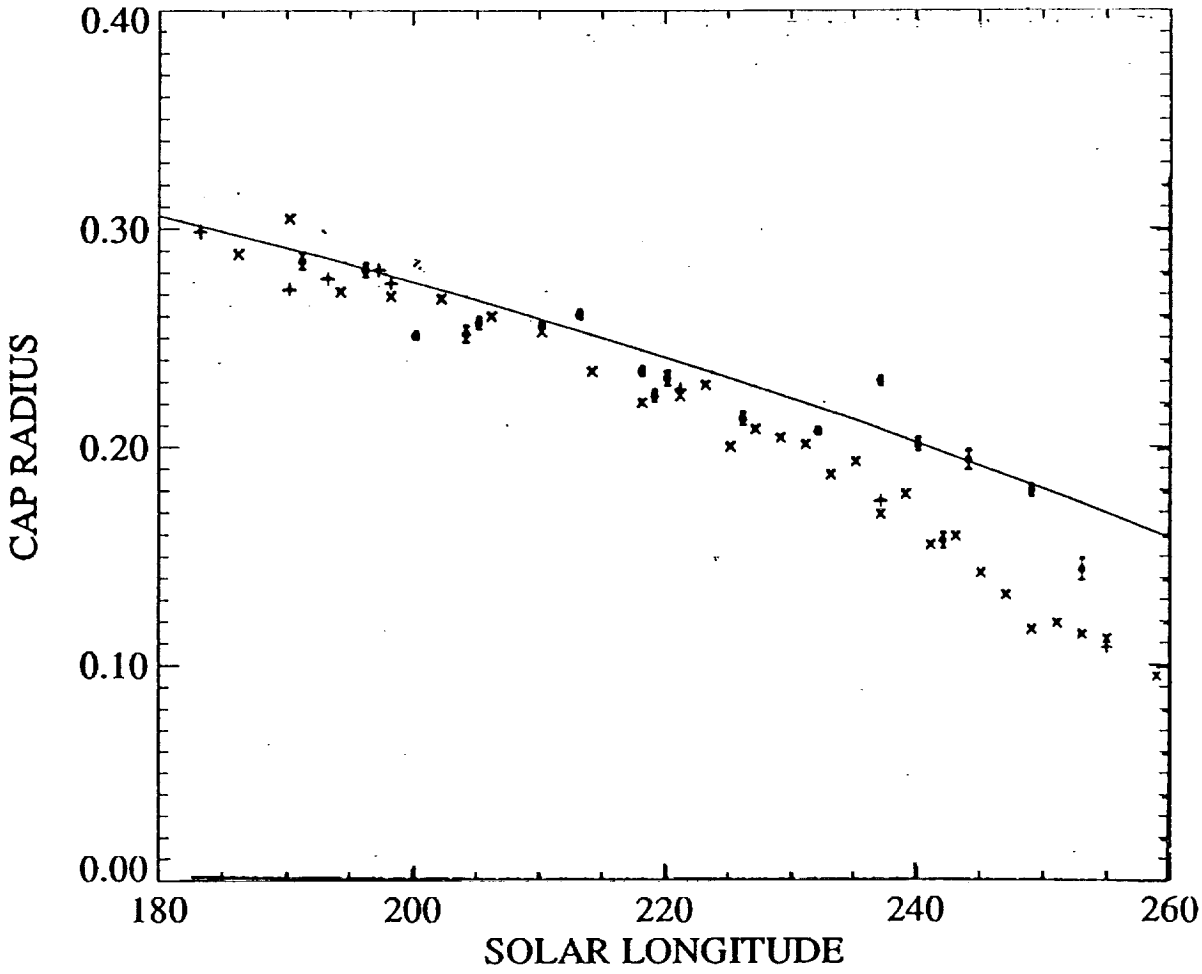

Fig. 17. The regression of the south polar cap, as observed in 1986 (solid circles), 1971 (crosses), and 1977 (plus signs) [taken from James et al., 1990] and as simulated by our model (thin line), as a function of the aerocentric longitude of the sun (L_s). Two-sigma error bars are indicated for the 1986 data; the errors are smaller for the denser 1971 data and for the 1977 Viking data.

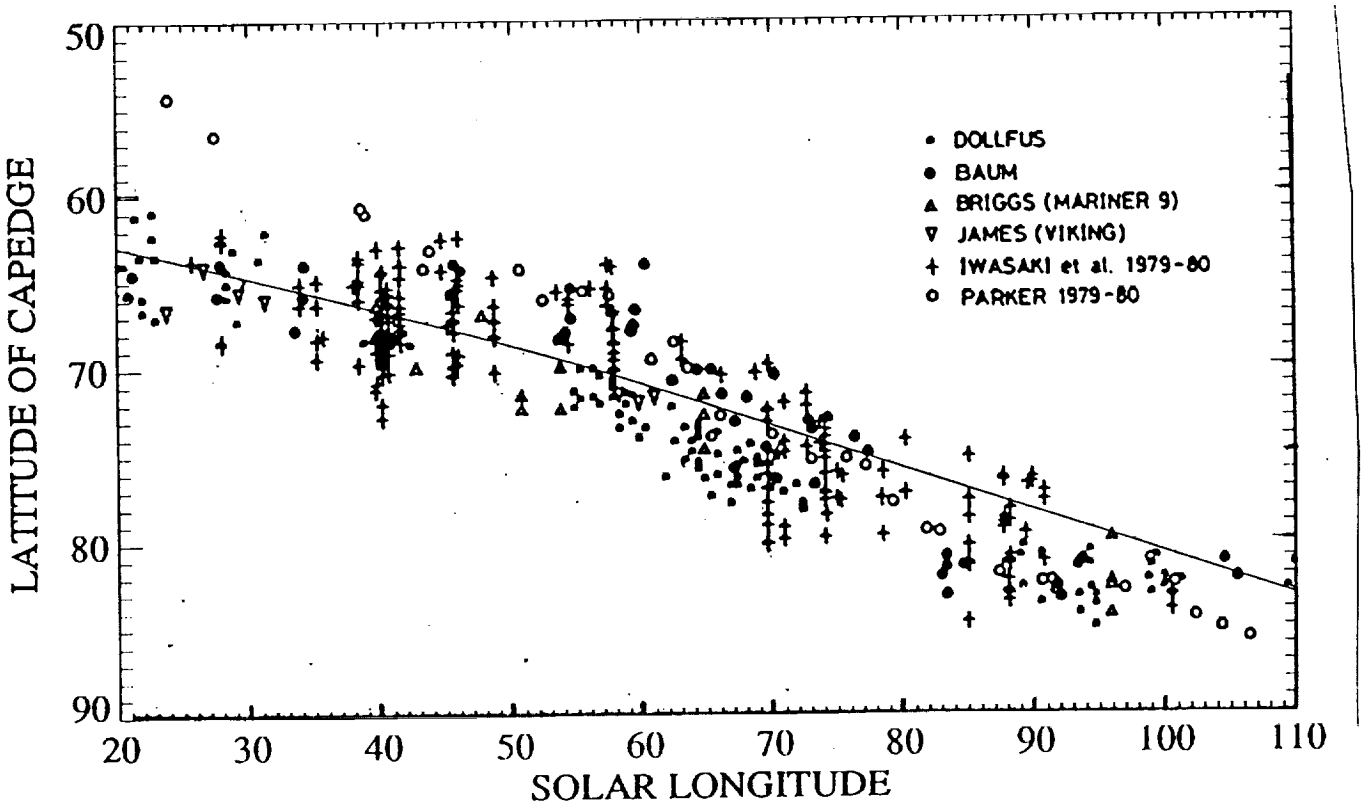

Fig. 18. The regression of the north polar cap, as observed for various years [taken from Iwasaki et al., 1982; symbols refer to Dollfus (1973), Baum (1974), Briggs(1974), James (1979), Capen and Parker (1981), Iwasaki et al. (1982)] and as simulated by our model (thin line), as a function of the aerocentric longitude of the sun (L_s).

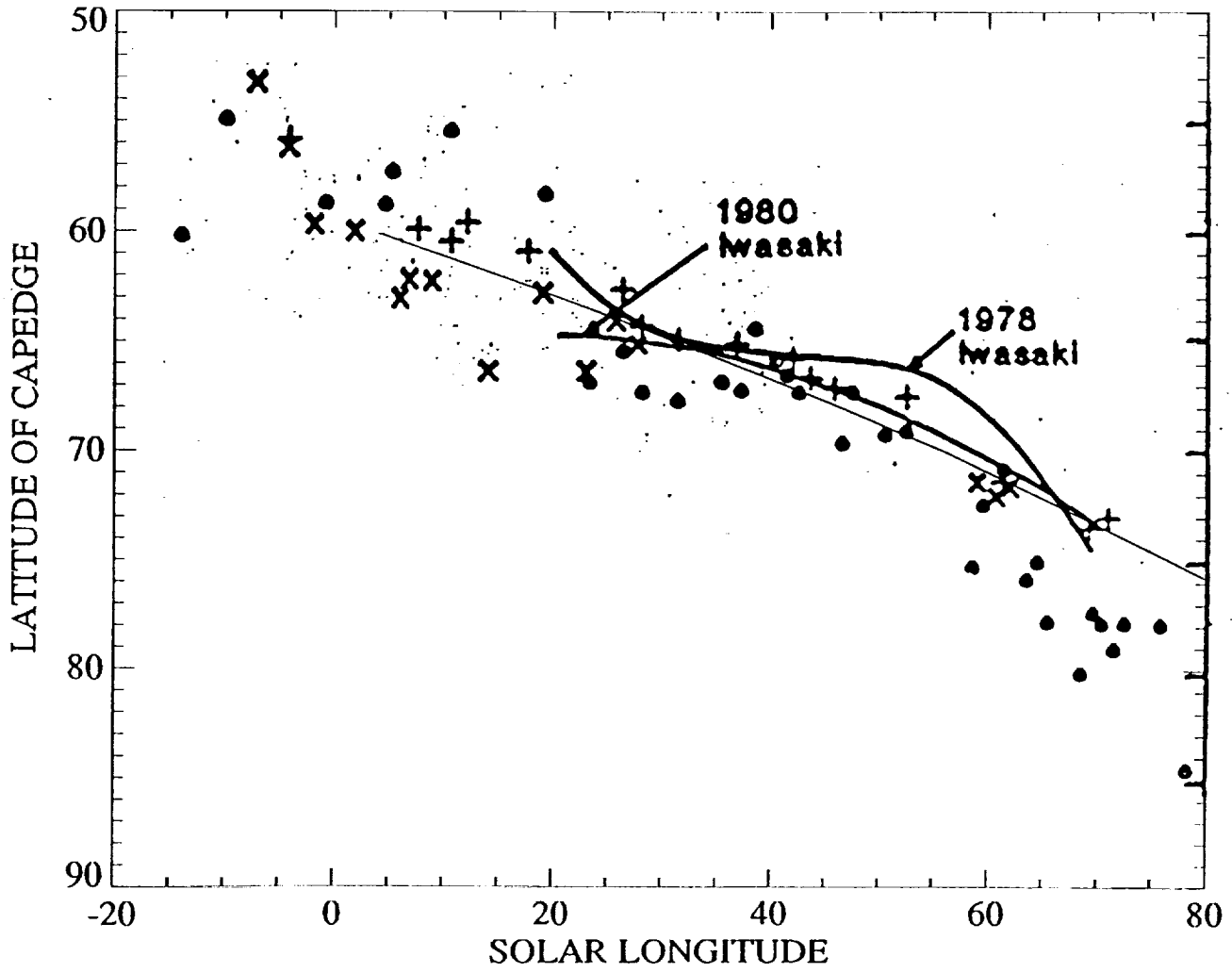

Fig. 19. The regression of the north polar cap, as simulated by our model (thin line) and as observed, as a function of the aerocentric longitude of the sun (L_s). Data are taken from James et al. (1987); also showing data of Iwasaki et al. (1979; 1982). The symbols stand for 1977-1978 and 1980 Viking data (x's and +'s respectively) and ground-based 1975-1980 data (circles).

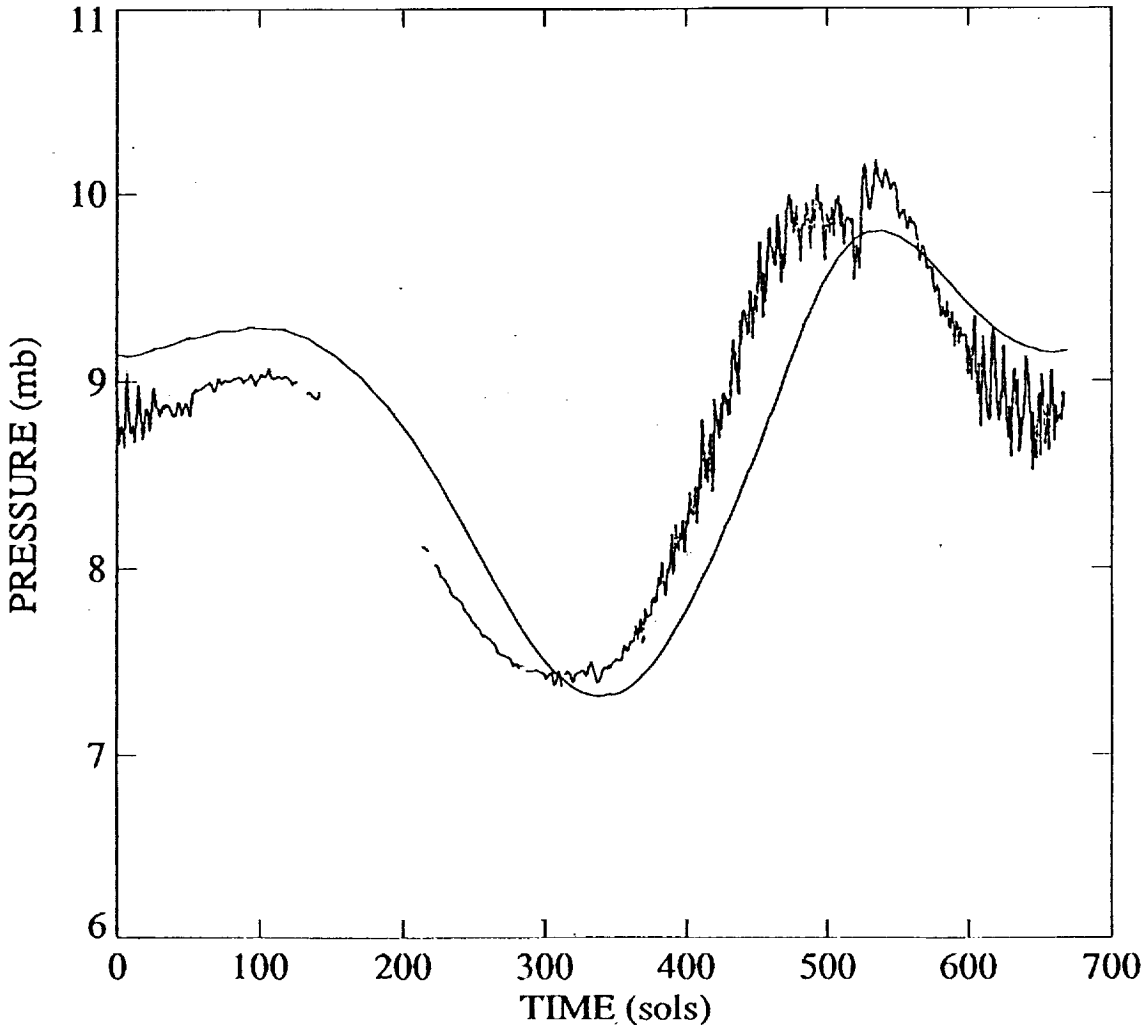

Fig. 20. Daily mean surface pressure at Viking Lander 2, showing observations (line with high-frequency oscillations) and simulations (smooth line) over the course of one martian year starting from the vernal equinox. Observations are taken from Hess et al. (1980), and gaps in the data are due to irretrievably lost data.

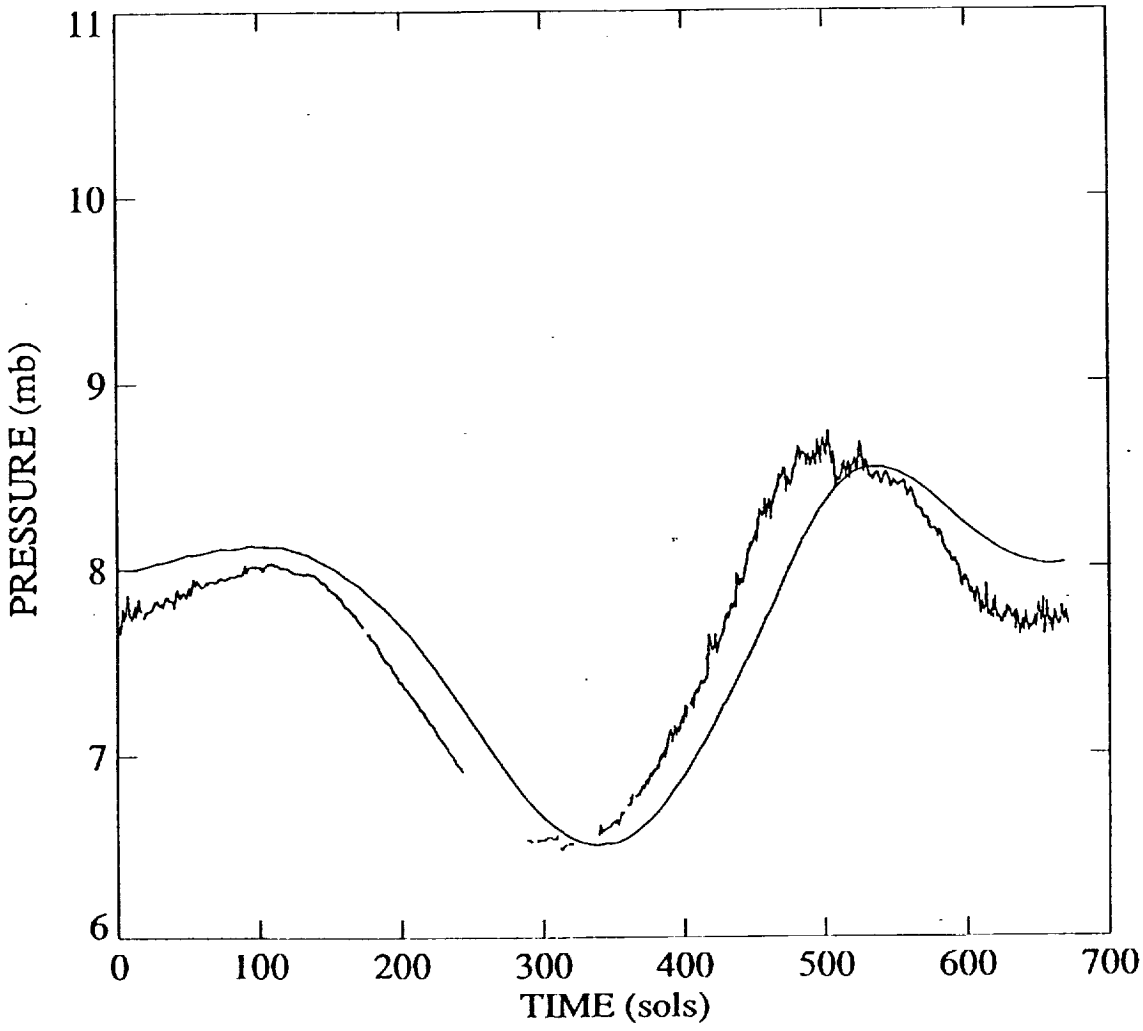

Fig. 21. Daily mean surface pressure at Viking Lander 1, showing observations (line with high-frequency oscillations) and simulations (smooth line) over the course of one martian year starting from the vernal equinox. Observations are taken from Hess et al. (1980), and gaps in the data are due to irretrievably lost data.

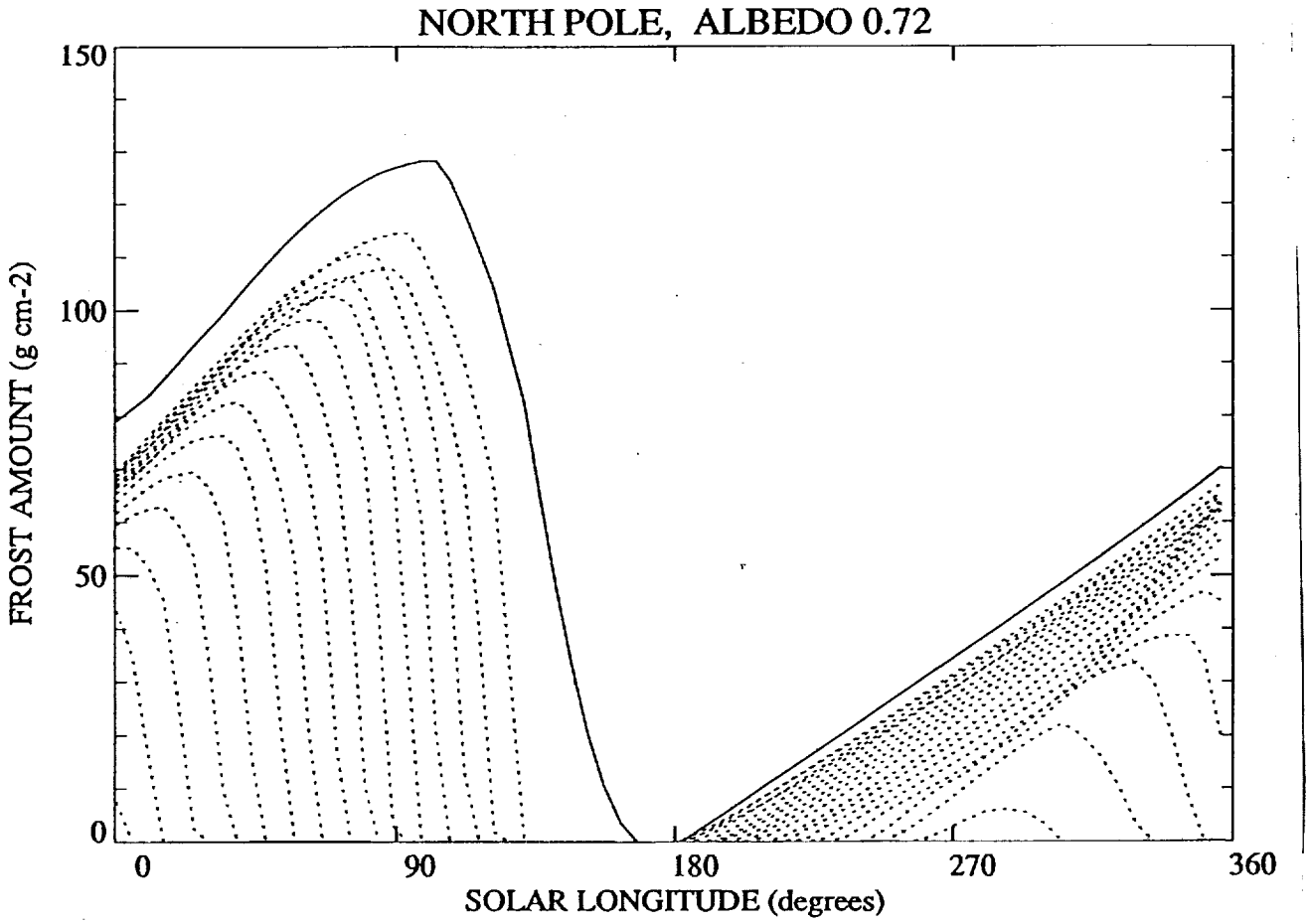

Fig. 22. Mass of CO_2 frost per cm^2 of surface at every 2 degrees of latitude in the northern hemisphere over one martian year starting at vernal equinox. The solid line is 90°N latitude.

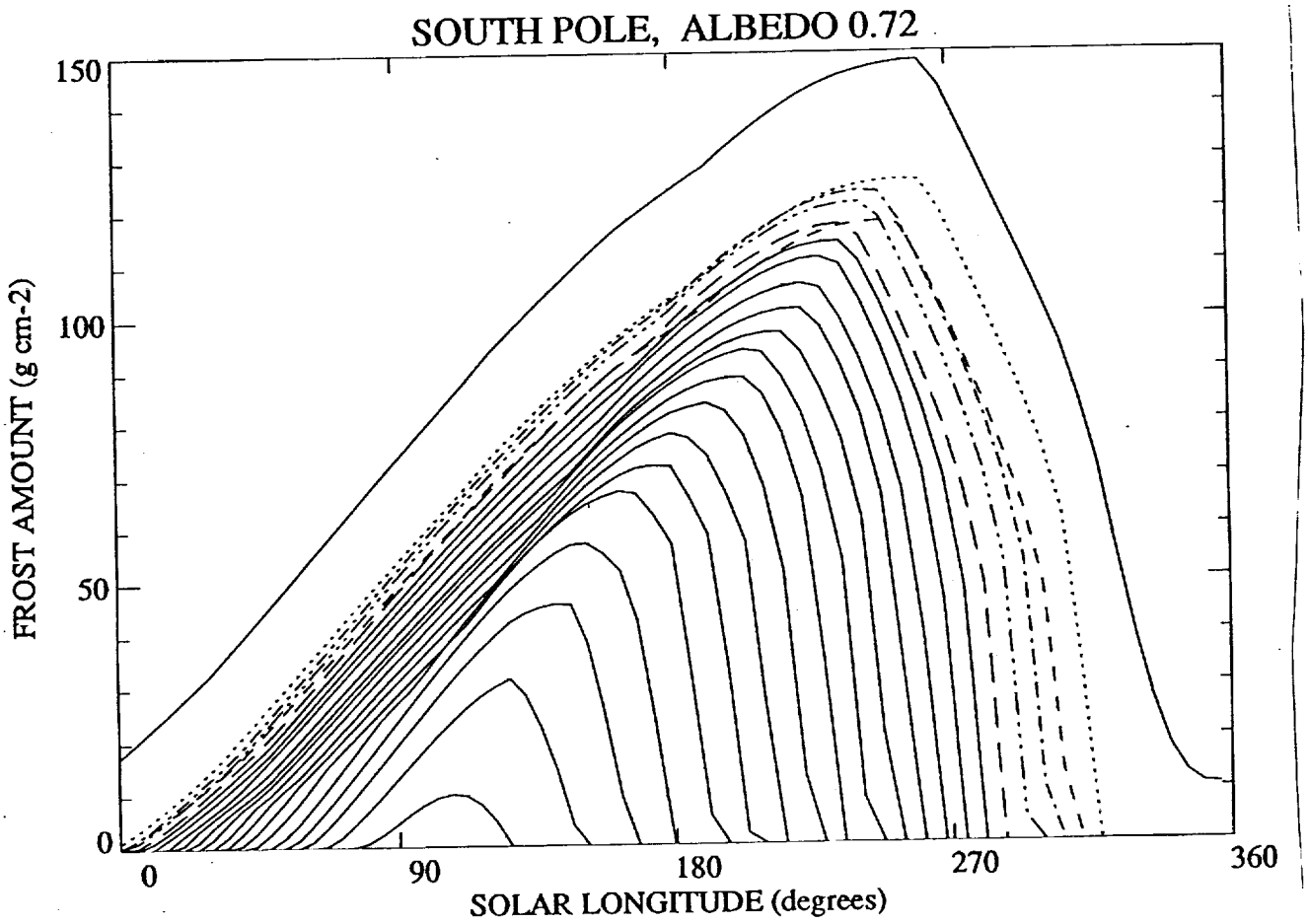

Fig. 23. Mass of CO_2 frost per cm^2 of surface at every 2 degrees of latitude in the southern hemisphere over one martian year starting at vernal equinox. The solid line is 90°S latitude.

II.7. Presentations made at conferences

Several conferences were attended which were supported in whole or in part by this contract. Reprints of papers and abstracts published at these meetings are included in the Appendix.

1989 DPS Conference

Dr. Lindner attended the AAS/DPS conference in Providence in October, 1989, and presented a paper entitled "The Martian Polar Cap: Radiative effects of ozone, clouds, and airborne dust", which discussed the theoretical aspects of this current work. The work was well received, and Dr. Lindner benefitted from discussions with Dr. Jakosky and others at the conference, and from listening to other talks. The abstract was published in the Bulletin of the American Astronomical Society, Volume 21, p. 979 (1989). NASA contract NASW-4444 paid for expenses.

LPS Conference

Dr. Lindner attended the Lunar and Planetary Science Conference in Houston in March, 1990 and presented a paper entitled "Solar and IR radiation near the martian surface: A parameterization for CO_2 transmittance" with T. Ackerman, J. Pollack, O.B. Toon and G.E. Thomas as secondary authors. This paper was published in Lunar and Planetary Science XXI, pp. 696-697. NASA contract NASW-4444 paid for some expenses (mostly just my labor), with the Lunar and Planetary Institute paying the rest of the expenses (airfare, rental car, and some food and

hotel) with a grant from the Mars Surface and Atmosphere Through Time (MSATT) program at NASA.

EGS Conference

Dr. Lindner attended the European Geophysical Society Assembly in Copenhagen, Denmark in April, 1990 and presented a paper entitled "CO_2 transmittance in the Mars atmosphere: An exponential-sum fit for use in multiple-scattering models" with J. Pollack and T. Ackerman as secondary authors. This abstract was published in Annales Geophysicae. NASA contract NASW-4444 paid all expenses.

Atmospheric Radiation Conference

Dr. Lindner attended the seventh conference on atmospheric radiation in San Francisco in July and presented a paper entitled "The effects of polar clouds and dust on the radiative budget of the martian polar cap". This paper was published in the conference proceedings by the American Meteorological Society. A. D.O.D. contract paid all expenses except for the publication and registration costs related to the Mars work as Dr. Lindner was there to present other research as well (Multi-spectral Cloud Property Retrieval by B.L. Lindner and R.G. Isaacs).

Cloud Physics Conference

Dr. Lindner attended the cloud physics conference in San Francisco in July (concurrent with the atmospheric radiation

conference) and presented a paper entitled "Clouds and Chemistry on Mars". This paper was published in the conference proceedings by the American Meteorological Society. A. D.O.D. contract paid all expenses except for the publication and registration costs related to the Mars work.

1990 DPS Conference

Dr. Lindner attended the AAS/DPS conference in Charlottesville, Virginia in October, 1990, and presented a paper entitled "Penetration of Light Into the Martian Polar Cap: Implications for the Energy Budget", which discussed the results presented in section II.4. The abstract was published in the Bulletin of the American Astronomical Society, Volume 22, p. 1060 (1989). NASA contract NASW-4444 paid for expenses.

II.7 Journal Publications

The text of the proposal for this contract was editted and published in the special Mars Polar Processes edition of the Journal of Geophysical Research, Solid Earth and Planets, Volume 95, pages 1367-1379, February 1990. A reprint is included in the Appendix.

A paper by Dr. Lindner entitled " Ozone heating in the martian atmosphere " has been submitted to Icarus. A preprint will be included in the final report.

III. Program of Research for the Next 6 Months

III.1. Research Tasks

Seeing that the primary contract objectives have been satisfied, and that all contract funds have been spent, the next and last 6 months of this contract will be spent preparing the results of this contract for publications and presentations, as outlined below.

III.2. Conferences

Dr. Lindner will attend the International Union of Geodesy and Geophysics Assembly in Vienna, Austria, in August 1991 to present a paper entitled " Mars seasonal CO_2-ice lifetimes and the angular dependence of albedo " in a special Mars climate session. The abstract will appear in the conference proceedings.

Dr. Lindner will also attend the International Symposium on the chemistry and physics of ice, held in Sapporo Japan in Sept. 1991, to present a paper entitled " Why is the north polar cap on Mars different than the south polar cap? " in the extraterrestrial ice session. The abstract will appear in the conference proceedings.

III.3. Publications in Progress

We are in the process of submitting a short paper to Geophysical Research Letters which will present the research presented in sections II.3 and II.4 of this report.

We are also preparing a manuscript to submit to either Nature or Science describing the results of sections II.5 and II.6.

III.4 Proposal to continue this work.

We intend to submit a proposal to NASA to continue this work. We would integrate more accurate simulations of heat transport into our polar-cap model. We would also investigate some processes touched on in the initial proposal to this work which haven't been investigated, such as terrain, snowfall, Warren et al. (1990) predictions of ice emissivity, and the wavelength dependence and bidirectional nature of ice albedo. (As predicted by several peer reviewers who read the proposal for this contract, I did not request sufficient funds for this research).

Publications under this contract

(reprints are in the appendix)

Lindner, B. L., The martian polar cap: Radiative effects of ozone, clouds, and airborne dust (abstract), Bull. Am. Astron. Soc., 21, 979, 1989.

Lindner, B. L., Clouds and chemistry on Mars, in Preprints, conference on cloud physics, pp. 226-227, held in San Francisco, July 23-27, published by Amer. Meteorol. Soc., Boston, 1990a.

Lindner, B. L., The effect of polar clouds and dust on the radiative budget of the martian polar cap, in Preprints, seventh conference on atmospheric radiation, pp. 200-201, held in San Francisco, July 23-27, published by Amer. Meteorol. Soc., Boston, 1990b.

Lindner, B. L., The martian polar cap: Radiative effects of ozone, clouds, and airborne dust, J. Geophys. Res., 95, 1367-1379, 1990c.

Lindner, B. L., The thermal and frost budgets of the martian seasonal polar caps including infiltration of solar radiation, submitted to Geophys. Res. Lett., 1991a.

Lindner, B. L., Ozone heating in the martian atmosphere, submitted to Icarus, 1991b.

Lindner, B. L., Why is the north polar cap on Mars different than the south polar cap?, Proceedings, International Symp. on the Phys. and Chem. of Ice, in Press, 1991c.

Lindner, B. L., Mars seasonal CO_2-ice lifetimes and the angular dependence of albedo, in Proceedings, International Union of Geodesy and Geophys. General Assembly, in Press, 1991d.

Lindner, B. L., The polar caps of Mars, in preparation, 1991e.

Lindner, B. L. and B. M. Jakosky, Penetration of light into the martian polar cap: Implications for the energy budget (abstract), Bull. Am. Astron. Soc., 22, 1060, 1990.

Lindner, B. L., T. P. Ackerman, and J. B. Pollack, An efficient and accurate technique to compute the absorption, emission, and transmission of radiation by the martian atmosphere, in Scientific results of the NASA-sponsored study project on Mars: Evolution of volcanism, tectonics and volatiles, S.C. Solomon, V.L. Sharpton, and J.R. Zimbelman, ed.s, p. 198-200, LPI Tech. Rpt. 90-06, Lunar and Planetary Institute, Houston, 322 pp., 1990c.

Lindner, B. L., T. P. Ackerman, J. B. Pollack, O. B. Toon, and G. E. Thomas, Solar and IR radiation near the martian surface: A parameterization for CO_2 transmittance, In Lunar and Planetary Science XXI, pp. 696-697, Lunar and Planetary Institute, Houston, 1990.

Lindner, B. L., J. B. Pollack, and T. P. Ackerman, CO_2 transmittance in the Mars atmosphere: An exponential-sum fit for use in multiple-scattering models (abstract), Annales Geophysicae, EGS special issue, p. 328, 1990.

Bibliography

Baum, W. A., Results of current Mars studies at the IAU Planetary Research Center, in Exploration of the Planetary System, edited by A. Woszczyk and C. Iwaniszewska, pp. 241-151, D. Reidel, Dordrecht, Netherlands, 1974.

Briggs, G. A., The nature of the residual Martian polar caps, Icarus, 23, 167-191, 1974.

Capen, C. G. and D. C. Parker, What is new on Mars - Martian 1979-1980 appartion report II, J. Assoc. Lunar Planet Observ., Jan. 1981.

Dollfus, A., New optical measurements of planetary diameters, IV. Size of the morth polar cap of Mars, Icarus, 18, 142-155, 1973.

Fischbacher, G.E., L.J. Martin, and W.A. Baum, Martian polar cap boundaries, final report, part A contract 951547 to Jet Propul. Lab., Pasadena, Calif., Planet. Res. Center, Lowell Observ. Flagstaff, Ariz., May 1969.

Hess, S. L., J. A. Ryan, J. E. Tillman, R. M. Henry, and C. B. Leovy, The annual cycle of pressure on Mars measured by Viking landers 1 and 2, Geophys. Res. Lett., 7, 197-200, 1980.

Iwasaki, K. Y. Saito, and T. Akabane, Behavior of the martian north polar cap, 1975-1978, J. Geophys. Res., 84, 8311-8316, 1979.

Iwasaki, K., Y. Saito and T. Akabane, Martian north polar cap 1979-1980, J. Geophys. Res., 87, 10265-10269, 1982.

Iwasaki, K., Y. Saito, and T. Akabane, martian north polar cap and haze 1981-1982, Publ. Astron. Soc. Jpn., 36, 347-356, 1984a.

Iwasaki, K., Y. Saito, and T. Akabane, Interannual difference in the regression of the south polar cap of Mars, Proceeding of the 17th ISAS Lunar and Planetary Symposium, pp. 5-6, Inst. Space and Astronaut. Sci., Tokyo, 1984b.

Iwasaki, K., Y. Saito, and T. Akabane, Interannual differences in the regressions of the polar caps of Mars, Mars: Evolution of its climate and atmosphere, LPI Tech. Rep. 87-01, pp. 57-59, Lunar and Planet. Inst., Houston, Tex., 1986b.

Iwasaki, K., Y. Saito, T. Akabane, Y. Nakai, E. Panjaitan, I. Radiman, and S.D. Wiramiharja, Martian south polar cap 1986, Vistas Astron., 31, 141-146, 1988.

Iwasaki, K., Y. Saito, Y. Nakai, T. Akabane, E. Panjaitan, I. Radiman, and S. Wiramihardja, Martian south polar cap 1988, J. Geophys. Res., 95, 14751-14754, 1990.

Jakosky, B. M., and R. M. Haberle, Year-to-year instability of the Mars south polar cap, J. Geophys. Res., 95, 1990.

James, P.B., Recession of Martian north polar cap: 1977-1978 Viking observations, J. Geophys. Res., 84, 8332-8334, 1979.

James, P. B. and K. Lumme, Martian south polar cap boudary: 1971 and 1973 data, Icarus, 50, 368-380, 1982.

James, P. B., M. Pierce, and L. J. Martin, Martian north polar cap and circumpolar clouds: 1975-1980 telescopic observations, Icarus, 71, 306-312, 1987.

James, P. B., L.J. Martin, J.R. Hensen, and P.V. Birch, Seasonal recession of Mars' south polar cap in 1986, J. Geophys. Res., 95, 1337-1341, 1990.

Kieffer, H. H., Water Grain size and the amount of dust in Mars' Residual north polar cap, J. Geophys. Res., 95, 1481, 1990.

Lindner, B. L., The aeronomy and radiative transfer of the Martian atmosphere, Ph.D. dissertation, 470 pp., Univ. of Colo., Boulder, Aug. 1985.

Lindner, B. L., The martian polar cap: Radiative effects of ozone, clouds, and airborne dust, J. Geophys. Res., 95, 1367-1379, 1990c.

Moore, J. M., Experimental studies of sublimation in ice-particulate mixtures: Applications to Mars, Bull. Amer. Astron. Soc., 20, 847, 1988.

Paige, D. A., The annual heat balance of the Martian polar caps from Viking observations, Ph.D. dissertation, 207 pp., Calif. Inst. of Technol., Pasadena, May 1985.

Pollack, J. B., D. Colburn, R. Kahn, J. Hunter, W. Van Camp, C. E. Carlston, and M. R. Wolf, Properties of aerosols in the Martian atmosphere as inferred from Viking Lander imaging data, J. Geophys. Res., 82, 4479-4496, 1977.

Pollack, J. B., R. M. Haberle, J. Schaeffer, and H. Lee, Simulations of the general circulation of the martian atmosphere. 1. Polar Processes, J. Geophys. Res., 95, 1447, 1990.

Warren, S.G., Wiscombe, W.J., and J.F. FIrestone, Spectral albedo and emissivity of carbon dioxide in martian polar

caps: Model results, J. Geophys. Res., 95, 14717-14741, 1990.

Appendix

Reprints of publications made under this contract

(in the order listed earlier)

[redacted] VISION FOR PLANETARY SCIENCE ABSTRACT FORM

Run.No._____ Sess.No._____
FOR EDITORIAL USE ONLY

The Martian Polar Cap: Radiative Effects of Ozone, Clouds, and Airborne Dust

B.L. Lindner (AER)

The solar and thermal flux striking the polar cap of Mars is computed for various ozone, dust, and cloud abundances and for three solar zenith angles. Ozone does not significantly affect the total energy budget of the polar cap. Hence, the observed hemispherical asymmetry in ozone abundance causes only an insignificant hemispherical asymmetry in the polar caps. Vertical optical depths of dust and cloud ranging from zero to one cause little change in the total flux absorbed by the polar cap near its edge, but increase the absorbed flux significantly as one travels poleward. Hemispherical asymmetries in dust abundance, cloud cover, and surface pressure combine to cause a significant hemispherical asymmetry in the total flux absorbed by the residual polar caps, which helps to explain the dichotomy in the residual polar caps on Mars. Other processes which affect the energy budget of the polar cap are proposed and reviewed, particularly with respect to their interaction with the radiative effects of clouds and dust.

Preferred Mode of Presentation ☐ ORAL ☐ POSTER

PAPER PRESENTED BY _____
(Please Print, Must be First Author)

SPECIAL INSTRUCTIONS:

First Author's Address – Print

Signature of First Author

Signature of Introducing Member, if Author is a Nonmember

Phone _____

Membership Status (First Author):

DPS-AAS Member ☐ Non-Member ☐ Student ☐

Is your abstract newsworthy, and if so would you be willing to assist our publicity staff with additional material or interviews for reporters.

Yes ☐ No ☐ Maybe ☐

Abstracts must conform to the AAS style as described on the back of this form.

The charge for publication of this abstract in the *Bulletin of the American Astronomical Society* will be included in the registration fee for this meeting.

Deadline for receipt of abstract: August 1, 1989.

SUBMIT ABSTRACT TO: **DPS Abstracts**
Publications Office, Stephanie Tindell
Lunar & Planetary Institute
3303 NASA Road One
Houston, TX 77058

Abstract Submitted for the Division for Planetary Sciences, Providence Meeting

Date Submitted_____ Form Version 5/89

FOR EDITORIAL USE ONLY

BAAS VOL_____ NO _____ 198___

CLOUDS AND CHEMISTRY ON MARS

Bernhard Lee Lindner

Atmospheric and Environmental Inc.
Cambridge, MA

1. INTRODUCTION

Martian O_3 shows strong seasonal and latitudinal variation, with a mixing ratio ranging from 2×10^{-3} ppm at equatorial latitudes to a maximum of 0.6ppm over the winter polar atmosphere (Barth et al., 1973). The wealth of data provided by Mariner 9 spawned many theoretical models to understand martian photochemistry. However, the polar hood (a layer of clouds at winter polar latitudes) has been neglected by both observational and theoretical studies of martian aeronomy, even though there have been no studies that have shown whether these effects are indeed negligible. Indeed, the abundance of O_3 within the polar hood is virtually unknown because of the inability of reflectance spectroscopy observations of O_3 to pierce the large optical depths (τ) of aerosols. This study examines the variation in the O_3 abundance on Mars with changes in cloud opacities from a theoretical basis; it also questions the efficacy of reflectance spectroscopy for observing O_3 abundances on Mars.

2. MODEL

The O_3 abundance is obtained by solving the coupled one-dimensional continuity equations for O_x, HO_x, O_3, $O(^3P)$, $O(^1D)$, H, OH, HO_2, and H_2O_2 (discussed in detail in Lindner and Jakosky, 1985; Lindner, 1988). H_2O_2 is allowed to condense. The surface is assumed covered with old ice with a albedo of 0.5. The vertical transport term in the one-dimensional continuity equation uses the eddy diffusion coefficient, K, to describe the processes which mix the atmosphere vertically. Heterogeneous catalytic decomposition of O_3 at the surface is accounted for using the parameterization of Kong and McElroy (1977), modified to account for the lower temperatures and snow cover at the winter poles. The radiative transfer used to calculate the intensity is described in detail elsewhere (Lindner, 1990; Lindner et al., 1990). The discrete ordinate method of Stamnes et al. (1988) is used to treat the scattering and absorption of radiation. The flux is calculated for 57 solar wavelength intervals, including Rayleigh scattering and the absorption and scattering by O_3, CO_2, O_2, H_2O, H_2O_2, HO_2, cloud ice, and dust. Three types of clouds are frequently observed in the polar hood and are selected to test the interaction between O_3 and the polar hood: a low-lying cloud or fog, a cloud layer, and a hazy cloud. The vertical optical depth at the surface (τ_v) used here is unity, which is typical of the polar hood. The single-scattering albedo ice is taken to be unity and the Henyey-Greenstein phase function is used.

3. OZONE AND THE POLAR HOOD

The effect of a hazy cloud on the number densities of O_x family members is shown in Figure 1. H_2O and H_2O_2 are controlled by temperature in the winter polar atmosphere and are not shown. O_3 number densities decrease at all altitudes, primarily because the dominant O_x loss occurs at an altitude of 20km through HO_x, and HO_x actually increases at this altitude. Unlike the other species, O_3 does not experience strong altitude-dependent changes because O_3 is nearly in diffusive equilibrium (O_x is nearly in diffusive equilibrium, and O_3 is the predominant O_x species below 30km). Decreases in O_3 number densities near the surface are nearly balanced by increases in O_3 number densities at high altitudes.

H, OH, HO_2, $O(^1D)$, and $O(^3P)$ number densities all exhibit increases above and within the upper part of the cloud, and decreases in the lower part of the cloud. As H, OH, $O(^3P)$, and $O(^1D)$ all have very short lifetimes, they are more dependent on the local photodissociation rates (J) than are O_3 and HO_2, and exhibit the same altitude dependence as the J's. J's increase as much as 10% above the cloud and within the upper 10km of the cloud because of the increase in the effective solar flux resulting from the scattering by the cloud. J's decrease over 20% in the lower part of the cloud because of a significant reduction in the solar radiation resulting from the scattering to space of the solar flux by the upper portion of the cloud.

Changing the optical depth of the cloud gives results similar to those shown, except that the magnitudes varied slightly. A cloud with $\tau_v = 3$ yields virtually the same results shown, indicating that large clouds (τ_v = 1-3) affect martian aeronomy similarly and irrespective of τ_v. Indeed, O_3 number densities are found to vary by at most a few percent for a cloud of any optical depth, which agrees with Mariner 9 observations (Barth and Dick, 1974).

The most surprising result is that J's are decreased by only 20% near the surface, when one would expect that a cloud with τ_v = 1 should cause far greater reductions in the available solar flux. The explanation lies in the large solar zenith angle. Without a cloud, the solar flux must traverse an effective optical depth of τ_v/μ_o, where τ_v is the vertical optical depth measured from the surface to infinity and μ_o

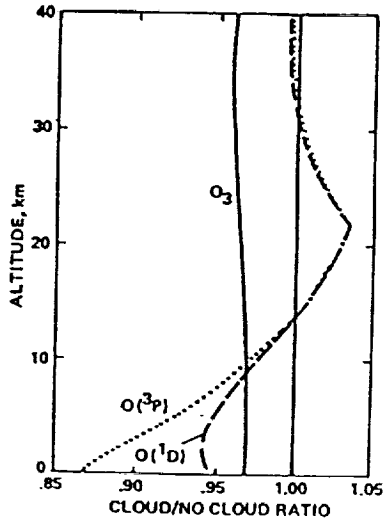

Figure 1. Ratio of the number densities for the hazy cloud case to those of the cloudless case.

is the cosine of the solar zenith angle. In the winter polar regions, μ_o is quite large. If a cloud is in the path of the solar rays, then most rays are scattered in all directions, although with strong forward scattering. Some solar rays are scattered to space and lost. However, a significant percentage of the solar photons are scattered downward at some angle θ which is usually less than the solar zenith angle. As a result, $\tau_v/\cos\theta$ is actually less than the optical depth traversed had the cloud not been there. When solar zenith angles are as large as they are in the winter polar regions, this is an important effect, explaining why the reduction in J's is only 20% when a factor of 2 or so could be expected. This effect is even more dramatic farther poleward where J's are actually larger at the surface when a cloud is present than they would be if no cloud were present.

The overall pattern in number densities with a low-lying cloud or fog is similar to the case of the hazy cloud, only shifted toward the surface. Again, O_3 is reduced 3-4% at all heights. When a cloud layer is present, the J's and number densities develop a discontinuity at the altitude of the cloud layer. All short-lived species also show a small increase near the surface, caused by a similar increase in the J's near the surface. Below the cloud, the effect of the cloud is to increase J's as the surface is approached because the solar flux passes through less atmosphere than it would if it traveled along the solar zenith angle, as explained before. The effect is stronger for the optically thick wavelengths that are important for $J(CO_2)$ and $J(H_2O)$.

Other latitudes and seasons are also examined. In general, O_3 varies only a few percent with the occurrence of clouds, sometimes increasing slightly, sometimes decreasing slightly.

4. DISCUSSION

Figure 2 shows the column abundance of O_3 observed by Mariner 9 in late winter (Barth, 1985). While a general trend in the O_3 abundance with latitude is apparent in Figure 2, significant scatter of data points can be seen, particularly at polar hood latitudes (poleward of 40° latitude). Furthermore, significant variability occurs in the O_3 measurements made over the polar hood, but not in the observations made over the polar cap when no clouds are present (Barth et al., 1973). As demonstrated by the modeling results, the presence of clouds does little to change the O_3 abundance, or even to change the altitude dependence of O_3. Variations in temperature (cold fronts) have been claimed to account for much of the scatter in the data points at any particular latitude, because the water vapor abundance would vary as well (see Barth et al., 1973; Barth and Dick, 1974; Barth, 1985). However, water vapor is a small source of odd hydrogen in the winter polar atmosphere, and may not account for most of the variability in Figure 2.

Masking by clouds may also account for some of the observed O_3 variability, because the nature and opacity of the clouds in the polar hood change dramatically in latitude and even on a day-to-day basis. As the maximum O_3 abundance resides near the surface, spacecraft must be able to observe through the entire cloud in order to actually see the total O_3 column abundance. If reflectance spectroscopy is used, as on Mariner 9, then the cloud and the airborne dust must be traversed twice; first by the incoming solar flux down to the surface, and then once again upon reflection from the surface out to the spacecraft. In addition, the large solar zenith angles at winter polar latitudes mean several times τ_v of the cloud and dust must be traversed. Indeed, part of the observed latitudinal variation in O_3 may be due to the inability of the spacecraft to observe through the increasing effective optical depths (τ_v/μ) as one goes poleward.

This work supported by NASA grant NASW-4444.

5. REFERENCES

Barth, C.A., Photochemistry of the atmosphere of Mars, The Photochemistry of Atmospheres, Earth, the Other Planets, and Comets, (Ed. J. Levine), 476 p., Academic Press, Orlando, Fla, 1985.

Barth, C.A. and Dick, M.L., Ozone and the polar hood of Mars, Icarus, 22, 205-211, 1974.

Barth, C.A., C.W. Hord, A.I. Stewart, A.L. Lane, M.L. Dick, and G.P. Anderson, Mariner 9 ultraviolet experiment: Seasonal variation of ozone on Mars, Science, 179, 795-796, 1973.

Kong, T.Y. and M.B. McElroy, The global distribution of O_3 on Mars, Planet. Space Sci., 25, 839-857, 1977.

Lindner, B.L., Ozone on Mars: The effects of clouds and airborne dust, Planet. Space Sci., 36, 125-144, 1988.

Lindner, B.L., The martian polar cap: Radiative effects of ozone, clouds, and airborne dust, J. Geophys. Res., 95, 1367-1379, 1990.

Lindner, B.L. and B.M. Jakosky, Martian atmospheric photochemistry and composition during periods of low obliquity, J. Geophys. Res., 90, 3435-3440, 1985.

Lindner, B.L., T. Ackerman, J. Pollack, O.B. Toon, and G.E. Thomas, Solar and IR radiation near the martian surface: A parameterization for CO_2 transmittance, In Lunar and Planetary Science XXI, pp. 696-697, Lunar and Planetary Institute, Houston, 1990.

Stamnes, K., S. Tsay, W. Wiscombe, and K. Jayaweera, Numerically stable algorithm for discrete-ordinate-method radiative transfer in multiple scattering and emitting layered media, App. Optics, 27, 2502, 1988.

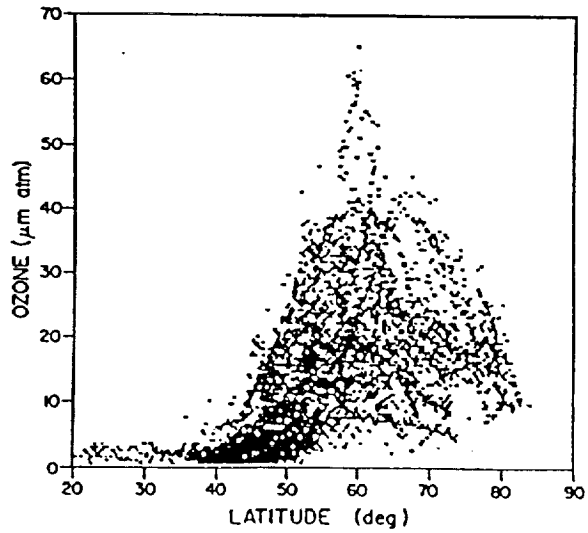

FIG. 2. *Mariner* 9 MEASUREMENTS OF THE O_3 COLUMN ABUNDANCE DURING THE NORTHERN WINTER, L_s = 330–360°, IN THE NORTHERN HEMISPHERE (TAKEN WITH PERMISSION FROM BARTH, 1985).

THE EFFECT OF POLAR CLOUDS AND DUST ON THE RADIATIVE BUDGET OF THE MARTIAN POLAR CAP

Bernhard Lee Lindner

Atmospheric and Environmental Research, Incorporated
Cambridge, Massachusetts.

1. INTRODUCTION

One of the most puzzling mysteries about the planet Mars is the hemispherical asymmetry in the polar caps. Every spring the seasonal polar cap of CO_2 recedes until the end of summer, when only a small part, the residual polar cap, remains. During the year that Viking observed Mars, the residual polar cap was composed of water ice in the northern hemisphere [Kieffer et al., 1976] but was primarily carbon dioxide ice in the southern hemisphere [Kieffer, 1979]. Scientists have sought to explain this asymmetry by modeling Viking lander observations of atmospheric pressure (since the seasonal polar caps are primarily frozen atmosphere, they are directly related to changes in atmospheric mass). These models are hereafter called "polar cap/atmospheric pressure" models because they examine the energy balance at the surface at all latitudes and seasons, thus simulating the condensation and evaporation of CO_2 ice over the winter polar region. They can therefore be compared to observations of atmospheric pressure and polar cap recession, which are reproduced fairly well, except for the asymmetry in the residual polar caps (Leighton and Murray, 1966; Cross, 1971; Briggs, 1974; Davies et al., 1977; James and North, 1982; Lindner, 1985, 1986). This paper will focus on how ozone, clouds, and airborne dust affect CO_2 ice formation and sublimation to see if they help explain the asymmetry in the residual polar caps.

2. MODELING PROCEDURE

The radiative flux striking the surface is calculated for 57 solar and 10 infrared wavelength intervals from 0 to 100 μm including the absorption, scattering, and emission by O_3, CO_2, clouds, and dust (see Lindner, 1990). Ultraviolet absorption by O_2, H_2O, HO_2, and H_2O_2 is also included, as is Rayleigh scattering. The discrete ordinate method of Stamnes et al. (1988) treats the scattering, emission, and absorption of monochromatic radiation. The exponential sum method allows CO_2 transmittance to be incorporated in a scattering model [see Lindner et al., 1990]. The albedo for the polar cap is 0.5 at solar wavelengths [Kieffer, 1979; James and Lumme, 1982]. The IR albedo of the polar cap is assumed to be zero [Kieffer, 1970; Smythe, 1975; Wiscombe and Warren, 1980]. Three latitude cases were studied: 57°N, 70°N, and 90°N, and late winter conditions were assumed (L_s = 343°). These three cases effectively simulate the edge of the polar cap, the edge of polar night, and polar night, respectively, for all solar longitudes and both polar caps. The temperature profile at 57°N latitude rises linearly with altitude from 150 K at the surface to 170 K at 6 km altitude and then falls to 130 K at 40 km [Lindal et al., 1979]. The temperature profile at 70°N had a peak temperature of 155 K at 6 km, and polar night temperatures fell linearly from 150 K at the surface to 130 K at 40 km. The value used for albedo and temperature had little effect on our conclusions.

3. THE EFFECT OF CLOUDS AND DUST

Sublimation depends on the total flux that is absorbed, which is a function of the cap albedo. Weighting the fluxes we calculate with the coalbedo results in the absorbed flux, as shown in Table 1. Almost no change in the absorbed flux occurs over the range that dust and cloud optical depth experiences in the atmosphere, a result also found by Davies [1979] and Paige [1985]. The increase in the infrared flux due to thermal emission by dust balances the decrease in the solar flux due to dust absorption.

It is at the polar night latitudes that the radiative effects of clouds and background dust are most significant, as shown in Table 2. IR fluxes absorbed by the polar cap increase up to an order of magnitude as the cloud opacity and dust opacity increase. Even simply a cloud optical depth of 0.5 and dust optical depth of 0.2 would result in the sublimation of the order of 40 cm of CO_2 ice over 1 martian year. When inserted in a model, this would accelerate the predicted loss of all the CO_2 ice on the northern

TABLE 1. Flux Absorbed by the Polar Cap Near Its Edge for Various Cloud and Dust Opacities (57°N Latitude, L_s = 343°)

	Dust Opacity			
Cloud Opacity	0.0	0.2	0.5	1.0
0.0	348.2	340.9	333.0	326.7
0.2	339.8	336.5	333.6	330.1
0.5	333.1	334.7	334.1	332.6
1.0	329.8	333.5	338.2	339.2

The vertical optical depth is given. Flux values are given in units of J cm^{-2} day^{-1}.

TABLE 2. Flux Absorbed by the Polar Cap in Polar Night for Various Cloud and Dust Opacities (90°N Latitude, L_s = 343°)

	Dust Opacity		
Cloud Opacity	0.0	0.2	0.5
0.0	14.7	43.7	74.8
0.2	36.5	60.9	88.7
0.5	60.9	81.7	105.9
1.0	90.3	107.9	128.4
3.0	152.4	164.7	178.1

The vertical optical depth is given. Flux values are given in units of J cm^{-2} day^{-1}.

polar cap by approximately 40 sols (based on ice depth vs. season from Leighton and Murray [1966], Cross [1971], Briggs [1974], Davies et al [1977], Lindner [1985], and Jakosky and Haberle [1990]).

While polar cap/atmospheric pressure models have been unable to explain the dichotomy of the residual polar caps, these models have been fairly successful at reproducing observations of atmospheric pressure and polar cap recession up to 75° or 80° latitude. The radiative effects of clouds and background dust have the added benefit of not significantly affecting model predictions of the annual variation in atmospheric pressure. Clouds and background dust have a neutral effect along the cap edge, becoming more important as one approaches the pole, particularly within 80° latitude. The integral of seasonal CO_2 ice over the 80°S to 90°S latitude band (where the residual polar cap exists) is an order of magnitude less than the integral of seasonal CO_2 ice over the planet. Hence, a process which affects primarily the residual polar cap area will not significantly affect predictions of atmospheric pressure. Also, the rate of recession of the seasonal polar cap would remain essentially the same as that predicted by polar cap/atmospheric pressure models equatorward of 75° latitude, where good agreement with observations was previously obtained. The behavior near the pole would be significantly modified, making for better agreement with observations than previously obtained. The rate of recession of the polar cap is an important test, especially since it repeats reliably over several years of observation [James and Lumme, 1982; James, 1982].

4. IMPLICATIONS FOR THE POLAR CAP ASYMMETRY

The radiative effects of clouds and background dust would be most noticeable near the residual polar cap, which spends all of the winter in polar night. Observational evidence suggests a greater abundance of clouds over the northern polar cap than over the southern polar cap. Moreover, it is also expected that the formation and sublimation phases of the seasonal southern polar cap will occur with higher background dust opacities than the formation and sublimation phases of the seasonal northern polar cap. Both of these asymmetries would preferentially increase the fluxes absorbed by the residual polar cap in the north.

Furthermore, the surface pressure is lower over the southern residual polar cap than the northern residual polar cap. If mixing ratios of cloud and dust are assumed to be the same for both poles, then the pressure differential between the poles would result in a dust and cloud opacity over the residual polar cap in the south that is 30% less than over the north during the crucial winter months. Mixing ratios of dust may actually be lower over the southern polar cap during winter months because the mechanisms for raising and maintaining atmospheric dust are pressure dependent [Pollack and Toon, 1982]. Lower mixing ratios over the southern pole would accentuate the asymmetry in cloud and dust opacity. These hemispherical asymmetries would allow relatively less frost to accumulate in the north during the fall and winter and cause the CO_2 surface ice to sublimate more rapidly in the north during the following spring and summer.

However, the effects of clouds and background dust would not allow CO_2 ice to survive year-round in the south, as is observed. Other processes which might allow that include penetration of radiation into and through the ice, bidirectional surface reflectance, ice albedo dependence on solar zenith angle, season, and latitude [Wiscombe and Warren, 1980; Squyres and Veverka, 1982; Paige 1985], lower ice emissivity (S. Warren, personal communication, 1988), decreased heat conduction from the surface due to existing ice [Jakosky and Haberle, 1990], snowfall [Pollack and Haberle, 1988], surface residues [Saunders et al., 1986], surface roughness, and wind shifting of ice [Briggs, 1974; James et al., 1979; Kieffer, 1979]. The importance of each of these processes is currently being assessed by B.L. Lindner and B.M. Jakosky. Most of these processes would lengthen CO_2 ice survivability either by increasing condensation or decreasing sublimation of CO_2 ice and would counter the increased sublimation caused by clouds and dust. However, most of these processes work equally effectively at both poles and do not generate an asymmetry. Hemispherical asymmetries in cloud and dust opacity and in surface elevation would result in a hemispherical asymmetry in the net radiative flux from clouds and dust which is absorbed by the polar cap, helping explain the asymmetry in the polar caps.

This work paid by NASA contract NASW-4444.

5. REFERENCES

Briggs, G.A., Icarus, 23, 167, 1974.
Cross, C.A., Icarus, 15, 110, 1971.
Davies, D.W., J. Geophys. Res., 84, 8289, 1979.
Davies, D.W., C.B. Farmer, and D.D. LaPorte, J. Geophys. Res., 82, 3815, 1977.
Hess, S., J. Ryan, J. Tillman, R. Henry, and C. Leovy, Geophys. Res. Lett., 7, 197, 1980.
Jakosky, B. and R. Haberle, J. Geophys. Res., 95, 1990.
James, P.B., Icarus, 52, 565, 1982.
James, P.B. and K. Lumme, Icarus, 50, 368, 1982.
James, P.B. and G.R. North, J. Geophys. Res., 87, 10,271, 1982.
Kieffer, H., J. Geophys. Res., 75, 501, 1970.
Kieffer, H.H., J. Geophys. Res., 84, 8263, 1979.
Kieffer, H., S. Chase, Jr., T. Martin, E. Miner, and F. Palluconi, Science, 194, 1341, 1976.
Leighton, R and B Murray, Science,153, 136, 1966.
Lindal, G et al, J. Geophys. Res., 84,8443, 1979.
Lindner, B.L., Ph.D. dissertation, 470 pp., Univ. of Colo., Boulder, Aug. 1985.
Lindner, B.L., Eos Trans. AGU, 67, 1078, 1986.
Lindner, B.L., J. Geophys. Res., 95, 1367, 1990.
Lindner, B.L., and G.E. Thomas, Bull. Am. Astron. Soc., 15, 849, 1983.
Lindner, B.L., T. Ackerman, J. Pollack, O.B. Toon, and G.E. Thomas, In Lunar and Planetary Science XXI, p. 696, LPI, Houston, 1990.
Paige, D.A., Ph.D. dissertation, 207 pp., Calif. Inst. of Technol., Pasadena, May 1985.
Pollack. J.B., and R.M. Haberle, Bull. Am. Astron. Soc., 20, 859, 1988.
Pollack, J., and B. Toon, Icarus, 50, 259, 1982.
Saunders, R., F. Fanale, T. Parker, J. Stephens, and S. Sutton, Icarus, 66, 94, 1986.
Smythe, W.D., Icarus, 24, 421, 1975.
Squyres, S, and J Veverka, Icarus, 50, 115, 1982
Stamnes, K., S. Tsay, W. Wiscombe, and K. Jayaweera, App. Optics, 27, 2502, 1988.
Wiscombe, W.J., and S.G. Warren, J. Atmos. Sci., 37, 2712, 1980.

JOURNAL OF GEOPHYSICAL RESEARCH, VOL. 95, NO. B2, PAGES 1367-1379, FEBRUARY 10, 1990

THE MARTIAN POLAR CAP: RADIATIVE EFFECTS OF OZONE, CLOUDS, AND AIRBORNE DUST

Bernhard Lee Lindner

Atmospheric and Environmental Research, Incorporated, Cambridge, Massachusetts

Abstract. The solar and thermal flux striking the polar cap of Mars is computed for various ozone, dust, and cloud abundances and for three solar zenith angles. Ozone does not significantly affect the total energy budget of the polar cap. Hence the observed hemispherical asymmetry in ozone abundance causes only an insignificant hemispherical asymmetry in the polar caps. Vertical optical depths of dust and cloud ranging from zero to 1 cause little change in the total flux absorbed by the polar cap near its edge but increase the absorbed flux significantly as one travels poleward. Hemispherical asymmetries in dust abundance, cloud cover, and surface pressure combine to cause a significant hemispherical asymmetry in the total flux absorbed by the residual polar caps, which helps to explain the dichotomy in the residual polar caps on Mars. Other processes which affect the energy budget of the polar cap are proposed and reviewed, particularly with respect to their interaction with the radiative effects of clouds and dust.

Introduction

One of the most puzzling mysteries about the planet Mars is the hemispherical asymmetry in the polar caps. Every spring the seasonal polar cap of CO_2 recedes until the end of summer, when only a small part, the residual polar cap, remains. During the year that Viking observed Mars, the residual polar cap was composed of water ice in the northern hemisphere [Kieffer et al., 1976] but was primarily carbon dioxide ice in the southern hemisphere [Kieffer, 1979]. Scientists have sought to explain this asymmetry by modeling Viking lander observations of atmospheric pressure (since the seasonal polar caps are primarily frozen atmosphere, they are directly related to changes in atmospheric mass). These models are hereafter called "polar cap/atmospheric pressure" models because they examine the energy balance at the surface at all latitudes and seasons, thus simulating the condensation and evaporation of CO_2 ice over the winter polar region, and can therefore be compared to observations of atmospheric pressure and polar cap recession [Leighton and Murray, 1966; Cross, 1971; Briggs, 1974; Davies et al., 1977; James and North, 1982; Lindner, 1985, 1986]. Polar cap/atmospheric pressure models reproduce most aspects of the observed annual variation in atmospheric pressure fairly accurately. Furthermore, the predicted recession of the northern polar cap in the spring agrees well with observations, including the fact that the CO_2 ice is predicted to completely sublime away. However, these models all predict that the carbon dioxide ice will also sublime away during the summer in the southern hemisphere, as shown in Figure 1. This paper will focus on how ozone, clouds, and airborne dust affect CO_2 ice formation and sublimation to see if they help explain the hemispherical asymmetry in the residual polar caps.

Paper number 89JB01426.
0148-0227/90/89JB-01426$05.00

Observations of Ozone, Clouds, and Airborne Dust

Ozone has been observed on Mars by Mariner 6 and Mariner 7 [Barth and Hord, 1971; Lane et al., 1973], by Mariner 9 [Barth et al., 1973; Lane et al., 1973; Barth and Dick, 1974], by MARS 5 [Krasnopol'skii et al., 1975], and by Earth-based experiments [Broadfoot and Wallace, 1970; Noxon et al., 1976; Traub et al., 1979]. Global-average ozone abundances integrated from the surface to space are of the order of 1 μm atm (1 micron atmosphere = 1 μm atm = 2.69×10^{15} cm^{-2}). Ozone experiences strong latitudinal variation, increasing significantly over the winter polar regions. In the northern hemisphere, the maximum abundance of ozone observed was 60 μm atm near 60°N latitude in late winter, while the maximum abundance observed in the southern hemisphere was 30 μm atm. This hemispherical asymmetry in ozone is reproduced by theoretical modeling [Kong and McElroy, 1977; Shimazaki and Shimizu, 1979; Lindner, 1985]. There is also strong day-to-day variability in ozone, which arises from the variability in temperature and in the polar hood [Barth and Dick, 1974; Lindner, 1988].

The polar hood, a blanket of clouds which covers the winter polar region, has been observed on a latitudinal and seasonal basis by Mariner 9, MARS 3, and Viking [Leovy et al., 1972; Masursky et al., 1972; Briggs and Leovy, 1974; Martin, 1975; Moroz, 1976; Briggs et al., 1977; Anderson and Leovy, 1978; Tillman et al., 1979; Kondrat'ev and Hunt, 1982; Kahn, 1984; Christensen and Zurek, 1984]. The following synopsis is extracted from these papers. The polar hood is first observed at high latitudes in the northern hemisphere at about the time of autumnal equinox, gradually spreading to obscure the surface to latitudes as low as 40°, and then retreating to the pole in the spring. The disappearance of the hood occurs at about the vernal equinox. At lower latitudes, the polar hood has strong daily variation and highly variable and often complex vertical structure and is diffuse on scales of less than 1 km [Briggs and Leovy, 1974]. The main bulk of the polar hood is below 20 km altitude. The thickness at one point is estimated at 1-2 km, centered at 15 km height, with an average mixing ratio of ice of the order of 10^{15} g cm^{-2}. The hood is often a wave cloud pattern at lower latitudes, and clouds 10 km high with half an optical depth can appear at the hood's edge. Equatorward of 60° latitude in winter the composition of the clouds may be primarily water ice. Poleward of that, the hood is more diffuse,

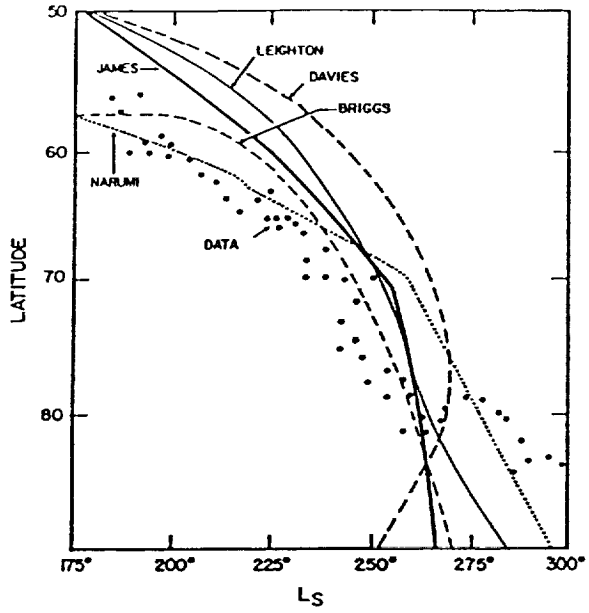

Fig. 1. The seasonal recession of the south polar cap as observed over the last 20 years [James and Lumme, 1982] and as predicted by Leighton and Murray [1966], Briggs [1974], Davies et al. [1977], Y. Narumi, (unpublished data, 1980) and James and North [1982]. (The aerocentric longitude of the Sun, L_s, is the seasonal index; L_s = 0°, 90°, 180°, and 270° correspond to northern spring equinox, summer solstice, autumnal equinox, and winter solstice, respectively.)

lower to the ground, and may be composed of carbon dioxide ice. In general, the polar hood is diffuse and structureless on scales smaller than a few kilometers.

Observers do note a reduction in polar hood clouds during global dust storms, although dust obscuration of most of the lower atmosphere causes the degree of any reduction in cloud cover to be inconclusive. Imaging observations of the polar hood in the polar night are nonexistent. However, CO_2 ice clouds have been inferred to exist in the polar night from Viking Infrared Thermal Mapper (IRTM) data [Hunt et al., 1980; Paige, 1985]. Morning fog is observed regularly over the Viking landers, and observations for several seasons have been reported [Pollack et al., 1977; Ryan and Sharman, 1981; Ryan et al., 1982; Jakosky, 1985]. However, morning fog is not expected at winter polar latitudes, since winter polar latitudes experience little diurnal temperature change.

Clouds are observed to be more prevalent over the edge of the northern polar cap than over the edge of the southern polar cap, although coverage is far from complete [James, 1983; Christensen and Zurek, 1983; James et al., 1987]. Clouds could not be seen in polar night with the imagers sent to Mars to date, although their existence has been suggested based on analysis of Viking infrared data [Hunt et al., 1980; Paige, 1985]. Observations in polar night are not able to discern whether or not any of the hemispherical asymmetry that may exist along the edge of the polar cap exists in polar night as well, although there is no evidence to suggest any other behavior.

The optical depth of dust in the atmosphere also experiences significant seasonal variation. Global dust storms tend to occur during southern spring, when Mars is near perihelion [Martin, 1984; Tillman and Leovy, 1984], and tend to have vertical optical depths of dust of 1.0 or greater at visible wavelengths [Pollack et al., 1979; Thorpe, 1981]. During the remainder of the year, atmospheric dust opacities are substantially lower, although still appreciable, and are hereafter called background dust. The vertical optical depth of background dust was observed to vary from 0.3 to 1.0 in the visible as determined by imaging the Sun from Viking landers 1 and 2 [Pollack et al., 1979]. Similar background dust optical depths were inferred from contrast observations by Viking orbiter imaging [Thorpe, 1981], inferred from Viking lander pressure oscillations [Zurek, 1981], deduced by studying polar cap reflection from Earth-based observations [Lumme and James, 1984], and inferred from modeling the annual variation in pressure [James and North, 1982].

The frequency and intensity of dust storms have apparently varied greatly from year to year over the past 60 years [Martin, 1984]. The second and third Mars years that Viking observed were relatively calm, while the fourth year had the most intense global dust storm observed by Viking, during which Viking lander 1 failed [Tillman and Leovy, 1984]. Earlier Mariner 9 imaging of surface contrast noted significantly less dust than observed by Viking, with optical depths of dust ranging from 0.1 to 2 [Leovy et al., 1972; Masursky et al., 1972]. The same variation in dust optical depth was inferred from Mariner 9 infrared interferometer spectrometer (IRIS) spectra at 3000 Å [Toon et al., 1977] and was determined by the reduction in the solar flux reflected by the polar cap, as observed by the Mariner 9 UV spectrometer [Pang and Hord, 1973].

Observations are inadequate to accurately describe any latitudinal variation in background dust opacity; orbiter data fail to note any significant latitudinal variation, other than a consistently lower dust opacity over both winter poles. Dust opacities in the winter polar atmosphere have been observed to be a factor of 2 or so lower than elsewhere over the planet when the global dust storms exist [Masursky et al., 1972; Leovy et al., 1972; Pang and Hord, 1973; Kieffer, 1979; James et al., 1979; Lumme and James, 1984; Jakosky and Martin, 1987], and the same may be true during background dust conditions. Surface dust is covered by ice at winter polar latitudes, hindering that source of dust; the winter polar atmosphere is stable, facilitating dust settling; and CO_2 snow forms using dust particles as nuclei, further accelerating dust removal [Pollack et al., 1979]. All of these processes may be active during background dust conditions, resulting in dust opacities that may be becoming gradually lower as one approaches the winter pole.

However, the dust seasonal cycle results in a background dust opacity over the Viking lander which is higher from L_s = 180° to 360° (southern winter and spring) than from L_s = 0° to 180° (northern winter and spring) [Pollack et al., 1979]. Assuming that little hemispherical asym-

metry occurs for the same time frame in background dust opacity [Martin, 1986], then the formation and sublimation phases of the southern polar cap will occur with higher background dust opacities than those of the northern polar cap. As a result, background dust could affect the formation and sublimation of the southern cap more than the northern cap at polar night latitudes.

Previous Work in This Area

Kuhn et al. [1979] suggested that ozone could play an important role in the energy budget of the polar cap. Kuhn et al. showed that ozone heating of the winter polar atmosphere was nonnegligible compared to CO_2 heating, particularly near 10 km altitude, and could therefore affect any CO_2 condensation in the atmosphere. However, atmospheric heating by aerosols in the winter polar atmosphere has since been shown to be greater than either O_3 or CO_2 heating, particularly near 10 km altitude [Lindner and Thomas, 1983; Lindner, 1985]. Thus, ozone does not make a large enough contribution to the atmospheric temperature to significantly affect downwelling thermal radiation which strikes the polar cap or any condensation of CO_2 in the atmosphere. Ozone also affects the surface energy budget by absorbing incoming solar radiation which would otherwise strike the surface. This issue is addressed in the results section of this paper.

Clouds will also affect the energy budget by scattering solar radiation and emitting thermal radiation. The radiative effects of clouds were shown to be important by Briggs [1974] and James and North [1982]. However, the magnitude of this importance was not accurately determined, since they ignored the effects of clouds at solar wavelengths. Furthermore, they included infrared effects with an atmospheric emissivity of 0.3 when clouds existed, an emissivity of 0.15 for cloudless conditions, and a single atmospheric temperature, assumptions which ignore the variations in cloud opacity and temperature which occur.

The attenuation of solar radiation due to absorption and scattering by dust and the increase in thermal radiation due to emission by dust will also influence the energy budget of polar cap, as previously suggested by Briggs [1974], Davies [1979], James et al. [1979], Kieffer [1979], Martin and Kieffer [1979], James and North [1982], and Paige [1985]. These studies all examined the radiative effects of the global dust storms, which occur primarily in southern spring, and showed that global dust storms do not appear to significantly affect polar cap recession. However, appreciable amounts of background dust exist year-round. Davies [1979], James and North [1982], and Paige [1985] examined the radiative effects of background dust and noted a neutral contribution on the whole (a slight decrease in some cases and a slight increase in others).

However, these background dust studies all ignored polar night latitudes (those latitudes and seasons where the Sun remains below the horizon all day). In addition, Paige [1985] studied only the 90° latitude in his study. Furthermore, all studies ignored the overlap of the radiative effects of CO_2 and dust in the 15-μm wavelength region, where both CO_2 and dust emit the most thermal radiation [Lindner, 1985], as well as the overlap of CO_2 and dust at near-infrared (NIR) wavelengths. Improper treatment of this overlap will result in errors in the downwelling thermal radiance of the order of 30% [Lindner, 1985]. Moreover, Davies [1979] and James and North [1982] accurately modeled the radiative effects at solar wavelengths, but included thermal heating of the surface by simply assuming that half of all the solar radiation absorbed by dust is radiated thermally to be absorbed by the surface. This hypothesis assumes that dust is the primary source of radiative heating and cooling; however, CO_2 heating and cooling is also appreciable during background dust conditions [e.g., Lindner, 1985]. Furthermore, atmospheric absorption of planetary thermal emission is also appreciable. A better approach to including IR heating of the polar cap is to compute the thermal emission based on the observed atmospheric temperatures, CO_2 opacities, and dust opacities, as is done here.

Modeling Procedure

The radiative flux striking the surface is calculated for 57 solar and 10 infrared wavelength intervals from 0 to 100 μm including the absorption, scattering, and emission by O_3, CO_2, clouds, and dust. Ultraviolet absorption of solar flux by O_2, H_2O, HO_2, and H_2O_2 is also included, as is Rayleigh scattering. Atmospheric composition is taken as 95% CO_2 and 0.13% O_2 [Owen et al., 1977]. Season-dependent CO_2 abundances are taken from Hess et al. [1980], after correcting for elevation [Lindal et al., 1979; Jakosky and Farmer, 1982] and accounting for possible circulation-induced pressure gradients [Haberle et al., 1979]. Ozone abundances were taken from Barth et al. [1973], assuming that ozone mixing ratios in the polar night were the same as at the edge of polar night and adopting altitude profiles from Lindner [1988]. H_2O abundances are based on the work of Jakosky and Farmer [1982] and Lindner [1988], and HO_2 and H_2O_2 abundances are taken from Lindner [1988].

Transmission functions for the 2.7-, 4.3-, and 15.0-μm bands of carbon dioxide are taken from the line-by-line model results of Gal'tsev and Osipov [1979]. The transmission function, Tr, as a function of temperature T, pressure P, and CO_2 column abundance U was extrapolated from the Gal'tsev and Osipov results (subscript G) to temperatures below 200 K by

$$Tr(T,P,U) = 1-[(1-Tr_G(200\ K,P,U))\ (T/200\ K)^Q]$$

The exponential Q was found to be 0.45, 0.3, and 0.8 for the 2.7-, 4.3-, and 15-μm bands, respectively, when the temperature dependencies for the Pollack et al. [1981] transmission functions were recast in this form. Using a modified version of the FASCOD transmission model (Clough et al., 1986), the accuracy of these transmission functions was confirmed, and transmission functions were obtained for the 1.3-, 1.4-, 1.6-, 2.0-, 4.8-, and 5.2-μm bands of CO_2 (B. L. Lindner et al., manuscript in preparation, 1989).

The properties of clouds and dust are extrapolated from observations at mid-latitudes, given

the lack of observations at winter polar latitudes. Background dust opacities over winter polar latitudes may be less than the Viking lander latitudes, where they vary from 0.2 to 1.0 [Pollack et al., 1979; Lumme and James, 1984]. However, vertical optical depths of background dust vary from 0 to 1.0 in this work to account for all possible scenarios. The wavelength dependence of the dust opacity is taken from Toon et al. [1977]. A Gaussian profile describes the vertical distribution of dust, with dust opacities confined mostly below 20 km altitude for normal conditions and 50 km altitude for dust storm conditions [see Anderson and Leovy, 1978; Zurek, 1982]. The single-scattering albedo of airborne dust as a function of wavelength is taken from Zurek [1978, 1982] and Toon et al. [1977] at solar and infrared wavelengths, respectively, using a solar average of 0.86 [Pollack et al., 1979]. The Haze-L phase function is used to describe the scattering of radiation by Martian dust [Toon et al., 1977]. The emissivity of airborne dust is high and has been calculated as a function of wavelength from theory and observations [Toon et al., 1977; Simpson et al., 1981].

Clouds were assumed to be diffuse, with a distribution in altitude of the mixing ratio of cloud ice like that assumed for airborne dust [Briggs and Leovy, 1974]. Cloud opacities are observed to vary significantly, and a range of 0 to 3 is used in this work. The single-scattering albedos of both CO_2 and H_2O ice clouds are high and are assumed to be unity at all wavelengths from UV to IR. This agrees with single-scattering albedos for Martian water ice clouds derived from IRTM data [Hunt, 1979] and derived for CO_2 ice clouds from Mie theory [Hunt et al., 1980] for all wavelengths, to the extent that ice particle radii are known. Single-scattering albedos for the clouds are also given by Moroz [1976] and Freeman and Liou [1979]. These observations agree well with theoretical calculations [Wiscombe and Warren, 1980]. The analytic phase function which has been used most extensively in the literature was introduced by Henyey and Greenstein [1941]. The Henyey-Greenstein phase function has been shown to be valid for ice [Hansen, 1969], and asymmetry factors as a function of wavelength from the UV to IR have been derived for Martian clouds, with a great deal of uncertainty [Hunt, 1979; Hunt et al., 1980].

The discrete ordinate method of Stamnes and Conklin [1984] treats the scattering, emission, and absorption of monochromatic radiation through the Martian atmosphere. The exponential sum method allows the banded wavelength structure of CO_2 in the infrared (IR) and near-infrared (NIR) to be treated as monochromatic, allowing for its incorporation in a scattering model [see Freeman and Liou, 1979]. Eight terms in the exponential sum were found to give a good approximation to the transmission in the 15-μm band of CO_2, while four terms were used for the NIR bands of CO_2 (B. L. Lindner et al., manuscript in preparation, 1989). The use of the exponential sum technique allows the overlap of CO_2 and dust opacities in the 15-μm and NIR wavelength regions to be properly treated.

Atmospheric properties are zonally averaged and assumed azimuthally independent. The region from the surface to 40 km altitude is broken into 20 2-km-thick layers to account for vertical inhomogeneity. The Chapman function is used to approximate the slant path in place of the secant function [e.g., Smith and Smith, 1972], because the winter polar atmosphere always has large solar zenith angles, and the secant function is in error for large angles. The model is diurnally averaged [e.g., Cogley and Borucki, 1976]. An albedo for the polar cap at solar wavelengths (0.3-5.4 μm) of 0.5 is used, which is appropriate for late northern winter [Kieffer, 1979; James and Lumme, 1982]. The IR (5.4-100 μm) albedo of the polar cap is assumed to be zero [Kieffer, 1970; Smythe, 1975; Wiscombe and Warren, 1980]. Three latitude cases were studied: 57°N, 70°N, and 90°N, and late winter conditions were assumed (L_s = 343°). These three cases effectively simulate the edge of the polar cap, the edge of polar night, and polar night, respectively, for all solar longitudes and both polar caps.

The temperature profile at 57°N latitude that is used in this study rises linearly with altitude from 150 K at the surface to 170 K at 6 km altitude and then falls with increasing altitude to 130 K at 40 km. This temperature profile is extracted from radio occulation observations made near winter polar latitudes during background dust conditions [Lindal et al., 1979]. These temperatures also agree with those obtained by the Viking IRTM experiment [Kieffer, 1979; Martin, 1984]. The diurnally averaged heating and cooling rates calculated using these temperatures were very nearly in balance. This indicates that the winter polar atmosphere is nearly in radiative equilibrium, which is the assumption that is used for calculating atmospheric temperatures farther poleward. The temperature profile at 70°N latitude was the same as that used at 57°N latitude except that it had a peak temperature of 155 K at 6 km. Polar night temperatures were assumed to have no inversion and fell linearly from 150 K at the surface to 130 K at 40 km. Temperatures are markedly higher at the time of the global dust storms [e.g., Pollack, 1978], but global dust storms are not considered here.

Radiative Fluxes at the Polar Cap Surface

Table 1 shows the radiative fluxes from 0 to 100 μm integrated over UV, visible, NIR, and three IR wavelength bands. O_3 absorbs almost two thirds of the available solar flux from 0 to 0.3 μm at 57°N latitude. (The flux in the 0- to 0.3-μm bin is 6 J cm^{-2} sol^{-1} for no dust and no O_3 scenarios for this latitude and season. 1 sol = 1 Martian day.) However, ozone absorption has only a minor effect on the overall flux at the surface, due to the small contribution that solar radiation in the UV makes to the overall energy budget. Very little O_3 or CO_2 absorption occurs in the 0.3- to 1.0-μm wavelength bin. Absorption in the CO_2 NIR bands prevents approximately 5% of the available solar flux from 1 to 5 μm from striking the surface at 57°N latitude and L_s = 343°. The 15-μm band of CO_2 is the dominant gaseous source of thermal radiation which strikes the polar cap [see Lindner, 1985]. The IR flux from the Sun can be seen in the 5.4- to 10-μm and 21- to 100-μm wavelength bins for the dust-free case.

TABLE 1. Flux Striking the Surface Near the Edge of the Polar Cap (57°N Latitude, L_s = 343°)

Wavelength Interval, μm	Dust Opacity 0.0	0.2	0.5	1.0
0.0-0.3	2.132	1.429	0.823	0.364
0.3-1.0	455.608	391.262	321.688	247.947
1.0-5.4	194.296	167.001	138.951	109.501
5.4-10.0	2.221	3.255	4.361	5.315
10.0-21.0	19.894	41.189	61.311	79.603
21.0-100.0	0.044	16.603	36.640	62.910
Total flux	674.195	620.739	563.774	505.640
Absorbed flux	348.177	340.893	333.043	326.734

The vertical optical depth of dust is given. Flux values are given in units of J cm^{-2} sol^{-1}.

Dust affects the energy budget of the polar cap by absorbing and scattering to space solar radiation that would otherwise strike the cap and by emitting thermal radiation, some of which strikes the cap. Dust absorbs and scatters strongly in the UV and moderately in the visible and NIR as seen in Table 1. Dust also emits thermally at all wavelengths. Note that the flux which strikes the surface from thermal emission by even small abundances of airborne dust is of the same order as thermal emission in the 15-μm band of CO_2. Clearly, both CO_2 and dust thermal emission are important for the energy budget of the polar cap. It is also important to note that in the 15-μm wavelength band, both dust and CO_2 emission are important. Hence, it is important to treat dust and CO_2 simultaneously as is done here, and not to calculate cooling rates individually and sum them.

The total wavelength-integrated flux decreases with increasing dust optical depth, as the increase in thermal radiation does not equal the decrease in solar flux. However, sublimation depends on the total flux that is absorbed, which is a function of the cap albedo. Whereas the typical albedo of old ice is 0.5 at solar wavelengths [Kieffer, 1979; James and Lumme, 1982], the albedo at IR wavelengths is close to zero [Kieffer, 1970; Smythe, 1975; Wiscombe and Warren, 1980]. Weighting the flux with the coalbedo (1-albedo) results in the absorbed flux, given at the bottom of Table 1. Almost no change in the absorbed flux occurs over the range that dust optical depth experiences in the Mars atmosphere (omitting dust storms), a result also found by Davies [1979] and Paige [1985]. The increase in the infrared flux due to thermal emission by dust balances the decrease in the solar flux due to dust absorption, although not completely, resulting in a slight decrease in absorbed flux. Global dust storms are another matter, as the atmospheric temperature and the meridional transport of heat are much higher. However, the effect of dust storms on polar cap recession was studied by Briggs [1974], James and North [1982], and Paige [1985], and dust storms do not appear to offer an explanation for the persistence of CO_2 ice in the southern hemisphere.

As shown in Table 2, all solar fluxes at 70°N latitude are lower than at 57°N latitude due to the increased solar zenith angle and decreased daylight hours. The larger slant path allows O_3, CO_2, and dust to be more effective at preventing solar flux from reaching the surface; effective optical depths are nearly an order of magnitude larger than vertical optical depths. Thermal fluxes at 70°N latitude are also lower than thermal fluxes at 57°N latitude (Table 1) because atmospheric temperatures are lower [Lindal et al., 1979]. However, the net effect on the flux absorbed by the polar cap is the same as at 57°N latitude, in that changes in dust opacities from 0 to 0.5 cause virtually no change in absorbed flux.

However, while dust has little influence on the total flux absorbed by the polar cap at sunlit latitudes, a noticeable result occurs in the polar night region (that part of the planet where the Sun does not illuminate the surface at all during an entire day). Table 3 shows the thermal

TABLE 2. Flux Striking the Surface of the Polar Cap Near the Edge of Polar Night (70°N Latitude, L_s = 343°)

Wavelength Interval, μm	Dust Opacity 0.0	0.2	0.5
0.0-0.3	1.105	0.552	0.264
0.3-1.0	220.890	164.544	121.753
1.0-5.4	93.550	73.743	58.566
5.4-10.0	1.078	1.731	2.432
10.0-21.0	16.348	32.923	48.696
21.0-100.0	0.021	14.497	32.051
Total flux	332.992	287.990	263.762
Absorbed flux	175.220	168.571	173.471

The vertical optical depth of dust is given. Flux values are given in units of J cm^{-2} sol^{-1}.

TABLE 3. Flux Striking the Surface of the Polar Cap in Polar Night (90°N Latitude, L_s = 343°)

Wavelength Interval, μm	Dust Opacity 0.0	0.2	0.5
5.4-10.0	0.000	0.708	1.391
10.0-21.0	14.714	29.441	43.465
21.0-100.0	0.000	13.511	29.909
Absorbed flux	14.714	43.660	74.765

The vertical optical depth of dust is given. Flux values are given in units of J cm^{-2} sol^{-1}.

flux absorbed by the polar cap for three dust opacities (solar fluxes are obviously zero). Again, note that thermal fluxes are lower at polar night latitudes than at sunlit latitudes (i.e., Tables 1 and 2) due to the extremely cold temperatures. Even so, there is a substantial increase in absorbed flux with dust opacity, even for very small opacities. For comparison, the thermal emission by the surface to space is only 260 J cm^{-2} sol^{-1}, assuming unit emissivity. In terms of a sublimation rate, 10 J cm^{-2} sol^{-1} would sublimate approximately 0.02 cm of CO_2 ice per sol (this assumes an ice density of 1 g cm^{-3}.) Hence, a period of 1 Martian year with a vertical optical depth of dust of 0.2 would result in a substantial loss of the order of 20 cm of CO_2 ice.

The Effect of Clouds

Clouds also affect the energy budget of the polar cap. At 57°N latitude, the radiative effects on the absorbed flux of a combination of clouds and dust are fairly neutral, with a slight downward bias (Table 4). Clouds slightly decrease the flux absorbed by the polar cap for small dust opacities (τD = 0 or 0.2), with the extent of the decrease proportional to the cloud opacity. However, clouds actually slightly increase the flux absorbed by the polar cap at 57°N latitude for moderate or large dust opacities (τD = 0.5 or 1). The explanation lies in the fact that cloud ice is strongly scattering and in the fact that the solar zenith angles are very large in the winter polar atmosphere. Without a cloud, the solar flux must traverse an effective optical depth of τ/μ_0, where τ is the vertical optical depth measured from the surface to infinity, and μ_0 is the cosine of the solar zenith angle. In the winter polar regions, μ_0 is quite small (diurnally averaged μ_0 is approximately 0.32 for this case). If a cloud is in the path of the solar rays, then most rays are scattered in all directions, although with strong forward scattering. Some solar rays are scattered to space and lost. However, a significant percentage of the solar photons are scattered downward at some angle θ which is usually less than the solar zenith angle. As a result, $\tau/\cos\theta$ is actually less than the optical depth traversed had the cloud not been there. When solar zenith angles are as large as they are in the winter polar regions, this is an important effect. This effect is even more dramatic farther poleward. The same effect is easily noticed on Earth, especially just after sunset. If a cloud is present, then the surface illumination can be significantly greater than if no cloud were present because the cloud scatters the solar flux down to the surface.

For low dust opacities, the effect of lowering the effective solar zenith angle is outweighed by the scattering of solar flux to space. For moderate or high dust opacities, lowering the effective solar zenith angle decreases the effective optical depth of dust that must be traversed and allows more solar radiation to reach the surface. This is even more important in NIR and UV wavelengths, where CO_2 and O_3 have absorption bands. This effect was noted to be particularly important for ozone photochemistry on Mars [Lindner, 1988]. Thermal emission by clouds increases the IR flux absorbed by the polar cap, most noticeably in the 21- to 100-μm wavelength range. Thermal emission by clouds in the 15-μm and can get absorbed by CO_2 before striking the surface.

At 70°N latitude, the radiative effect is also neutral for small cloud opacities and all dust opacities, as shown in Table 5. However, moderate and large clouds cause up to a 15% increase in the flux absorbed by the polar cap. At 70°N

TABLE 4. Flux Absorbed by the Polar Cap Near Its Edge for Various Cloud and Dust Opacities (57°N Latitude, L_s = 343°)

Cloud Opacity	Dust Opacity 0.0	0.2	0.5	1.0
0.0	348.177	340.893	333.043	326.734
0.2	339.769	336.545	333.569	330.136
0.5	333.106	334.744	334.143	332.564
1.0	329.832	333.467	338.226	339.172

The vertical optical depth is given. Flux values are given in units of J cm^{-2} sol^{-1}.

TABLE 5. Flux Absorbed by the Polar Cap Near the Edge of Polar Night for Various Cloud and Dust Opacities (70°N Latitude, L_s = 343°)

Cloud Opacity	Dust Opacity 0.0	0.2	0.5
0.0	175.220	168.571	173.471
0.2	167.139	170.336	181.032
0.5	169.478	178.580	192.287
1.0	184.456	208.631	195.178

The vertical optical depth is given. Flux values are given in units of J cm^{-2} sol^{-1}.

latitude the solar flux traverses approximately 8 times as much atmosphere as it would if it traveled vertically. The cloud acts to shorten the path of the solar radiation, allowing for less absorption on the path toward the surface and accounting for the increase in absorbed flux. This is especially noticeable in the UV, where the flux reaching the surface is 50% higher when the radiative effects of a cloud of opacity 1 and dust of opacity 1/2 are included. The total solar flux which reaches the surface at 70°N latitude is only reduced by 10% from "clear" atmospheric conditions when a cloud opacity of 1 and dust opacity of 1/2 are included, which is more than offset by the increase in thermal flux, even though colder atmospheric temperatures exist at 70°N latitude.

It is at the polar night latitudes that the radiative effects of clouds and background dust are most significant, as shown in Table 6 (solar fluxes are obviously zero). IR fluxes absorbed by the polar cap increase up to an order of magnitude as the cloud opacity and dust opacity increase. While dust optical depths of 0.5 are shown for completeness, they are unlikely except during dust storms. As discussed earlier, dust opacities may be lower in the winter polar atmosphere than over the Viking landers, making background dust opacities of 0.5 unlikely. Also,

TABLE 6. Flux Absorbed by the Polar Cap in Polar Night for Various Cloud and Dust Opacities (90°N Latitude, L_s = 343°)

Cloud Opacity	Dust Opacity 0.0	0.2	0.5
0.0	14.714	43.660	74.765
0.2	36.506	60.984	88.694
0.5	60.951	81.669	105.963
1.0	90.255	107.864	128.389
3.0	152.423	164.712	178.094

The vertical optical depth is given. Flux values are given in units of J cm^{-2} sol^{-1}.

while cloud optical depths as large as 3 could occur, optical depths of 0.5 are probably more common. However, even simply a cloud optical depth of 0.5 and dust optical depth of 0.2 would result in the sublimation of the order of 40 cm of CO_2 ice over 1 Martian year. When inserted in a polar cap/atmospheric pressure model, this would accelerate the predicted loss of all the CO_2 ice on the northern polar cap by approximately 40 sols (based on ice depth versus season as shown by Leighton and Murray [1966], Cross [1971], Briggs [1974], Davies et al. [1977], Lindner [1985], and Jakosky and Haberle [this issue]).

As discussed in the introduction, while polar cap/atmospheric pressure models have been unable to explain the dichotomy of the residual polar caps, these models have been fairly successful at reproducing observations of atmospheric pressure and polar cap recession up to 75° or 80° latitude. The radiative effects of clouds and background dust have the added benefit of not significantly affecting polar cap/atmospheric pressure model predictions of the annual variation in atmospheric pressure. Clouds and background dust have a neutral effect along the cap edge, becoming more important as one approaches the pole, particularly within 80° latitude. The integral of seasonal CO_2 ice over the 80°S to 90°S latitude band (where the residual polar cap exists) is an order of magnitude less than the integral of seasonal CO_2 ice over the planet [Leighton and Murray, 1966; Briggs, 1974; Davies et al., 1977; Lindner, 1985]. Hence, a process which affects primarily the residual polar cap area will not significantly affect model predictions of atmospheric pressure. Also, the rate of recession of the seasonal polar cap would remain essentially the same as that predicted by polar cap/atmospheric pressure models equatorward of 75° latitude, where good agreement with observations was previously obtained. The behavior near the pole would be significantly modified, making for better agreement with observations than previously obtained. The rate of recession of the polar cap is an important test, especially since it repeats reliably over several years of observation [Veverka and Goguen, 1973; James et al., 1979; James and Lumme, 1982; James, 1982].

The Effect of Albedo and Temperature on Our Results

A polar cap albedo of 0.5 at visible wavelengths was selected for the calculations presented here, which is appropriate during the sublimation phase of the polar cap (late winter, spring) [Kieffer, 1979; James and Lumme, 1982]. One would expect higher albedos during the formation phase of the polar cap (fall, early winter) because of the freshly formed ice; unfortunately, observations of the polar cap albedo during the formation phase of the polar cap are not available, due to the extensive cloud cover at this time. Higher polar cap albedos would lessen the amount of absorbed solar flux, making the thermal effects of clouds and dust relatively more important to the energy budget of the polar cap. A polar cap albedo of 1 would change the polar cap energy budget by nullifying the solar contributions in Tables 1 and 2. For dust-free, cloud-free cases, the total flux absorbed by the polar

cap at 57°N latitude in late winter would be only 5% of the value obtained for an albedo of 0.5. However, a scenario with a cloud of vertical optical depth 1 and dust of vertical optical depth 0.5 at 57°N latitude in late winter would still result in a flux absorbed by the polar cap for an albedo of 1 that is 50% of the flux absorbed for an albedo of 0.5. Hence, the presence of clouds and dust lessens the ability for a high albedo to preserve CO_2 ice. Furthermore, polar cap albedo does not have a linear effect on the energy budget, as clouds and dust will reflect some of the flux reflected from the polar cap back onto the polar cap. Also, a high albedo at solar wavelengths is of no consequence at polar night latitudes where the Sun never shines.

Similarly, a low albedo at solar wavelengths is not as damaging for the preservation of CO_2 ice as might be expected, because a substantial portion of the energy budget of the polar cap is received from IR emission by clouds and background dust. Hence, any increase in absorbed flux at solar wavelengths from a decrease in albedo is not as important to the energy budget as it would be in the absence of clouds and dust. A polar cap albedo of zero would approximately double the absorbed solar flux given in the tables, but the percentage increase to the total energy budget is smaller when the effects of clouds and dust are included. Furthermore, a low albedo at solar wavelengths has no importance at polar night latitudes.

Atmospheric temperatures used in this model for the edge of the polar cap were some of the coldest observed at polar cap edge latitudes by the Viking orbiter [Lindal et al., 1979]. Higher atmospheric temperatures than those used here would actually increase the thermal emission by dust and cloud even more, making their radiative effects yet more important to the overall energy budget. However, the temperatures used are not as important as one might expect, because most atmospheric dust and cloud lie near the surface (about 60% is within 8 km of the surface; one atmospheric scale height at 160 K), and atmospheric temperatures near the surface remain very close to the CO_2 frost point temperature during winter except during dust storms [Lindal et al., 1979].

Implications for the Polar Cap Asymmetry

As ozone is more prevalent at northern latitudes [Barth et al., 1973], ozone was proposed to be partly responsible for the hemispherical asymmetry in residual polar caps [Kuhn et al., 1979]. The maximum ozone abundance observed by Mariner 9 is used to test this hypothesis. Higher ozone abundances probably exist under cloudy and dusty conditions through which the reflectance spectroscopy technique employed by Mariner 9 researchers would have had difficulty detecting ozone [Lindner, 1988]. However, both ozone heating of the atmosphere and the reduction in UV light striking the surface would be less important under very cloudy, dusty conditions [Lindner, 1988].

Ozone does absorb most of the ultraviolet insolation, which increases the lifetime of CO_2 ice. However, ultraviolet insolation is only 1% of the total insolation. Thus, even if O_3 absorbed all ultraviolet insolation, CO_2 ice lifetimes would only be marginally changed. Ozone heating of the atmosphere is also minor compared to CO_2 and dust heating [Lindner and Thomas, 1983; Lindner, 1985]. Hence, ozone would not cause any appreciable hemispherical asymmetry in atmospheric temperature, and therefore in the atmospheric thermal emission which strikes the polar cap, or in any CO_2 condensation which may take place in the atmosphere.

However, the cloud and dust results have more important implications regarding the hemispherical asymmetry of the residual polar caps. Although the results are dependent on the polar cap albedo and atmospheric temperatures, it does appear that the radiative effects of both clouds and background dust will appreciably increase sublimation of the polar cap at polar night latitudes. Hence, the radiative effects of clouds and background dust would be most noticeable near the residual polar cap, which spends all of the winter in polar night. As discussed in the introduction, observational evidence suggests a greater abundance of clouds over the northern polar cap than over the southern polar cap. Moreover, as also discussed in the introduction, it is also expected that the formation and sublimation phases of the seasonal southern polar cap will occur with higher background dust opacities than the formation and sublimation phases of the seasonal northern polar cap. Both of these hemispherical asymmetries would preferentially increase the fluxes absorbed by the polar cap at polar night latitudes in the north, particularly by the residual polar cap area in the north.

Furthermore, the surface pressure during winter months is lower over the southern residual polar cap than the northern residual polar cap, due to differences in elevation [Wolceshyn, 1974; Lindal et al., 1979] and due to the annual cycle in surface pressure [Hess et al., 1980]. If mixing ratios of cloud and dust are assumed to be the same for both poles, then the pressure differential between the poles would result in a dust and cloud opacity over the residual polar cap in the south that is 30% less than over the residual polar cap in the north during the crucial winter months. Mixing ratios of dust may actually be lower over the southern polar cap than over the northern polar cap during winter months because the mechanisms for raising and maintaining atmospheric dust are pressure dependent [Pollack et al., 1976, 1979; Pollack and Toon, 1982]. Lower mixing ratios over the southern pole would accentuate the asymmetry in cloud and dust opacity due to the asymmetry in surface pressure.

The net result of all these hemispherical asymmetries is that the solar and infrared flux absorbed by the residual polar cap area in the north during the winter is greater than that absorbed by the residual polar cap area in the south. This would allow relatively less frost to accumulate over the residual polar cap in the north during the fall and winter than in the south and cause the CO_2 surface ice to sublimate more rapidly in the north during the following spring and summer. These suspected hemispherical asymmetries in background dust and atmospheric pressure have not been included in prior polar cap/atmospheric pressure studies.

Other Processes Neglected by Prior Polar Cap/Atmospheric Pressure Models

The radiative effects of cloud and dust are not the only processes responsible for the hemispherical asymmetry in the residual polar caps. Prior polar cap/atmospheric pressure studies determined that CO_2 ice would completely sublime away from both polar caps. This study has shown that clouds and background dust serve to increase sublimation over the poles, albeit to a greater extent over the northern pole. Some other phenomenon that has not been included in prior polar cap/atmospheric pressure models is causing the ice to sublime more slowly, to allow CO_2 ice to survive southern summer.

Previous polar cap/atmospheric pressure models have assumed that all absorption of sunlight occurs at the top surface of the polar cap, when in reality it can be distributed over as much as several meters depth [Clow, 1987]. This simplified treatment of ice microphysics by prior models yields incorrect sublimation rates for three reasons. First, the rate of sublimation/condensation of a column of ice depends on the integral of the energy imbalances at each level within the ice, which is not the same as assuming that all sources and sinks occur at the top surface. Second, accurate treatment of ice microphysics is particularly important for thin ice, as much of the incoming radiation would go through the cap and get absorbed by the surface under the cap. Considering that the seasonal cap is at most 1 m thick [Leighton and Murray, 1966; Briggs, 1974; Davies et al., 1977; Lindner, 1985], this effect alone should extend the predicted stability of surface ice in the summer. Third, previous models of the sublimation of Martian ice used an empirical relationship for sublimation developed for turbulent-driven evaporation from terrestrial oceans [Clow, 1987]. This parameterization fails to account for environmental differences between the Earth and Mars and differences between aerodynamically rough and smooth surfaces or atmospheric stability conditions; and the predicted sublimation rates are substantially in error (G. Clow, personal communication, 1988).

Furthermore, all prior models ignored CO_2 absorption by the atmosphere in the NIR, which is more important at winter polar latitudes where the slant paths are so large [Lindner, 1985]. As much as 10% of the solar flux can be absorbed, which would allow CO_2 ice to linger longer into the summer months. Moreover, heating within the polar cap in near-infrared wavelengths is actually larger than heating in visible wavelengths in the top few millimeters of ice, because near-infrared radiation does not penetrate the ice as deeply as visible radiation [Clow, 1987]. This accentuates the effect that atmospheric absorption of near-infrared sunlight has on polar cap sublimation.

Previous models assumed a Lambertian (isotropic) surface albedo. However, ice does not scatter isotropically, particularly for solar zenith angles above 66° where ice is strongly forward scattering [Taylor and Stowe, 1984]. Since the solar zenith angle in the winter polar region of Mars is usually much greater than 66°, the assumption of an isotropic albedo for the polar cap is in error. This error becomes important when the atmospheric feedbacks of clouds and dust become important, because clouds and dust do scatter a significant amount of solar radiation which has been reflected by the polar cap back onto the polar cap. This is particularly important for high-albedo objects such as the polar caps and the polar hood where solar radiation can reflect back and forth many times before escaping to space or getting absorbed.

Furthermore, the total albedo of ice has a strong dependence on solar zenith angle [Lian and Cess, 1977; Wiscombe and Warren, 1980; Squyres and Veverka, 1982; Paige 1985], which previous polar cap/atmospheric pressure models have ignored. Ice brightens significantly at high solar zenith angles. This is an important effect to consider in the winter polar regions where solar zenith angles vary significantly. The inclusion of the dependence of ice albedo on the solar zenith angle should help explain why CO_2 ice is retained year-round at the south pole. Since the albedo of ice increases and becomes more forward scattering at higher solar zenith angles, and since the solar zenith angle becomes higher as one approaches the pole, the effect will cause the albedo to be greatest at the pole. This will decrease absorption of sunlight, hence increasing survivability of CO_2 ice. Furthermore, at the pole the Sun is above the horizon all day, but at a very high zenith angle. As one goes toward the equator, the Sun spends less time at high zenith angles. This will accentuate the solar zenith angle effect on ice albedo at the pole even more.

This is particularly important when viewed together with the radiative effects of clouds and dust. Assuming that the hemispherical asymmetries in clouds and dust mentioned earlier do indeed exist, then the combination of the effects of solar zenith angle on albedo and the effects of clouds and dust could act to extend the lifetime of CO_2 ice on the south pole relatively more than on the north pole. Another positive aspect of solar zenith angle effects on ice albedo is that the extension of CO_2 ice lifetimes at the pole due to the inclusion of solar zenith angle effects on ice albedo should not appreciably change model predictions of the annual cycle of pressure or polar cap recession equatorward of 75° latitude, since approximately 90% of the seasonal CO_2 frost is equatorward of 80° latitude [Leighton and Murray, 1966; Briggs, 1974; Davies et al., 1977; Lindner, 1985]. Hence, the good model agreement to polar cap recession equatorward of 80° latitude is retained there.

Recent studies of the wavelength dependence for the albedo of ice should also be incorporated in future polar cap/atmospheric pressure studies, given the direct relationship between ice albedo and ice sublimation. Compilations of the optical constants of water ice and CO_2 ice exist from UV to microwave wavelengths [Warren, 1984, 1986]. Not only does experimental work report the wavelength dependence of CO_2/H_2O ice mixtures [Kieffer, 1970], but experimental studies also document the change in this wavelength dependence for various ice/dust mixing ratios, various radius sizes of ice particles, and various dust types [Wiscombe and Warren, 1980; Warren and Wiscombe, 1980; Clark, 1981]. This is of particular importance in the near-infrared where the albedo of ice is highly variable, since significant subli-

mation of the polar cap occurs in the near-infrared [Clow, 1987]. The albedo of ice is sensitive to grain size in the near-infrared and sensitive to the dust/ice mixing ratio in the visible [Warren and Wiscombe, 1980; Wiscombe and Warren, 1980].

Seasonal and latitudinal variations in ice albedo occur on the Earth due to changes in dust mixing ratios and ice age [Wiscombe and Warren, 1980; Warren and Wiscombe, 1980] and should also exist on Mars. Latitudinal variations in ice albedo have been inferred from Mariner 7 spectra [Martin, 1988], and a consistently higher albedo for surface ice is inferred to exist in the southern hemisphere based on Viking orbiter observations [Paige, 1985]. This would lower the energy absorbed by the southern polar cap and allow the CO_2 ice to survive the summer. Seasonal and latitudinal variations in polar cap albedo have been noted to make better agreement between polar cap/atmospheric pressure models and observations of atmospheric pressure [Lindner, 1986].

Previous polar cap/atmospheric pressure models have only examined the condensation of frost and have ignored snowfall. Snowfall could be an appreciable component of the polar cap [Pollack and Haberle, 1988], as it is on Earth, and therefore could account for the lingering of carbon dioxide ice. Carbon dioxide clouds probably exist over part of the polar cap [Briggs and Leovy, 1974; Hunt et al., 1980; Paige, 1985], and carbon dioxide snow could also be expected to form. Furthermore, snowfall should occur mostly at polar night latitudes. Sunlit polar winter latitudes have a strong inversion which keeps atmospheric temperatures well above the CO_2 condensation temperature even while frost is condensing on the surface [Lindal et al., 1979]. However, in polar night the heat sources which support the temperature inversion at lower latitudes are not as effective, allowing for lower atmospheric temperatures which favor the formation of CO_2 clouds and snow. Hence, snowfall might not be an important contributor to the polar energy budget at latitudes equatorward of 70°, which is where most of the CO_2 frost occurs [Leighton and Murray, 1966; Briggs, 1974; Davies et al., 1977; Lindner, 1985]. Thus, including snowfall in polar cap/atmospheric pressure models will not appreciably change the predictions of the annual cycle in pressure or the predictions of polar cap recession equatorward of 70° latitude, both of which agree fairly well with observations. However, snowfall might be appreciable poleward of 70° latitude, particularly at 90° latitude, where previous models have been incorrect. Snowfall would also help counterbalance the radiative effects of clouds and dust, which were also most important in polar night. Furthermore, southern winter is colder and longer than northern winter due to the large eccentricity of the Martian orbit. Thus, the southern pole might accumulate more snowfall than the northern pole, which also might help explain why CO_2 frost remains yearround at 90°S latitude and not at 90°N latitude.

Jakosky and Haberle [this issue] noted that prior polar cap/atmospheric pressure models always began with the assumption that the south pole was bare of a CO_2 ice residual polar cap. This allowed the surface to warm during summer and hence delayed the onset of frost in the fall. Jakosky and Haberle showed that the assumption that a CO_2 ice residual polar cap existed in southern summer resulted in CO_2 frost accumulating earlier the following fall and hence allowed it to survive longer the next summer. This idea has the added benefit of being most important at polar night latitudes and would therefore help to counter the radiative effects of clouds and dust, which are also most important at polar night latitudes.

Recent radar observations of the south polar cap suggest the presence of significant roughness (D. O. Muhleman, personal communication through B. M. Jakosky, 1988). Theoretically, surface roughness in the form of penitentes (spikes of ice) may occur in the polar caps [Svitek and Murray, 1988]. Surface roughness will change the effective solar zenith angle. Surface roughness will also allow radiation to be reflected from one part of the polar cap directly to another part of the polar cap without atmospheric scattering as an intermediary.

Recent calculations of the emissivity of CO_2 ice as a function of wavelength from the UV to the IR under Marslike conditions show strong variability in emissivity with dust content and ice age (S. Warren, personal communication, 1988). Under certain conditions, the emissivity can be quite low, which would decrease the ability of the ice to radiate in the IR.

Other possibilities include an insulating residue on the polar ice [Saunders et al., 1986], which would reduce the rate of sublimation. Wind shifting of the polar cap ice may also change the recession rate of the polar cap by moving ice toward the pole [Briggs, 1974; James et al., 1979; Kieffer, 1979; Saunders et al., 1985].

Summary

Polar cap/atmospheric pressure models have been unable to explain the observed hemispherical asymmetry in the composition of the residual polar caps on Mars. However, the radiative effects of ozone, clouds, and background dust were not fully modeled. Ozone has only a minor effect on the energy budget of the polar cap. Clouds and dust have a net radiative effect that is quite small near the edge of the polar cap, but it becomes more substantial in increasing the sublimation rate as one goes poleward. In fact, the net radiative effect of clouds and dust at the pole itself increases the loss of CO_2 ice over 1 Martian year of the order of 40 cm or more, which would result in the loss of CO_2 ice of the order of 40 sols earlier than previously predicted.

However, several other processes have also not been fully included in polar cap/atmospheric pressure models. These processes include penetration of radiation into and through the ice, bidirectional surface reflectance, ice albedo dependence on solar zenith angle, season, and latitude, lower ice emissivity, decreased heat conduction from the surface due to existing ice, snowfall, surface residues, surface roughness, and wind shifting of ice. The importance of each of these processes to the energy budget is currently being assessed by B. L. Lindner and B. M. Jakosky. Most of these processes would lengthen

CO_2 ice survivability either by increasing condensation or decreasing sublimation of CO_2 ice and would counter the increased sublimation caused by clouds and dust. However, most of these processes work equally effectively at both poles and do not generate an asymmetry. Hemispherical asymmetries in cloud and dust opacity and in surface elevation would result in a hemispherical asymmetry in the net radiative flux from clouds and dust which is absorbed by the polar cap. The key point is that the net radiative effect of clouds and background dust is to shorten ice lifetimes on the north pole relative to the south pole, helping to explain the asymmetry in the residual polar caps on Mars. Furthermore, the radiative effects of clouds and dust do not appear to significantly affect model predictions of polar cap recession equatorward of 75° latitude or model predictions of the annual cycle in atmospheric pressure, both of which agreed fairly well with observations. The presence of clouds and dust also lessens the ability for a higher albedo to preserve CO_2 ice and for a lower albedo to increase sublimation, decreasing the importance of albedo in determining ice sublimation rates.

Acknowledgments. My thesis advisor, Gary Thomas, was invaluable in pointing out errors and improvements in the radiative transfer. Knut Stamnes, Tom Ackerman, Brian Toon, and Warren Wiscombe are thanked for providing computer codes. Bruce Jakosky, Bob Haberle, Brian Toon, and the reviewers provided valuable discussion. This work was funded by NSF grant ATM 8305841, NASA grants NAGW-389 and NAGW-552, NASA contract NASW-4444, the National Research Council, the NASA Ames Research Center, and Atmospheric and Environmental Research, Inc.

References

Anderson, E., and C. Leovy, Mariner 9 television limb observations of dust and ice hazes on Mars, J. Atmos. Sci., 35, 723-734, 1978.

Barth, C. A., and M. L. Dick, Ozone and the polar hood of Mars, Icarus, 22, 205-211, 1974.

Barth, C. A., and C. W. Hord, Mariner ultraviolet spectrometer: Topography and polar cap, Science, 173, 197-201, 1971.

Barth, C. A., C. W. Hord, A. I. Stewart, A. L. Lane, M. L. Dick, and G. P. Anderson, Mariner 9 ultraviolet experiment: Seasonal variation of ozone on Mars, Science, 179, 795-796, 1973.

Briggs, G. A., The nature of the residual Martian polar caps, Icarus, 23, 167-191, 1974.

Briggs, G. A., and C. B. Leovy, Mariner 9 observations of the Mars north polar hood, Bull. Am. Meteorol. Soc., 55, 278-296, 1974.

Briggs, G., K. Klaasen, T. Thorpe, J. Wellman, and W. Baum, Martian dynamical phenomena during June-November 1976: Viking orbiter imaging results, J. Geophys. Res., 82, 4121-4149, 1977.

Broadfoot, A. L., and L. Wallace, Reflectivity of Mars, 2550-3300 Å, Astrophys. J., 161, 303-307, 1970.

Christensen, P. R., and R. W. Zurek, Martian water-ice clouds: Location and seasonal variation (abstract), Bull. Am. Astron. Soc., 15, 847, 1983.

Christensen, P. R., and R. W. Zurek, Martian north polar hazes and surface ice: Results from the Viking survey/completion mission, J. Geophys. Res., 89, 4587-4596, 1984.

Clark, R. N., Water frost and ice: The near-infrared spectral reflectance 0.65-2.5 microns, J. Geophys. Res., 86, 3087-3096, 1981.

Clough, S. A., F. X. Kneizys, E. P. Shettle, and G. P. Anderson, Atmospheric Radiance and Transmission: FASCOD2, Proceedings of the Sixth Conference on Atmospheric Radiation, Williamsburg, VA, 1986.

Clow, G. D., Generation of liquid water on Mars through the melting of a dusty snowpack, Icarus, 72, 95-127, 1987.

Cogley, A. C., and W. J. Borucki, Exponential approximations for daily average solar heating or photolysis, J. Atmos. Sci., 33, 1347-1356, 1976.

Cross, C. A., The heat balance of the Martian polar caps, Icarus, 15, 110-114, 1971.

Davies, D. W., Effects of dust on the heating of Mars' surface and atmosphere, J. Geophys. Res., 84, 8289-8293, 1979.

Davies, D. W., C. B. Farmer, and D. D. LaPorte, Behavior of volatiles in Mars' polar areas: A model incorporating new experimental data, J. Geophys. Res., 82, 3815-3822, 1977.

Freeman, K. P., and K. N. Liou, Climatic effects of cirrus clouds, Adv. Geophys., 21, 231-287, 1979.

Gal'tsev, A. P., and V. M. Osipov, Spectral transmission functions of CO_2 for the conditions of the Martian atmosphere, Izv. Acad. Sci. USSR Atmos. Oceanic Phys., Engl. Transl., 15, 767-769, 1979.

Haberle, R. M., C. B. Leovy, and J. B. Pollack, A numerical model of the Martian polar cap winds, Icarus, 39, 151-183, 1979.

Hansen, J. E., Exact and approximate solutions for multiple scattering by cloudy and hazy planetary atmospheres, J. Atmos. Sci., 26, 478-487, 1969.

Henyey, L. G., and J. L. Greenstein, Diffuse radiation in the galaxy, Astrophys. J., 93, 70-83, 1941.

Hess, S. L., J. A. Ryan, J. E. Tillman, R. M. Henry, and C. B. Leovy, The annual cycle of pressure on Mars measured by Viking landers 1 and 2, Geophys. Res. Lett., 7, 197-200, 1980.

Hunt, G. E., Thermal infrared properties of the Martian atmosphere, 4, Predictions of the presence of dust and ice clouds from Viking IRTM spectral measurements, J. Geophys. Res., 84, 2865-2874, 1979.

Hunt, G. E., E. A. Mitchell, H. H. Kieffer, and R. Ditteon, Scattering and absorption properties of carbon dioxide ice spheres in the region 360-4000 cm^{-1}, J. Quant. Spectrosc. Radiat. Transfer, 24, 141-146, 1980.

Jakosky, B. M., The seasonal cycle of water on Mars, Space Sci. Rev., 41, 131-200, 1985.

Jakosky, B. M., and C. B. Farmer, The seasonal and global behavior of water vapor in the Mars atmosphere: Complete global results of the Viking atmospheric water detector experiment, J. Geophys. Res., 87, 2999-3019, 1982.

Jakosky, B. M., and R. M. Haberle, Year-to-year instability of the Mars south polar cap, J. Geophys. Res., this issue.

Jakosky, B. M., and T. Z. Martin, Mars: North

polar atmospheric warming during dust storms, Icarus, 72, 528-534, 1987.

James, P. B., Recession of Martian north polar cap: 1979-1980 Viking observations, Icarus, 52, 565-569, 1982.

James, P. B., Condensation phase of the Martian south polar cap (abstract), Bull. Am. Astron. Soc., 15, 846-847, 1983.

James, P. B., and K. Lumme, Martian south polar cap boundary: 1971 and 1973 data, Icarus, 50, 368-380, 1982.

James, P. B., and G. R. North, The seasonal CO_2 cycle on Mars: An application of an energy-balance climate model, J. Geophys. Res., 87, 10,271-10,283, 1982.

James, P. B., G. Briggs, J. Barnes, and A. Spruck, Seasonal recession of Mars' south polar cap as seen by Viking, J. Geophys. Res., 84, 2889-2922, 1979.

James, P. B., M. Pierce, and L. J. Martin, Martian north polar cap and circumpolar clouds: 1975-1980 telescopic observations, Icarus, 71, 306-312, 1987.

Kahn, R., The spatial and seasonal distribution of Martian clouds and some meteorological implications, J. Geophys. Res., 89, 6671-6688, 1984.

Kieffer, H., Spectral reflectance of carbon dioxide-water vapor frosts, J. Geophys. Res., 75, 501-509, 1970.

Kieffer, H. H., Mars south polar spring and summer temperatures: A residual CO_2 frost, J. Geophys. Res., 84, 8263-8288, 1979.

Kieffer, H. H., S. C. Chase, Jr., T. Z. Martin, E. D. Miner, and F. D. Palluconi, Martian north pole summer temperatures: Dirty water ice, Science, 194, 1341-1343, 1976.

Kondrat'ev, K. Ya., and G. E. Hunt, Weather and Climate on Planets, Pergamon, New York, 1982

Kong, T. Y., and M. B. McElroy, The global distribution of O_3 on Mars, Planet. Space Sci., 25, 839-857, 1977.

Krasnopol'skii, V. A., A. A. Krys'ko, and V. N. Rogachev, Measurement of ozone in a planetary atmosphere by space probe MARS 5, Kosm. Issled., 13, 37-41, 1975. (Cosmic Res., Engl. transl. 13, 31-34, 1975.)

Kuhn, W. R., S. K. Atreya, and S. E. Postawko, The influence of ozone on Martian atmospheric temperature, J. Geophys. Res., 84, 8341-8342, 1979.

Lane, A. L., C. A. Barth, C. W. Hord, and A. I. Stewart, Mariner 9 ultraviolet spectrometer experiment: Observations of ozone on Mars, Icarus, 18, 102-108, 1973.

Leighton, R. B., and B. C. Murray, Behavior of carbon dioxide and other volatiles on Mars, Science, 153, 136-144, 1966.

Leovy, C. B., G. A. Briggs, A. T. Young, B. A. Smith, J. B. Pollack, E. N. Shipley, and R. L. Wildey, The Martian atmosphere: Mariner 9 television experiment progress report, Icarus, 17, 373-393, 1972.

Lian, M. S., and R. D. Cess, Energy-balance climate models: A reappraisal of ice-albedo feedback, J. Atmos. Sci., 34, 1058-1062, 1977.

Lindal, G. F., H. B. Hotz, D. N. Sweetnam, Z. Shippony, J. P. Brenkle, G. V. Hartsell, R. T. Spear, and W. H. Michael, Jr., Viking radio occultation measurements of the atmosphere and topography of Mars: Data acquired during 1 Martian year of tracking, J. Geophys. Res., 84, 8443-8456, 1979.

Lindner, B. L., The aeronomy and radiative transfer of the Martian atmosphere, Ph.D. dissertation, 470 pp., Univ. of Colo., Boulder, Aug. 1985.

Lindner, B. L., Albedo of the polar caps on Mars (abstract), Eos Trans. AGU, 67, 1078, 1986.

Lindner, B. L., Ozone on Mars: The effect of clouds and airborne dust, Planet. Space Sci., 36, 125-144, 1988.

Lindner, B. L., and G. E. Thomas, On the importance of ozone heating in the Mars atmosphere (abstract), Bull. Am. Astron. Soc., 15, 849, 1983.

Lumme, K., and P. B. James, Some photometric properties of the Martian south polar cap region during the 1971 apparition, Icarus, 58, 363-376, 1984.

Martin, L. J., North polar hood observations during Martian dust storms, Icarus, 26, 341-352, 1975.

Martin, L. J., Clearing the Martian air: The troubled history of dust storms, Icarus, 57, 317-321, 1984.

Martin, T. Z., Thermal infrared opacity of the Mars atmosphere, Icarus, 66, 2-21, 1986.

Martin, T. Z., Mariner 7 spectra of the Mars south polar CO_2 cap (abstract), Bull. Am. Astron. Soc., 20, 851, 1988.

Martin, T. Z., and H. H. Kieffer, Thermal infrared properties of the Martian atmosphere, 2, The 15 micron band measurements, J. Geophys. Res., 84, 2843-2852, 1979.

Masursky, H., et al., Mariner 9 television reconnaissance of Mars and its satellites: Preliminary results, Science, 175, 294-305, 1972.

Moroz, V. I., Clouds on Mars: Some results from observations on MARS 3, Kosm. Issled., 14, 406-416, 1976. (Cosmic Res., Eng. transl., 14, 364-372, 1976.)

Noxon, J. F., W. A. Traub, N. P. Carleton, and P. Connes, Detection of O_2 dayglow emission from Mars and the Martian ozone abundance, Astrophys. J., 207, 1025-1035, 1976.

Owen, T., K. Biemann, D. R. Rushneck, J. E. Biller, D. W. Howarth, and A. L. Lafleur, The composition of the atmosphere at the surface of Mars, J. Geophys. Res., 82, 4635-4639, 1977.

Paige, D. A., The annual heat balance of the Martian polar caps from Viking observations, Ph.D. dissertation, 207 pp., Calif. Inst. of Technol., Pasadena, May 1985.

Pang, K., and C. W. Hord, Mariner 9 ultraviolet spectrometer experiment: 1971 Mars' dust storm, Icarus, 18, 481-488, 1973.

Pollack, J. B., Properties of dust in the Martian atmosphere and its effect on temperature structure, the Mars Reference Atmosphere, edited by A. Kliore, pp. 63-80, Jet Propulsion Lab., Calif. Inst. of Technol., Pasadena, 1978.

Pollack, J. B., and R. M. Haberle, Simulations of the general circulation of the Martian atmosphere (abstract), Bull. Am. Astron. Soc., 20, 859, 1988.

Pollack, J. B., and O. B. Toon, Quasi-periodic climate changes on Mars: A review, Icarus, 50, 259-287, 1982.

Pollack, J. B., C. B. Leovy, Y. H. Mintz, and W.

Van Camp, Winds on Mars during the Viking season: Predictions based on a general circulation model with topography, Geophys. Res. Lett., 3, 479-482, 1976.

Pollack, J. B., D. Colburn, R. Kahn, J. Hunter, W. Van Camp, C. E. Carlston, and M. R. Wolf, Properties of aerosols in the Martian atmosphere as inferred from Viking Lander imaging data, J. Geophys. Res., 82, 4479-4496, 1977.

Pollack, J. B., D. S. Colburn, F. M. Flasar, R. Kahn, C. E. Carlston, and D. Pidek, Properties and effects of dust particles suspended in the Martian atmosphere, J. Geophys. Res., 84, 2929-2945, 1979.

Pollack, J. B., C. B. Leovy, P. W. Greiman, and Y. Mintz, A Martian general circulation experiment with large topography, J. Atmos. Sci., 38, 3-29, 1981.

Ryan, J. A., and R. D. Sharman, H_2O frost point detection on Mars, J. Geophys. Res., 86, 503-511, 1981.

Ryan, J. A., R. D. Sharman, and R. D. Lucich, Mars water vapor, near-surface, J. Geophys. Res., 87, 7279-7284, 1982.

Saunders, R. S., T. J. Parker, J. B. Stephens, E. G. Laue, and F. P. Fanale, Sediment-water deposition and erosion in the Martian polar regions (abstract), Workshop on Water on Mars, edited by S. Clifford, Tech. Rep. 85-03, pp. 68-70, Lunar and Planet. Inst., Houston, Tex., 1985.

Saunders, R. S., F. P. Fanale, T. J. Parker, J. B. Stephens, and S. Sutton, Properties of filamentary sublimation residuals from dispersions of clay in ice, Icarus, 66, 94-104, 1986.

Shimazaki, T., and M. Shimizu, The seasonal variation of ozone density in the Martian atmosphere, J. Geophys. Res., 84, 1269-1276, 1979.

Simpson, J. P., J. N. Cuzzi, E. F. Erickson, D. W. Strecker, and A. T. Tokunaga, Mars: Far-infrared spectra and thermal-emission models, Icarus, 48, 230-245, 1981.

Smith, F. L., III, and C. Smith, Numerical evaluation of Chapman's grazing incidence integral ch (X, X), J. Geophys. Res., 77, 3592-3597, 1972.

Smythe, W. D., Spectra of hydrate frosts: Their application to the outer solar system, Icarus, 24, 421-427, 1975.

Squyres, S. W., and J. Veverka, Variation of albedo with solar incidence angle on planetary surfaces, Icarus, 50, 115-122, 1982.

Stamnes, K., and P. Conklin, A new multi-layer discrete ordinate approach to radiative transfer in vertically inhomogeneous atmospheres, J. Quant. Spectrosc. Radiat. Transfer, 31, 273-282, 1984.

Svitek, T., and B. C. Murray, Penitentes on Mars? (abstract), Bull. Am. Astron. Soc., 20, 847-848, 1988.

Taylor, V. R., and L. L. Stowe, Reflectance characteristics of uniform Earth and cloud surfaces derived from Nimbus 7 ERB, J. Geophys. Res., 89, 4987-4996, 1984.

Thorpe, T. E., Mars atmospheric opacity effects observed in the northern hemisphere by Viking orbiter imaging, J. Geophys. Res., 86, 11,419-11,429, 1981.

Tillman, J. E., and C. B. Leovy, Dustiness on Mars as determined from surface meteorological measurements: Variability over three years (abstract), Bull. Am. Astron. Soc., 16, 672, 1984.

Tillman, J. E., R. M. Henry, and S. L. Hess, Frontal systems during passage of the Martian north polar hood over the Viking Lander 2 site prior to the first 1977 dust storm, J. Geophys. Res., 84, 2947-2955, 1979.

Toon, O. B., J. B. Pollack, and C. Sagan, Physical properties of the particles composing the Martian dust storm of 1971-1972, Icarus, 30, 663-696, 1977.

Traub, W. A., N. P. Carleton, P. Connes, and J. F. Noxon, The latitude variation of O_2 dayglow and O_3 abundance on Mars, Astrophys. J., 299, 846-850, 1979.

Veverka, J., and J. Goguen, The nonuniform recession of the south polar cap of Mars, J. R. Astron. Soc. Can., 67, 273-290, 1973.

Warren, S. G., Optical constants of ice from the ultraviolet to the microwave, Appl. Opt., 23, 1206-1225, 1984.

Warren, S. G., Optical constants of carbon dioxide ice, Appl. Opt., 25, 2650-2674, 1986.

Warren, S. G., and W. J. Wiscombe, A model for the spectral albedo of snow, II, Snow containing atmospheric aerosols, J. Atmos. Sci., 37, 2734-2745, 1980.

Wiscombe, W. J., and S. G. Warren, A model for the spectral albedo of snow, I, Pure snow, J. Atmos. Sci., 37, 2712-2733, 1980.

Woiceshyn, P. M., Global seasonal atmospheric fluctuations on Mars, Icarus, 22, 325-344, 1974.

Zurek, R. W., Solar heating of the Martian dusty atmosphere, Icarus, 35, 196-208, 1978.

Zurek, R. W., Inference of dust opacities for the 1977 Martian great dust storms from Viking Lander 1 pressure data, Icarus, 45, 202-215, 1981.

Zurek, R. W., Martian great dust storms: An update, Icarus, 50, 288-310, 1982.

B. L. Lindner, Atmospheric and Environmental Research, Incorporated, Cambridge, MA 02139.

(Received September 1, 1988
Revised June 5, 1989
Accepted June 8, 1989.)

Penetration of Light Into the Martian Polar Cap: Implications for the Energy Budget

B.L. Lindner (AER) and B.M. Jakosky (U. Colo.)

We have modified the Jakosky and Haberle (J. Geophys. Res., 95, 1359, 1990) model of the seasonal polar cap on Mars to include penetration of solar radiation into the cap itself, based on the theoretical work of Clow (Icarus, 72, 95, 1987). We find that the inclusion of light penetration slightly decreases the albedo needed in the model to keep CO_2-ice year-round at the south pole by on the order of 1%. The required albedo is decreased because some solar radiation is used to heat the subsurface, and not all of this heat is transported back to the surface. Furthermore, the number of sols for which the north pole is free of CO_2-ice is increased slightly by approx. 5 sols. By allowing solar radiation to be absorbed at depth, the surface does not become as warm. This decreases the infrared radiation emitted by the surface and increases the heat conduction from the subsurface, which in turn delays the onset of frost formation in the fall.

Overall, we conclude that the penetration of light into the polar cap has only a small effect on the energy budget of the polar cap. Given the uncertainties currently present in albedo and other parameters, the effect of light penetration is second order, and can be neglected in models of the polar cap energy budget.

AN EFFICIENT AND ACCURATE TECHNIQUE TO COMPUTE THE ABSORPTION, EMISSION, AND TRANSMISSION OF RADIATION BY THE MARTIAN ATMOSPHERE. Bernhard Lee Lindner, AER Inc., 840 Memorial Drive, Cambridge, MA 02139; Thomas P. Ackerman, Dept. of Meteor., Penn. State Univ., University Park, PA 16802; and James B. Pollack, NASA/ARC, Moffett Field, CA 94035.

INTRODUCTION. CO_2 comprises 95% of the composition of the martian atmosphere [1]. However, the martian atmosphere also has a high aerosol content. Dust opacities vary from less than 0.2 to greater than 3.0, primarily on a seasonal basis with the occurrence of global dust storms during southern spring [2]. Ice-cloud opacities vary from 0 to greater than 1, with large amounts occurring at winter polar latitudes [3]. CO_2 is an active absorber and emitter in near-IR and IR wavelengths; the near-IR absorption bands of CO_2 provide significant heating of the atmosphere, and the 15 μm band provides rapid cooling[4-7]. However, dust and ice-cloud aerosols have high scattering albedoes in solar wavelengths, and are highly absorbing at infrared wavelengths, and are as important as CO_2 in the atmospheric energy budget [5].

Including both CO_2 and aerosol radiative transfer simultaneously in a model is difficult. Aerosol radiative transfer requires a multiple-scattering code, while CO_2 radiative transfer must deal with complex wavelength structure, as shown in Fig. 1. The problem can be solved exactly by inserting the CO_2 absorptance for each spectral line into a multiple-scattering code, but the 15μm band alone has on the order of 10,000 lines, making such a computation tedious and expensive. It is this difficulty of simultaneously treating aerosol multiple scattering and the banded absorption structure of CO_2 that prompts most radiative-transfer studies of the martian atmosphere to consider either a pure-CO_2 or pure-dust atmosphere. This approximation simplifies treatment, but is inaccurate.

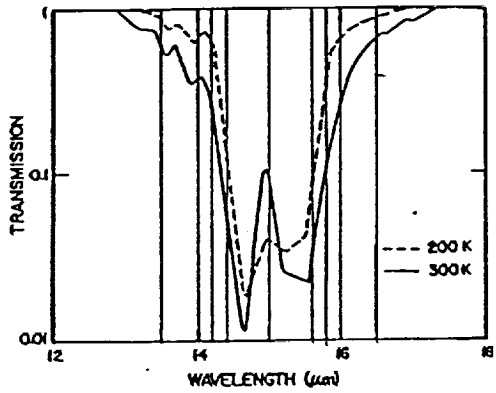

Figure 1. CO_2 15 μm band transmission at 20 km altitude looking upward, at temperatures of 200 and 300K [25]. Also shown are the sub-intervals used for the 8 term and 16 term fits.

One alternative technique that has recently been developed for atmospheric applications is the exponential-sum or k-distribution approximation [8-21]. The transmission of a homogeneous atmosphere is actually independent of the ordering of the absorption coefficient, k, in frequency space within a spectral interval, depending only upon the percentage of the spectral interval that has a particular value of k. The percentage of the spectral interval which has values between k and k + Δk can be formulated in a probability density function f(k) shown schematically in Fig. 2. The chief advantage of the exponential-sum approach is that the integration over k space of f(k) can be computed more quickly than the integration of k_ν over frequency. The exponential-sum approach is superior to the photon-path-distribution and emissivity techniques for dusty conditions [22, 19, 23]. Our work is the first application of the exponential-sum approach to martian conditions.

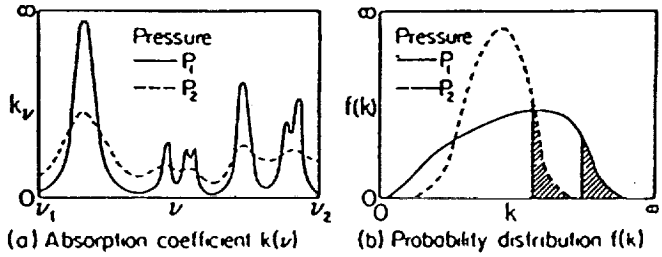

Figure 2. A schematic illustration portraying the essence of the exponential-sum approach. (a) shows a schematic of absorption line spectra at two different pressures. In (b) the two probability density functions f(k) associated with (a) are illustrated. The shaded area depicts the strongest absorption (i.e., largest k) for the same spectral interval (i.e., f(k) for different pressures are correlated). Integration of f(k) over k replaces the integration of k_ν over ν (modified from [28], [29]).

THEORETICAL APPROACH. The transmittance of the 15 μm band and the near-IR bands of CO_2 was computed using the FASCOD line-by-line transmittance model [24], modified for martian conditions. Computations with the modified FASCOD model were made at 3 temperatures (125K, 200K, 300K) and 5 pressures (100 mb, 10 mb, 1 mb, 0.1 mb, 0.01 mb); these cover the range of temperature and pressure currently observed in the atmosphere at all latitudes, seasons, and altitudes up to 40 km, and also can be used for early Mars, dense atmosphere studies. The near-IR and 15μm bands were broken into spectral sub-intervals (see Fig. 1), and the

transmittance for each layer, Tr, as a function of CO_2 column abundance within that layer, u, was fit with a series of weighting coefficients, a_i, and exponential coefficients, b_i:

$$Tr(u) \approx \sum_{i=1}^{n} a_i \exp(-b_i u) \quad (1)$$

We tried fitting procedures based on Wiscombe and Evans [14] and an improved version of Ackerman et al. [13], and found both yielded similar results. Both of these procedures avoid the ill-conditioning of earlier exponential-sum routines, and produce more accurate and unique solutions [13,14]. The exponential-sum fit reproduced the FASCOD transmittances to better than 10^{-4} for all CO_2 abundances considered. The frequency sub-intervals are picked to try to minimize the variation in line strengths within the sub-interval. As shown in Fig. 1, 2 sub-intervals covered the band center, 2 covered the far line wings, 2 covered the near line wings, and 2 covered the transition from wings to band center. The vertical inhomogeneity of the atmosphere is treated by using homogeneous layers, with the absorption coefficients k for all layers correlated in frequency space, i.e. the sub-intervals of the spectral band which have the maximum absorption also have the largest k values (Ackerman et al., 1976). An interpolation is used for temperatures and pressures which fall in between the values at which the exponential-sum coefficients were computed. We compared a logarithmic interpolation to a linear interpolation, and found the logarithmic interpolation to be more accurate.

INCORPORATION IN MULTIPLE-SCATTERING MODELS. Vertical optical depths of CO_2 absorption for each term number, frequency sub-interval, and atmospheric layer are $b_i u$. CO_2 is combined with dust and cloud in that the total optical depth T_i, single-scattering albedo $\tilde{\omega}_i$, and phase function P for each term, frequency sub-interval, and layer are given by[16]:

$$T_i = b_i u + \tau^R + \tau_s^D + \tau_a^D + \tau_s^C + \tau_a^C \quad (2)$$

$$\tilde{\omega}_i = (\tau^R + \tau_s^D + \tau_s^C) / T_i \quad (3)$$

$$P = \frac{\tau_s^D P^D + \tau_s^C P^C + \tau^R P^R}{\tau_s^D + \tau_s^C + \tau^R} \quad (4)$$

where: τ^R - Rayleigh scattering optical depth for that layer

$\tau_{s,a}^{D,C}$ - Dust (D) and Cloud (C) scattering (s) and absorption (a) optical depth for that layer

$P^{D,C,R}$ - dust (D), cloud (C), and Rayleigh scattering (R) phase function

The multiple-scattering code is run once for each term in the sum using the T, $\tilde{\omega}_i$, and P appropriate to that term, and the resultant fluxes, F_i, (or intensities) are then summed and weighted by a_i to give the total flux, F, (or intensity) over the frequency sub-interval:

$$F = \sum_{i=1}^{n} a_i F_i(b_i u) \quad (5)$$

Tables of the exponential-sum coefficients, a_i and b_i, can be obtained from the authors.

NUMERICAL STUDIES. The number of terms in the series of exponentials (n in equation 1) and the number of sub-intervals into which the spectral band is broken can be varied to increase the desired accuracy. Figure 3 shows a comparison between the 15 μm cooling rates computed using various numbers of frequency sub-intervals and terms within each sub-interval. The temperature of the atmospheric model rose linearly from 150K at the surface to 160K at 10km altitude, and then fell linearly to 130K at 40km altitude. These temperatures are typical of the winter polar atmosphere on Mars. Using 4 terms and 4 sub-intervals results in an error of less than 10% in the lowest 10 km, but results in substantial errors at higher altitudes. The explanation is that the 4 term fit could not capture the effects of both the band center and the wings at all altitudes, and in this case we emphasized the wings, which are more important at lower altitudes where the band center is saturated (see Fig. 1). Adding additional terms from 8 to 16 is far less noticeable.

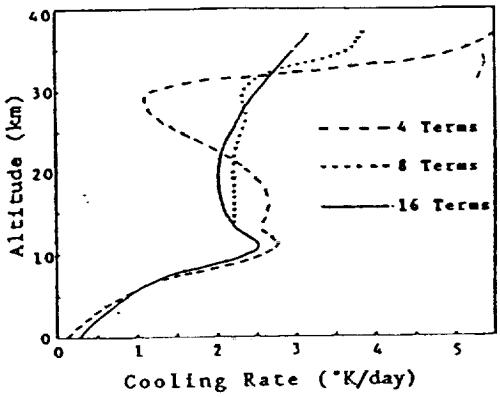

Figure 3. 15 μm band cooling rates calculated with an exponential-sum approach using 4 frequency sub-intervals and 4 terms in the sum, 10 sub-intervals and 8 terms, and 10 sub-intervals and 16 terms. A winter polar temperature profile is used (see text), but only 200K exponential-sum coefficients are used for comparison purposes.

We also separately derived exponential-sum coefficients based on the Gal'tsev and Osipov [25] line-by-line calculations of the 15 μm band. The number of terms in the fit (n in equation 1) were varied, to confirm our FASCOD work on the number of terms required to give an accurate fit. Figure 4 shows cooling rates computed with several fits to the Gal'tsev and Osipov parameterizations, as well as to the FASCOD transmittances. Cooling rates compare favorably in the lower atmosphere (below 10 km altitude). Gal'tsev and Osipov only considered temperatures as cold as 200K. We extrapolated the temperature dependence to colder temperatures [26]. Discrepancies between the Gal'tsev and Osipov and FASCOD cooling rates are due to the inaccuracy in the temperature extrapolation, particularly at the higher, colder altitudes. Again, note that the 4 and 5 term fits become inaccurate above 10 km altitude, as in Fig. 3. Also, the 15 term fit yields no marked improvement over the 8 term fit, as also shown with the FASCOD fits in Fig. 3.

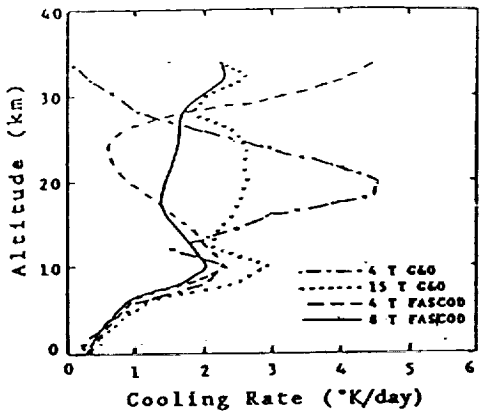

Figure 4. 15 μm band cooling rates calculated with 4 types of exponential-sum coefficients: 4 and 15 term fits to the transmission parameterizations of [25] (abbrev. G&O), and 4 and 8 term fits to the FASCOD transmission model. The winter polar atmosphere model is used, with logarithmic temperature interpolation for the exponential coefficients.

Cooling rates computed using the FASCOD exponential-sum transmittances also compared well below 10 km altitude with cooling rates computed using the Pollack et al. [27,4] parameterizations of CO_2 transmittance. At higher altitudes, discrepancies exist due to the use of the strong-line approximation by Pollack et al, which emphasizes the effects of the line wings. However, comparisons of our exponential-sum transmittances with techniques commonly used for the terrestrial atmosphere have indicated that our exponential-sum transmittances could be in error above 20 km altitude. J. Pollack is seeking to modify our exponential-sum approach to use two sets of sums, one applied to the line centers and one applied to the line wings. Initial tests seem to show better agreement in the upper atmosphere of Mars.

B.L. Lindner acknowledges support by NASA contract NASW-4444.

REFERENCES. [1]Owen, T. et al., J. Geophys. Res., 82, 4635, 1977. [2]Pollack, J. et al., J. Geophys. Res., 84, 2929, 1979. [3]Briggs, G. and C. Leovy, Bull. Amer. Met. Soc., 55, 278, 1974. [4]Gierasch, P. and R. Goody, Planet. Space. Sci., 15, 1465, 1967. [5]Kondratyev, K. et al., Sov. Phys. Dokl., 24, 81, 1979. [6]Pollack, J. et al., J. Atmos. Sci., 38, 3, 1981. [7]Lindner, B.L., The aeronomy and radiative transfer of the martian atmosphere, Ph.D. Dissertation, 470 pp., University of Colorado, Boulder, 1985. [8]Kondratyev, K., Radiation in the Atmosphere, Academic Press, 1969. [9]Arking, A. and K. Grossman, J. Atmos. Sci., 29, 937, 1972. [10]Raschke, E. and U. Stucke, Beitr. Phys. Atmosph., 46, 203, 1973. [11]Liou, K. and T. Sasamori, J. Atmos. Sci., 32, 2166, 1975. [12]Kerschgens, M. et al., Beitr. Phys. Atmosph., 49, 81, 1976. [13]Ackerman, T. et al., J. App. Meteor., 15, 28, 1976. [14]Wiscombe, W. and J. Evans, J. Computational Phys., 24, 416, 1977. [15]Morcrete, J., Beitr. Phys. Atmosph., 51, 338, 1978. [16]Freeman, K. and K. Liou, Adv. Geophys., 21, 231, 1979. [17]Evans, J. et al., Math. of Computat., 34, 203, 1980. [18]Chou, M. and A. Arking, J. Atmos. Sci., 38, 798, 1981. [19]Zdunkowski, W. et al., Beitr. Phys. Atmos., 55, 215, 1982. [20]Slingo, A. and H. Schrecker, Quart. J. R. Met. Soc., 108, 407, 1982. [21]Wang, W. and G. Shi, J. Quant. Spectrosc. Radiat. Transfer, 39, 387, 1988. [22]Bakan, S. et al., Beitr. Phys. Atmosph., 51, 28, 1978. [23]Wiscombe, W., Rev. Geophys. Space Phys., 21, 997, 1983. [24]Clough, S. et al., Proceedings of the Sixth Conference on Atmospheric Radiation, Williamsburg, VA, 1986. [25]Gal'tsev, A. and V. Osipov, Bull. (Izv.) Acad. Sci. USSR, Atmos. Ocean. Phys., 15, 767, 1979. [26]Lindner, B.L., The martian polar cap: Radiative effects of ozone, clouds, and airborne dust, J. Geophys. Res., 95, 1367, 1990. [27]Pollack, J. et al., Geophys. Res. Lett., 3, 479, 1976. [28]Stephens, G., Mon. Wea. Rev., 112, 826, 1984. [29] Hansen, J. et al., Mon. Wea. Rev., 111, 609, 1983.

SOLAR AND IR RADIATION NEAR THE MARTIAN SURFACE: A PARAMETERIZATION FOR CO_2 TRANSMITTANCE. Bernhard Lee Lindner, AER Inc., 840 Memorial Drive, Cambridge, MA 02139; Thomas P. Ackerman, Dept. of Meteor., Penn. State Univ., University Park, PA 16802; James B. Pollack and O. Brian Toon, NASA-/ARC, Moffett Field, CA 94035; Gary E. Thomas, APAS Dept., Univ. of Colorado, Boulder, CO 80309

INTRODUCTION. CO_2 comprises 95% of the atmospheric composition of the martian atmosphere [1]. CO_2 is an active absorber and emitter in near-IR and IR wavelengths; the near-IR absorption bands of CO_2 provide significant heating of the atmosphere, and the 15 μm band provides rapid cooling [2-5]. However, the Mars atmosphere also has a high aerosol content. Dust opacities vary from less than 0.2 to greater than 3.0, primarily on a seasonal basis with the occurrence of global dust storms during southern spring [6]. Ice-cloud opacities vary from 0 to greater than 1, with large amounts occurring at winter polar latitudes [7]. Dust and ice-cloud aerosols have high scattering albedoes in solar wavelengths, and are highly absorbing at infrared wavelengths, and are as important as CO_2 in the atmospheric energy budget [5].

Including both CO_2 and aerosol radiative transfer simultaneously in a model is difficult. Aerosol radiative transfer requires a multiple-scattering code, while CO_2 radiative transfer must deal with complex wavelength structure. The problem can be solved exactly by inserting the CO_2 absorptance for each spectral line into a multiple-scattering code, but the 15μm band alone has on the order of 10,000 lines, making such a computation tedious and expensive. It is this difficulty of simultaneously treating aerosol multiple scattering and the banded absorption structure of CO_2 that prompts most radiative-transfer studies of the martian atmosphere to consider either a pure-CO_2 or pure-dust atmosphere. This approximation simplifies treatment, but is inaccurate.

One alternative technique that has recently been developed for atmospheric applications is the exponential-sum or k-distribution approximation [8-21]. The transmission of a homogeneous atmosphere is actually independent of the ordering of the absorption coefficient, k, in frequency space within a spectral interval, depending only upon the percentage of the spectral interval that has a particular value of k. The percentage of the spectral interval which has values between k and k + ΔT can be formulated in a probability density function f(k) shown schematically in Figure 1. The chief advantage of the exponential-sum approach is that the integration over k space of f(k) can be computed more quickly than the integration of k_ν over frequency. The exponential-sum approach is superior to the photon-path-distribution and emissivity techniques for dusty conditions [22, 19, 23]. Our work is the first application of the exponential-sum approach to martian conditions.

THEORETICAL APPROACH. The transmittance of the 15 μm band and the near-IR bands of CO_2 was computed using the FASCOD line-by-line transmittance model [24], modified for martian conditions. Computations with the modified FASCOD model were made at 3 temperatures (125K, 200K, 300K) and 5 pressures (100 mb, 10 mb, 1 mb, 0.1 mb, 0.01 mb); these cover the range of temperature and pressure currently observed in the atmosphere at all latitudes, seasons, and altitudes up to 40 km, and also can be used for early Mars, dense atmosphere studies. The near-IR and 15 μm bands were broken into spectral sub-intervals, and the transmittance for each layer, Tr, as a function of CO_2 column abundance within that layer, u, was fit with a series of weighting coefficients, a_i, and exponential coefficients, b_i: $Tr(u) = \sum_{i=1,n} a_i \exp(-b_i u)$ from term number 1 to n. We tried fitting procedures based on Wiscombe and Evans [14] and an improved version of Ackerman et al. [13], and found both yielded similar results. Both of these procedures avoid the ill-conditioning of earlier exponential-sum routines, and produce more accurate and unique solutions [13,14]. The exponential-sum fit reproduced the FASCOD transmittances to better than 10^{-4} for all CO_2 abundances considered. The sub-intervals are picked to try to minimize the variation in line strengths within the sub-interval. Vertical optical depths of CO_2 absorption for each term number, frequency sub-interval, and atmospheric layer are $b_i u$. This CO_2 absorption opacity and the Rayleigh scattering opacity is combined with dust and cloud opacities, single-scattering albedoes and phase functions (e.g., [16]). The multiple-scattering code is run once for each term in the sum using the T, $\tilde{\omega}$, and P appropriate to that term, and the resultant fluxes (or intensities) are then summed and weighted by the a_i to give the total flux (or intensity) over the spectral sub-interval. An interpolation is used for temperatures and pressures which fall in between the values at which the exponential-sum coefficients were computed. We compared a logarithmic interpolation to a linear interpolation, and found the logarithmic interpolation to be more accurate. Tables of the exponential-sum coefficients, a_i and b_i, can be obtained from the authors.

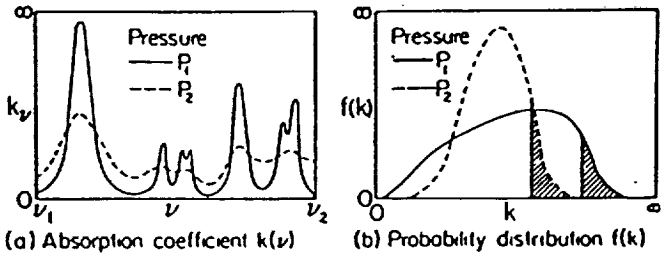

(a) Absorption coefficient $k(\nu)$ (b) Probability distribution f(k)

Figure 1. A schematic illustration portraying the essence of the exponential-sum approach. (a) shows a schematic of absorption line spectra at two different pressures. In (b) the two probability density functions f(k) associated with (a) are illustrated. The shaded area depicts the strongest absorption (i.e., largest k) for the same spectral interval (i.e., f(k) for different pressures are correlated). Integration of f(k) over k replaces the integration of k_ν over ν (reproduced from [28]).

RESULTS. The number of terms in the series of exponentials and the number of sub-intervals into which the spectral band is broken can be varied to increase the desired accuracy. Figure 2 shows a comparison between the 15 μm cooling rates computed using various numbers of frequency sub-intervals and terms within each sub-interval. The temperature of the atmospheric model rose linearly from 150K at the surface to 160K at 10km altitude, and then fell linearly to 130K at 40km altitude. These temperatures are typical of the winter polar atmosphere on Mars. Using 4 terms and 4 sub-intervals results in an error of less than 10% in the lowest 10 km, but results in substantial errors at higher altitudes. The explanation is that the 4 term fit could not capture the effects of both the band center and the wings at all altitudes, and in this case we emphasized the wings, which are more important at lower altitudes where the band center is saturated. Adding additional terms from 8 to 16 is far less noticeable. However, very recent work by J. Pollack comparing these exponential-sum transmittances with techniques commonly used for the terrestrial atmosphere have indicated that our exponential-sum transmittances could be in error above 20 km altitude. J. Pollack is seeking to modify our exponential-sum approach to use two sets of sums, one applied to the line centers and one applied to the line wings. Initial tests seem to show better agreement in the upper atmosphere of Mars.

We also separately derived exponential-sum coefficients based on the Gal'tsev and Osipov [25] line-by-line calculations of the 15 μm band. The number of terms in the fit were varied, to confirm our FASCOD work on the number of terms required to give an accurate fit. Figure 3 shows cooling rates computed with several fits to the Gal'tsev and Osipov parameterizations, as well as to the FASCOD transmittances. Cooling rates compare favorably in the lower atmosphere (below 10 km altitude). Gal'tsev and Osipov only considered temperatures as cold as 200K. We extrapolated the temperature dependence to colder temperatures [26]. Discrepancies between the Gal'tsev and Osipov and FASCOD cooling rates are due to the inaccuracy in the temperature extrapolation, particularly at the higher, colder altitudes. Again, note that the 4 and 5 term fits become inaccurate above 10 km altitude, as in Figure 2. Also, the 15 term fit yields no marked improvement over the 8 term fit, as also shown with the FASCOD fits in Figure 2.

Cooling rates computed using the FASCOD exponential-sum transmittances also compared well below 10 km altitude with cooling rates computed using the Pollack et al. [27,4] parameterizations of CO_2 transmittance. At higher altitudes, discrepancies exist due to the use of the strong-line approximation by Pollack et al, which emphasizes the effects of the line wings.

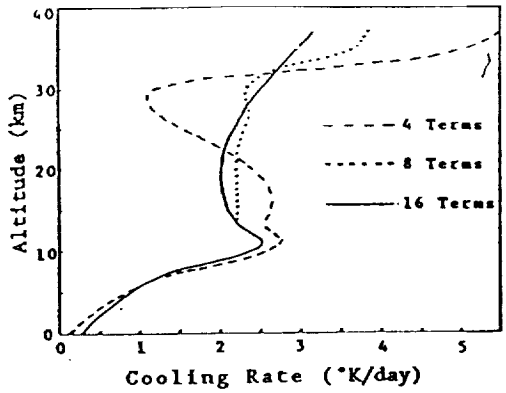

Figure 2. 15 μm band cooling rates calculated with an exponential-sum approach using 4 frequency sub-intervals and 4 terms in the sum, 10 sub-intervals and 8 terms, and 10 sub-intervals and 16 terms. A winter polar temperature profile is used (see text), but only 200K exponential-sum coefficients are used for comparison purposes.

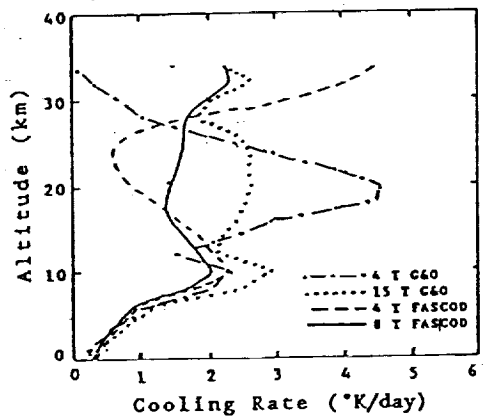

Figure 3. 15 μm band cooling rates calculated with 4 types of exponential-sum coefficients: 4 and 15 term fits to the transmission parameterizations of [25] (abbrev. G&O), and 4 and 8 term fits to the FASCOD transmission model. The winter polar atmosphere model is used, with logarithmic temperature interpolation for the exponential coefficients.

B.L. Lindner acknowledges support by NASA contract NASW-4444.

REFERENCES. [1]Oven, T. et al., J. Geophys. Res., 82, 4635, 1977. [2]Gierasch, P. and R. Goody, Planet. Space. Sci., 15, 1465, 1967. [3]Kondratyev, K. et al., Sov. Phys. Dokl., 24, 81, 1979. [4]Pollack, J. et al., J. Atmos. Sci., 38, 3, 1981. [5]Lindner, B., The aeronomy and radiative transfer of the martian atmosphere, Ph.D. Dissertation, 470 pp., University of Colorado, Boulder, 1985. [6]Pollack, J. et al., J. Geophys. Res., 84, 2929, 1979. [7]Briggs, G. and C. Leovy, Bull. Amer. Met. Soc., 55, 278, 1974. [8]Kondratyev, K., Radiation in the Atmosphere, Academic Press, 1969. [9]Arking, A. and K. Grossman, J. Atmos. Sci., 29, 937, 1972. [10]Raschke, E. and U. Stucke, Beitr. Phys. Atmosph., 46, 203, 1973. [11]Liou, K. and T. Sasamori, J. Atmos. Sci., 32, 2166, 1975. [12]Kerschgens, M. et al., Beitr. Phys. Atmosph., 49, 81, 1976. [13]Ackerman, T. et al., J. App. Meteor., 15, 28, 1976. [14]Wiscombe, W. and J. Evans, J. Computational Phys., 24, 416, 1977. [15]Morcrette, J., Beitr. Phys. Atmosph., 51, 338, 1978. [16]Freeman, K. and K. Liou, Adv. Geophys., 21, 231, 1979. [17]Evans, J. et al., Math. of Computat., 34, 203, 1980. [18]Chou, M. and A. Arking, J. Atmos. Sci., 38, 798, 1981. [19]Zdunkowski, W. et al., Beitr. Phys. Atmos., 55, 215, 1982. [20]Slingo, A. and H. Schrecker, Quart. J. R. Met. Soc., 108, 407, 1982. [21]Wang, W. and G. Shi, J. Quant. Spectrosc. Radiat. Transfer, 39, 387, 1988. [22]Bakan, S. et al., Beitr. Phys. Atmosph., 51, 28, 1978. [23]Wiscombe, W., Rev. Geophys. Space Phys., 21, 997, 1983. [24]Clough, S. et al., Proceedings of the Sixth Conference on Atmospheric Radiation, Williamsburg, VA, 1986. [25]Gal'tsev, A. and V. Osipov, Bull. (Izv.) Acad. Sci. USSR, Atmos. Ocean. Phys., 15, 767, 1979. [26]Lindner, B., The martian polar cap: Radiative effects of ozone, clouds, and airborne dust, J. Geophys. Res., In Press, 1990. [27]Pollack, J. et al., Geophys. Res. Lett., 3, 479, 1976. [28]Stephens, G., Mon. Wea. Rev., 112, 826, 1984.

CO_2 TRANSMITTANCE IN THE MARTIAN ATMOSPHERE: AN EXPONENTIAL-SUM FIT FOR USE IN MULTIPLE-SCATTERING MODELS

Bernhard Lee Lindner (Atmospheric and Environmental Research Inc., 840 Memorial Drive, Cambridge, MA 02139, U.S.A.)
James B. Pollack (NASA/Ames Research Center, Moffett Field, CA 94035, U.S.A.)
Thomas P. Ackerman (Dept. of Meteorology, Penn. State Univ., University Park, PA 16802 USA)

CO_2 and airborne dust are both important in heating and cooling the martian atmosphere. However, theoretical modeling of both CO_2 and dust radiative transfer simultaneously is difficult because dust radiative transfer requires a multiple scattering code, while CO_2 radiative transfer must deal with complex wavelength structure.

We have approximated the CO_2 transmittance at near-IR and IR wavelengths in the lower martian atmosphere with an exponential-sum fit. Exponential-sum fitting allows for the incorporation of CO_2 absorption and emission in a multiple scattering computer model in a straightforward, efficient and accurate manner. This makes it possible for CO_2 and dust heating and cooling of the martian atmosphere to be easily treated simultaneously.

Comparison of our CO_2 cooling and heating rates to those derived from several other techniques shows good agreement in the lower atmosphere below 20 km altitude, particularly near the surface. An improved version of the exponential-sum approach is being developed to treat higher altitudes as well.

Tables of exponential-sum coefficients are available from the authors.

1. Dr. Bernhard Lee Lindner
AER Inc.
840 Memorial Drive
Cambridge, Mass. 02139
United States of America

Telephone:
(617) 547-6207 (day)
(617) 277-2812 (night)

Fax: (617) 876-7158

Telex: 95-1417

2. Symposia JS.4

3. Dr. T. Encrenaz
Dr. N.F. Pissarenko

4. None

5. Oral
(but poster acceptable)

MARS SEASONAL CO_2-ICE LIFETIMES AND THE ANGULAR DEPENDENCE OF ALBEDO

Bernhard Lee Lindner, AER, 840 Memorial Drive, Cambridge MA 02139 USA

The albedo of the polar caps on Mars brightens appreciably at high solar zenith angle (Warren et al., J. Geophys. Res., 95, 14717, 1990), an effect not included in prior polar-cap energy-balance models. This decreases absorption of sunlight by the polar cap, hence decreasing sublimation of CO_2 ice. Lindner (J. Geophys. Res., 95, 1367, 1990) has shown that the radiative effects of clouds and airborne dust will increase sublimation of CO_2 ice over that predicted by prior polar-cap energy-balance models. Furthermore, observations hint that more clouds may exist in the northern hemisphere, which Lindner (1990) has shown would sublime CO_2 ice more quickly in the north than in the south. I show here that the effects of the solar zenith angle dependence of albedo and the radiative effects of clouds and dust offset each other, but act to extend the lifetime of CO_2 ice on the south pole more than on the north pole, possibly explaining the observed hemispherical asymmetry in the residual polar caps without the need of a hemispherical asymmetry in polar-cap albedo required by prior models. Another positive aspect of this solution is that neither the inclusion of the solar zenith angle dependence of albedo nor the radiative effects of clouds and dust should appreciably change prior model agreement with observations of the annual cycle of surface pressure and the recession of the polar caps equatorward of 75° latitude.

· LINDNER, Bernhard Lee, Ph.D., Atmospheric and Environmental Research, Inc., 840 Memorial Drive, Cambridge, MA 02139 USA

· The Climate of Mars Symposium, Symposium M13

· Oral presentation preferred

· 1 overhead projector

WHY IS THE NORTH POLAR CAP ON MARS DIFFERENT THAN THE SOUTH POLAR CAP?

Bernhard Lee Lindner, Atmospheric and Environmental Research, Inc.
840 Memorial Drive, Cambridge, Mass. 02139-3794, USA

Introduction. One of the most puzzling mysteries about the planet Mars is the hemispherical asymmetry in the polar caps. Every spring the seasonal polar cap of CO_2 recedes until the end of summer, when only a small part, the residual polar cap, remains. During the year that Viking observed Mars, the residual polar cap was composed of water ice in the northern hemisphere [Kieffer et al., Science, 194, 1341, 1976] but was primarily carbon dioxide ice in the southern hemisphere [Kieffer, J. Geophys. Res., 84, 8263, 1979]. Scientists have sought to explain this asymmetry by modeling observations of the latitudinal recession of the polar cap and seasonal variations in atmospheric pressure (since the seasonal polar caps are primarily frozen atmosphere, they are directly related to changes in atmospheric mass). These models reproduce most aspects of the observed annual variation in atmospheric pressure fairly accurately. Furthermore, the predicted latitudinal recession of the northern polar cap in the spring agrees well with observations, including the fact that the CO_2 ice is predicted to completely sublime away. However, these models all predict that the carbon dioxide ice will also sublime away during the summer in the southern hemisphere, unlike what is observed. This paper will show how the radiative effects of ozone, clouds, and airborne dust, light penetration into and through the polar cap, and the dependence of albedo on solar zenith angle affect CO_2 ice formation and sublimation, and how they help explain the hemispherical asymmetry in the residual polar caps. These effects have not been studied with prior polar cap models.

Ozone, Clouds, and Airborne Dust. Since O_3 is more prevalent in the northern hemisphere than in the southern hemisphere, O_3 was suggested as a cause for the hemispherical asymmetry in the residual polar caps by Kuhn et al. (J. Geophys. Res., 84, 8341, 1979). However, Lindner (submitted to Icarus, 1991) has shown that O_3 has a minor effect on the atmospheric temperature, and hence on the infrared radiation which strikes the polar cap, and Lindner (J. Geophys. Res., 95, 1367, 1990) has shown that O_3 absorbs less than 1% of the total solar radiation absorbed by the polar cap. Thus, O_3 is not an important consideration in the polar cap energy budget.

Lindner (1990) has computed the solar and thermal flux striking the polar cap of Mars for various ozone, dust, and cloud abundances and for three solar zenith angles. These calculations have been inserted in the polar-cap models

of Lindner (Eos Trans. AGU, 67, 1078, 1986) and Jakosky and Haberle (J. Geophys. Res., 95, 1359, 1990). Vertical optical depths of dust and cloud ranging from zero to 1 cause little change in the total flux absorbed by the polar cap near its edge but increase the absorbed flux significantly as one travels poleward. Observed hemispherical asymmetries in dust abundance, cloud cover, and surface pressure combine to cause a significant hemispherical asymmetry in the total flux absorbed by the residual polar caps, which helps to explain the dichotomy in the residual polar caps on Mars.

Light Penetration. Penetration of solar radiation into the cap itself is included in my polar cap model, based on the theoretical work of Clow (Icarus, 72, 95, 1987). I find that the inclusion of light penetration slightly decreases the albedo needed in the model to keep CO_2-ice year-round at the south pole by on the order of 1%. The required albedo is decreased because some solar radiation is used to heat the subsurface, and not all of this heat is transported back to the surface. Overall, I conclude that penetration of light into the polar cap has only a small effect on the polarcap energy budget.

Albedo and the Solar Zenith Angle. Warren et al. (J. Geophys. Res., 95, 14717, 1990) has computed the dependence of the albedo of the martian polar caps on solar zenith angle, and these calculations have been included in my polar cap model. Since the albedo of ice increases and becomes more forward scattering at higher solar zenith angles, and since the solar zenith angle becomes higher as one approaches the pole, the albedo is greatest at the pole. This decreases absorption of sunlight, hence increasing survivability of CO_2 ice. In fact, this increases the survivability of ice enough to offset the decrease in survivability of ice due to the radiative effects of clouds and dust.

Discussion. The combination of the effects of solar zenith angle on albedo and the radiative effects of clouds and dust act to extend the lifetime of CO_2 ice on the south pole relatively more than on the north pole, explaining the hemispherical asymmetry in the residual polar caps without the need of a hemispherical asymmetry in polar cap albedo. Another positive aspect this solution is that neither the inclusion of solar zenith angle effects on ice albedo nor the radiative effects of clouds and dust should appreciably change model predictions of the annual cycle of pressure or polar cap recession equatorward of 75° latitude, since approximately 90% of the seasonal CO_2 frost is equatorward of 80° latitude. Hence, the good model agreement noted by prior researchers to the seasonal cycle in atmospheric pressure and to the recession of the polar cap equatorward of 80° latitude is retained.